STUDIES ON

POWER SYSTEM CHARACTERISTICS OF SUPERCONDUCTING MAGNETIC ENERGY STORAGE

BY

YASUYUKI SHIRAI

FEBRUARY 1988

FACULTY OF ENGINEERING
KYOTO UNIVERSITY

JAPAN

STUDIES ON

POWER SYSTEM CHARACTERISTICS OF SUPERCONDUCTING MAGNETIC ENERGY STORAGE

BY

YASUYUKI SHIRAI

FEBRUARY 1988

FACULTY OF ENGINEERING
KYOTO UNIVERSITY

JAPAN

STUDIES ON

POWER SYSTEM CHARACTERISTICS OF SUPERCONDUCTING MAGNETIC ENERGY STORAGE

BY

YASUYUKI SHIRAI

FEBRUARY 1988

FACULTY OF ENGINEERING
KYOTO UNIVERSITY

JAPAN

ACKNOWLEDGMENT

The author wishes to express his sincere gratitude to Dr.Takao Okada, Professor of Kyoto University. for his continual encouragement and earnest guidance during the course of this work.

The author wishes to express his hearty appreciation to Dr.Tanzo Nitta, associate Professor of Kyoto University, for his valuable suggestions and discussions and for his careful reading of the manuscript.

The author would like to thank Dr.Junya Matsuki, Lecturer of Kyoto University, for his valuable discussions and useful advices.

The author is deeply indebted to Dr.Toshio Shintani, associate Professor of Fukuyama university, for his useful discussions.

Acknowledgement must be made to Mr.Tadashi Kojima, Mr.Atsushi Kishima, Mr.Yasuhiro Tanaka, Mr.Hiroyuki Seriu, Mr.Hisashi Kondoh and other staffs and graduate students of Professor Okada's reseaching groups for their excellent cooperations.

CONTENTS

STUDIES ON

POWER SYSTEM CHARACTERISTICS OF SUPERCONDUCTING MAGNETIC ENERGY STORAGE

BACKGROUND

In recent electric power systems, the difference between peak load and the lowest load in a day or a season is getting larger and larger. It leads to declining of a load factor. On the other hand, nuclear power plants which generate main part of total energy are desirable to operate at a constant output power. From this point of view, energy storage plants are necessary in electric power systems and are useful for power system planning. If energy storage plants can control powers with quick responsibility and have high efficiency, it is useful to meet peak shaving or load leveling, moreover, to improve power system stability.

By now, pumped hydro-storage plants are in use for peak shaving. However, they have some problems on efficiency, place to be installed at and response speed.

Several new energy storage methods are studied and developed, for example, new types of battery, flywheel, compressed air, thermal energy storage and so on. One of them is Superconducting Magnetic Energy Storage system(:abbr. SMES).

In comparison with the others, Superconducting Magnetic Energy Storage (SMES) has many advantages as an energy storage apparatus in power systems as follows:

1) High efficiency,

2) Quick responsibility,

3) No problem on short-circuit capacity in power systems, and so on.

For these advantages, many studies on SMES for several applications have been done. That is,

1)Static VAR Compensator[1]

2)Fault Current Limiter[2],[3]

3)Pulsed Power Source for Accelerator or Fusion Technology

4)Energy Storage Unit for Electric Power System

5)For Electric Power System Stabilization

and so on. For Application 4), the feasibility studies and concept design studies are reported.[4]-[8] For Application 5), the effect of SMES on power system stability are discussed by use of simulation studies[9]-[12] and experimental approaches[13]-[14]. The 30[MJ]-SMES installed to the commercial power system for BPA transmission line stabilization is reported.[15]

The important problems to put SMES in practice in electric power systems are considered as follows: 1)design and construction problems of large superconducting magnets, 2)protection system, 3)cryogenic problem, 4)Electrical power converter[16]-[18], 5)power system characteristics and so on.

This thesis aims at investigating power system characteristics of SMES. SMES has different features with comparison to the other power system apparatus now in use. It is necessary to reveal problems on installation of SMES to real power systems.

ABSTRACT

Power charging and discharging of SMES are made by changing current through superconducting magnet. Then in a strict sense, there is no steady state on operating SMES, that is, firing angles of converters always change and so on. On this point, we have problems as follows. What are problems on operating SMES in power systems? How does SMES behave in power systems? Those are points of our studies on SMES.

From these points of view, we have been studying power system characteristics of SMES and investigating problems on operations of SMES in power systems by use of small superconducting magnets, thyristorized converters, power control equipments and artificial transmission lines.

In chapter 1, basic structure of SMES for electrical power system are discussed. Fundamental characteristics of SMES are also discussed based on power controls. Power control schemes of SMES are considered in case of single and double bridge thyristorized converters. A basic design of SMES for a power system is examined.

When we study interaction between SMES and power systems, it is significant problems where SMES is installed and what capacity of SMES is needed in a certain power system. Before considering power system characteristics of SMES, we examine a case where SMES is connected to a bus of large capacity (that is, it is assumed to be an infinite bus) in chapter 2. Fundamental characteristics of exchanging powers between a superconducting magnet and an infinite bus(power source) are experimentally investigated by use of a model SMES system. Active power control and active and reactive powers simultaneous control are described.

In chapter 3, a computer simulation of power system including SMES which takes commutations of converters into account is proposed. The simulation method has flexibility for

change of power systems. Simulation studies are performed corresponding to the experimental system.

When SMES is installed at a certain point of transmission lines like a pumped hydro plants, it is necessary to take impedances of power systems viewed from terminal of SMES into account. As typical examples of such cases, characteristics of SMES are investigated experimentally taking up the following two cases.

In chapter 4, characteristics of SMES connected to a large power source through transmission lines are studied experimentally. Problems on current harmonics and lagging reactive power produced by SMES are discussed.

In chapter 5, characteristics of power system including generators and SMES are studied. Interaction between SMES and generator is discussed experimentally.

CHAPTER.1

SUPERCONDUCTING MAGNETIC ENERGY STORAGE[1]

1-1. INTRODUCTION

In this thesis, Superconducting Magnetic Energy Storage (SMES) is considered as an energy storage unit in an electric power system. Energy is stored as a magnetic energy by flowing DC current through a superconducting magnet. Because an electric power system is of AC three phase in general, an AC/DC converter is necessary to connect a superconducting magnet to AC system. As DC current through a superconducting magnet is comparably large and voltage across the magnet is low, transformers are also necessary to connect a magnet to AC system. A cooling system is needed to maintain superconductivity of a magnet. Many control schemes of SMES are considered according to utilities. When it is connected to the electrical power system, powers flowing into or out of SMES should be chosen as basic control valuables.

In Section 1-2, basic structure of SMES for electrical power system are discussed.

In Section 1-3, fundamental power characteristics of SMES is studied.

In Section 1-4, power control schemes of SMES are considered and discussed in case of single and double bridge thyristorized converters.

In Section 1-5, a basic design of SMES for a power system are examined.

1-2. BASIC STRUCTURE OF SMES

Main components of SMES are 1)large superconducting magnet, 2)AC/DC converter, 3)transformers, 4)cooling systems, 5)control equipments as mentioned above.

As to AC/DC converters, Motor-Generator sets or semiconductor power converters are considered. The Motor-Generator set is inferior to semiconductor converter in efficiency, maintenance and quick responsibility. Natural commutation type thyristors are now used widely, for example, in converters of High Voltage Direct Current (abbr.:HVDC) transmission lines.

Forced commutation type thyristors, which are superior to normal type thyristors(natural commutation) in controllability, are recently developed in capacity of conducting current. However, they have a possibility to open a circuit by themselves. On the other hand, normal type thyristors have little possibility. It is quite serious problem to open a circuit including superconducting magnet in series. Because it means the open circuit of large inductor with large current. Since energy stored in magnet has no path to be consumed, quite high voltage is induced at the open terminal. The voltage may lead to fatal damage of superconducting magnet. The gate turn off(GTO) thyristor is one of forced commutation type. GTO converters are superior in controllability for reactive power and harmonics. However, they are inferior to normal type thyristors in reliability for converters of SMES. Moreover large turn-off gate current is necessary to switch off conducting current.(The gate-gain is not so high.) It is one of disadvantages to turn off large current of superconducting magnet.

As a result of the above discussion, normal types of thyristor are used for converters in the following studies.

Next, let us consider how many pulses of converter shall we use. Three phase bridge connection(6-pulses) converter(Graetz bridge) are well in use. Several Graetz bridges are connected in series and parallel for safety of operations and reduction of harmonics as converters in HVDC transmission lines.

In case of SMES, however, the arrangement of several number of bridges in series leads to the decrease of reliability. The more the thyristors are used, the more the possibility of the breakdown of the thyristor becomes. It is unfavorable in efficiency because losses of thyristors become large in low voltage and large current systems such as SMES. The parallel arrangement of converters should be discussed for reduction of load on each thyristor. Here we put it as a future problem.

In the following discussions, a 12-pulse converter, which is generally used, is chosen for studies.

The more discussion on converters for SMES will be necessary. In this chapter, however, for investigation of fundamental characteristics of SMES, it may be sufficient to discuss the basic structure, where a superconducting magnet is connected to a power system through transformers and thyristorized converters as shown in Fig.1-1. Two Graetz bridges in series(called double-bridge) with two transformers of D-Y and D-D transformer connections is chosen as a basic structure for discussion in comparison with the one bridge(called single-bridge). Transformers have D-connection windings to eliminate the 3-rd harmonics.

1-3. TERMINAL CHARACTERISTICS OF SMES

1-3-1. FUNDAMENTAL CHARACTERISTICS

Here we discuss fundamental power characteristics of SMES by use of the basic structure shown in Fig.1-1. A superconducting magnet is connected to a power system through the transformers and the converters (thyristorized 3-phase bridge connection converter). When SMES is considered to be a power system plant, the main control variables should be powers flow into or out of SMES. The charging or discharging powers are controlled by the firing angles of the thyristorized converters. As the

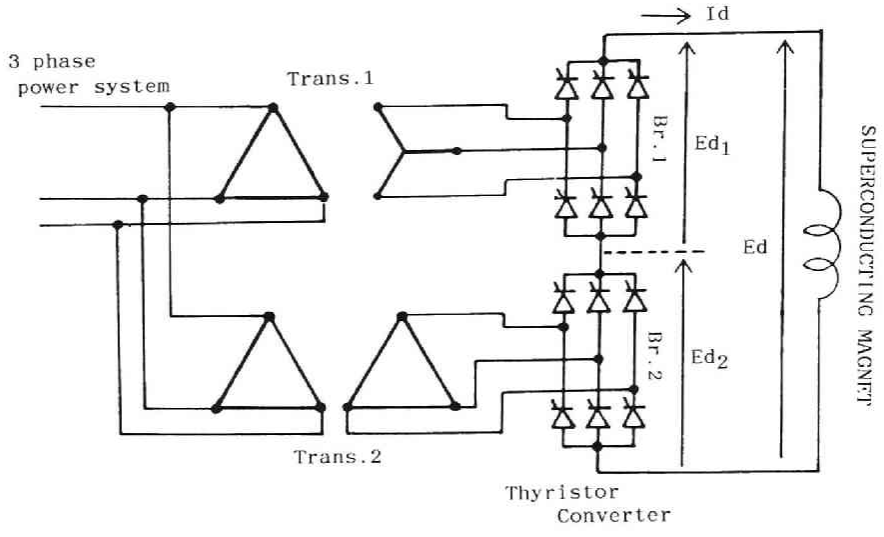

Fig.1-1 Schema of Superconducting magnetic energy storage

firing angles are able to be changed quickly, SMES has quick responsibility. By using two Graetz bridges in series shown in Fig.1-1, not only active power but also reactive power can be controlled and the current harmonics can be decreased to a certain extent as described below.

A voltage Ed across the superconducting magnet is written by use of magnet current Id and inductance L of the magnet as

$$Ed = L \frac{d\,Id}{dt} \qquad (1\text{-}1)$$

Stored energy W_L of the superconducting magnet is given as

$$W_L = \frac{1}{2} LId^2 \qquad (1\text{-}2)$$

Therefore the maximum stored energy is determined by the inductance and the rated current of the superconducting magnet.

It is important problem to decide inductance and rated current of superconducting magnet for a certain required stored energy.

An active power Pd charging into or discharging out of the superconducting magnet is obtained as derivative of stored energy W_L with respect to time.

$$Pd = \frac{d\ W_L}{dt} = L \frac{d\ Id}{dt} Id = EdId \qquad (1\text{-}3)$$

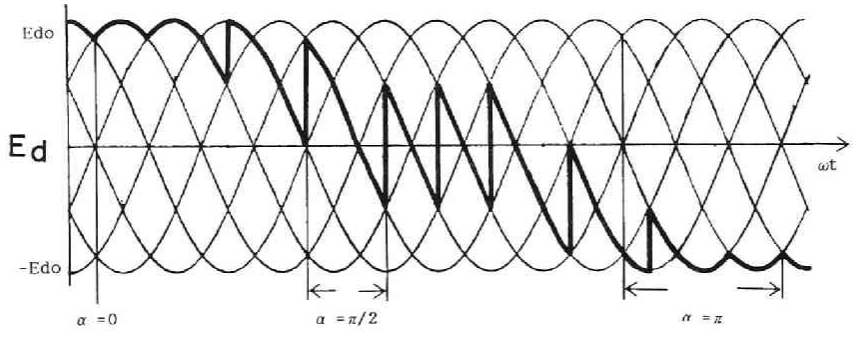

(a) without overlap

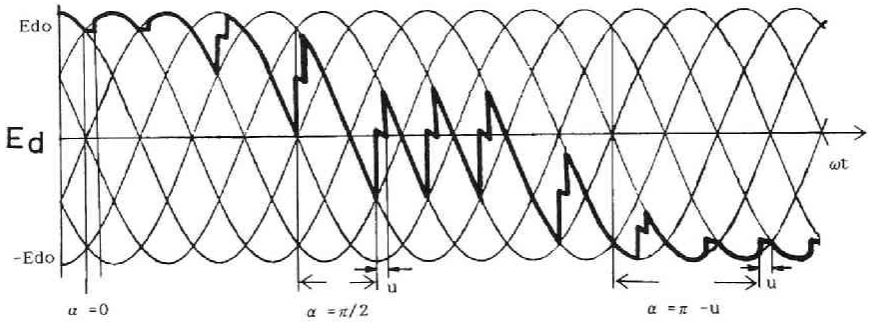

(b) with overlap (overlap angle u)

Fig.1-2 Instantaneous direct voltage of bridge converter with firing angle α (shown by heavy solid line)
(a) without overlap
(b) with overlap (overlap angle u)

When thyristorized converter is consist of the three phase Graetz bridge connection(considering single-bridge), a voltage across the superconducting magnet is of 6 phase commutating wave (see Fig.1-2). The no-load average voltage $Ed_{no-load}$ is given as

$$Ed_{no-load}= \frac{6}{2\pi}\int_{-\pi/6+\alpha}^{\pi/6+\alpha} \sqrt{2}E_2\cos\theta \, d\theta = \frac{3\sqrt{2}}{\pi}E_2\cos\alpha$$

$$= Edo^{(1)}\cos\alpha \qquad (1\text{-}4)$$

$$; \; Edo^{(1)}=\frac{3\sqrt{2}}{\pi} E_2$$

where E_2 denotes a line to line voltage across low voltage terminal of the transformer, α denotes a firing angle of thyristor, $Edo^{(1)}$ is named as the maximum average voltage at no-load.

Active power $Pd^{(1)}$ flowing into or out of the superconducting magnet through one converter bridge is given as

$$Pd^{(1)}=Ed^{(1)} \cdot Id=Edo^{(1)}\cos\alpha \cdot Id \qquad (1\text{-}5)$$

An apparent power $Pa^{(1)}$ for each converter bridge is defined as

$$Pa^{(1)}=Edo^{(1)} \cdot Id \qquad (1\text{-}6)$$

Therefore a reactive power $Qd^{(1)}$ is defined by DC values as

$$Qd^{(1)}=(Pa^{(1)2}-Pd^{(1)2})1/2 \qquad (1\text{-}7)$$

$$=Edo^{(1)} \cdot Id \cdot \sin\alpha$$

Equation (1-5) shows that active power can be controlled continuously by changing firing angle α, that is, charging mode($0° < \alpha < 90°$) and discharging mode($90° < \alpha < 180°$). Apparent power $Pa^{(1)}$ and reactive power $Qd^{(1)}$ change with active power control.

The above discussion is on the single-bridge converter. To

connect two or more bridges in series has several advantages. Here, we pick up the double-bridge converter for studies.

When two thyristorized converters are connected in series, magnet voltage is given as a sum of voltages of two converters. By neglecting leakage reactances of transformers and voltage drops across thyristors, voltage Ed across the superconducting magnet is obtained as

$$Ed=Edo\cdot(\cos\alpha_1+\cos\alpha_2)/2 \qquad (1\text{-}8)$$
$$;\ Edo=2\cdot Edo^{(1)}$$

where Edo is the maximum converter voltage at no load for two bridges in series ($Edo=2Edo^{(1)}$) and α_i is firing angle of the i-th converter(i=1,2).

Charging or discharging power Pd, reactive power Qd (lag:plus) and apparent power Pa for double-bridge converter are given from Eq.(1-5)-(1-7), respectively, as

$$Pd=\frac{EdoId}{2}(\cos\alpha_1+\cos\alpha_2)=EdId \qquad (1\text{-}9)$$

$$Qd=\frac{EdoId}{2}(\sin\alpha_1+\sin\alpha_2) \qquad (1\text{-}10)$$

$$Pa=\frac{EdoId}{2}[2+2\cos(\alpha_1-\alpha_2)]^{1/2} \qquad (1\text{-}11)$$

Since we can control two firing angles of converters α_1 and α_2, both Pd and Pa (that is, the reactive power Qd) are controlled simultaneously for a certain magnet current Id. It is useful to be able to control both the active power and the reactive power simultaneously (named P-Q simultaneous control) for electrical power systems. However, since Pd and Qd are also functions of Id , α_1 and α_2, there are restrictions in a set of (Pd,Qd,Id) for a P-Q simultaneous control.

Because of leakage reactances, a commutation period u is taken into account at load. The average voltage drop e_{xi} because of the commutation is obtained as follows.

$$e_{xi} = \frac{3X_i}{\pi} Id \qquad (1\text{-}12)$$

where X_i is leakage reactance per phase of i-th transformer. Therefore average voltage Ed at load is given as

$$Ed_i = Ed_{no\text{-}load} - e_{xi} = Edo \cdot \cos\alpha_i/2 - e_{xi} \qquad (1\text{-}13)$$

$$Ed = Ed_1 + Ed_2$$

$$= \frac{Edo}{2}(\cos\alpha_1 + \cos\alpha_2) - \frac{3(X_1+X_2)}{\pi} Id \qquad (1\text{-}14)$$

The subscript i denotes the upper(1) or the lower(2) thyristorized bridge. Active power Pd and reactive power Qd considering leakage reactances are respectively given as

$$Pd = Pd_1 + Pd_2$$

$$= \frac{EdoId}{2}(\cos\alpha_1 + \cos\alpha_2) - \frac{3(X_1+X_2)}{\pi} Id^2 \qquad (1\text{-}15)$$

$$;Pd_i = Ed_i Id$$

$$Qd = \left[\left(\frac{EdoId}{2}\right)^2 - Pd_1{}^2\right]^{1/2} + \left[\left(\frac{EdoId}{2}\right)^2 - Pd_2{}^2\right]^{1/2} \qquad (1\text{-}16)$$

If angles α_1' and α_2' are defined as

$$\alpha_i' = \cos^{-1}\left[\cos\alpha_i - \frac{6X_i}{\pi\, Edo} Id\right] \quad , \qquad (1\text{-}17)$$

powers Pd , Qd and Pa considering leakage reactances X_i are given by replacing α_1 and α_2 to $\alpha_1'$and α_2' in Eq.(1-9), (1-10) and (1-11), respectively.

1-3-2. POWER CHARACTERISTICS

Let us consider vector diagrams for power characteristics of SMES. A power vector diagram is drawn as shown in Fig.1-3 according to the discussion in Section 1-3-1. The largest

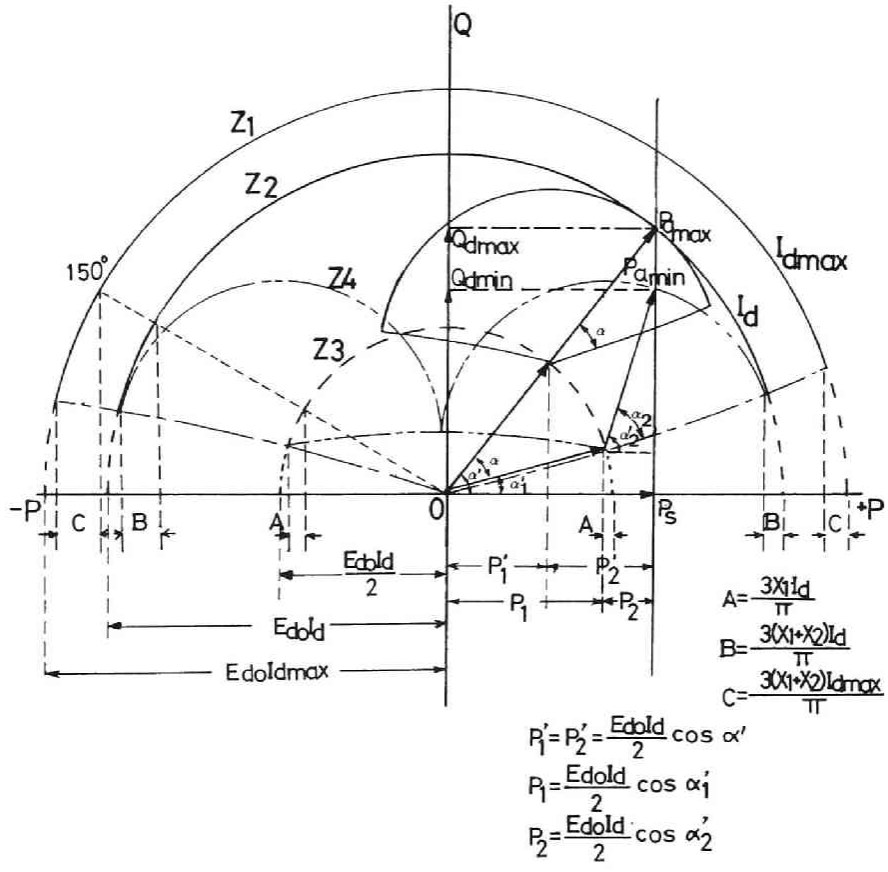

Fig.1-3 Power vector diagram of SMES using double bridge converter

circular arch Z_1 indicates the active and reactive power of SMES (P-Q characteristics) at the maximum magnet current Id_{max}, that is, the capacity of the system. Since margin for commutation mistakes must be taken into account, firing angles α_1 and α_2 should be between 0° and 150° . Because of leakage reactances X, the circular archs are inclined towards the positive direction of firing angle α .

For a magnet current Id, a set of active and reactive powers flowing into or out of the upper bridge is on the dotted arch line Z_3. As the firing angle α_1 is larger, the set of Pd_1 and

Qd_1 move from right to left along the circular arch. A power characteristics for the lower bridge is drawn in the solid line where the center of the circle is a point on the dotted line which indicates apparent power vector for the upper bridge. When two firing angles are same($\alpha_1=\alpha_2$), the power vector is on the circular arch Z_2. A length of the vector has the maximum value Pa_{max}. On the other hand, when difference between two firing angles is maximum, the power vector has the minimum value Pa_{min} and is on the line Z_4. Therefore when the magnet is charged at active power Ps, apparent power can be changed ($Pa_{min}<Pa<Pa_{max}$), and so reactive power also can be changed ($Qd_{min}<Qd<Qd_{max}$) by varying a set of firing angles as shown in Fig.1-3.

1-4. POWER CONTROL OF SMES

1-4-1. ACTIVE POWER CONTROL

A constant active power control by use of single-bridge converter is considered. The differential equation (1-3) is solved as a function of time t under the condition of constant power Pd. And we obtain

$$(Id^2-I_o^2)=\frac{2Pd}{L}t \qquad (1\text{-}18)$$

Where I_o is an initial magnet current. The maximum operating time T_{max} is obtained as

$$T_{max}=\frac{L(Id_{max}^2-I_o^2)}{2Pd} \qquad (1\text{-}19)$$

The magnet voltage Ed and the magnet current Id vary with time as

$$Id=\left(\frac{2Pd}{L}t+I_o^2\right)^{1/2} \qquad (1\text{-}20)$$

$$Ed = Pd/Id = \left[\frac{2}{PdL} t + \left(\frac{1}{E_o}\right)^2 \right]^{1/2} \qquad (1\text{-}21)$$

where $Pd = E_o I_o$, E_o ; initial voltage

I_o ; initial current

respectively. Time variations of voltage and current are illustrated schematically as shown in Fig.1-4.

The voltage Ed satisfies following inequality.

$$Ed_{min} \leqq Ed \leqq Ed_{max} \qquad (1\text{-}22)$$

where ; $Ed_{min} = -\frac{\sqrt{3}}{2} Edo - \frac{3(X_1+X_2)}{\pi} Id$

; $Ed_{max} = Edo - \frac{3(X_1+X_2)}{\pi} Id$

Constant active power (Pd) control can be performed in the region where magnet current Id exceeds the minimum value of Pd/Ed_{max} in charging mode and $|Pd/Ed_{min}|$ in discharging mode.

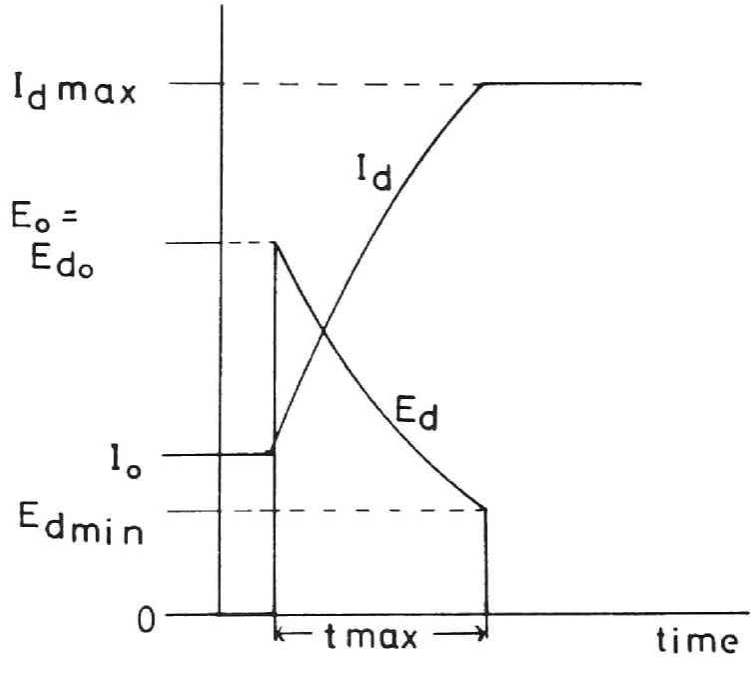

Fig.1-4 Magnet voltage and current at charging.

An example of control pattern is shown in Fig.1-5. As the magnet current Id increases and decreases, the magnet voltage is controlled in order to keep the active power constant. Then the reactive power Qd increases or decreases as the magnet current changes. In the next section, a control method by which not only active power but also reactive power are kept constant is studied.

1-4-2. ACTIVE AND REACTIVE POWER SIMULTANEOUS CONTROL

Constant active and reactive power simultaneous controls are examined and possible regions of the control is discussed.

As is mentioned above, in a constant active power control by use of double thyristorized bridges, two firing angles are changeable independently. A set of firing angles cannot be determined uniquely for a certain constant Pd. In other words, a apparent power Pa and a reactive power Qd can be controlled by choosing a set of firing angles for a certain active power. It is one of the advantages of SMES in power systems that not only active power but also reactive power are controllable.

In a constant active power control for a certain value of Id, we examine two firing angle control schemes as

$$\begin{aligned} &\text{C- i)} \quad \alpha_1 = \alpha_2 \\ &\text{C-ii)} \quad |\alpha_1 - \alpha_2| \rightarrow \text{maximum} \end{aligned} \tag{1-23}$$

For a constant active power Ps, reactive power is controlled to be maximum(Qd_{max}) on C-i)(maximum reactive power-control). On the contrary, reactive power is controlled to be minimum(Qd_{min}) on C-ii)(minimum reactive power-control). It is because apparent power Pa contains a function of $\cos(\alpha_1 - \alpha_2)$ shown in Eq.(1-11).

P-Q simultaneous control can be performed for the reactive power between Qd_{max} and Qd_{min}. In Fig.1-6, the lines (I) are P-Q characteristics on C-i) and the lines (II) are those on C-ii) for a magnet current Id. If a set of (Pd,Qd) is in the shaded

region between these two lines, P-Q simultaneous control can be performed.

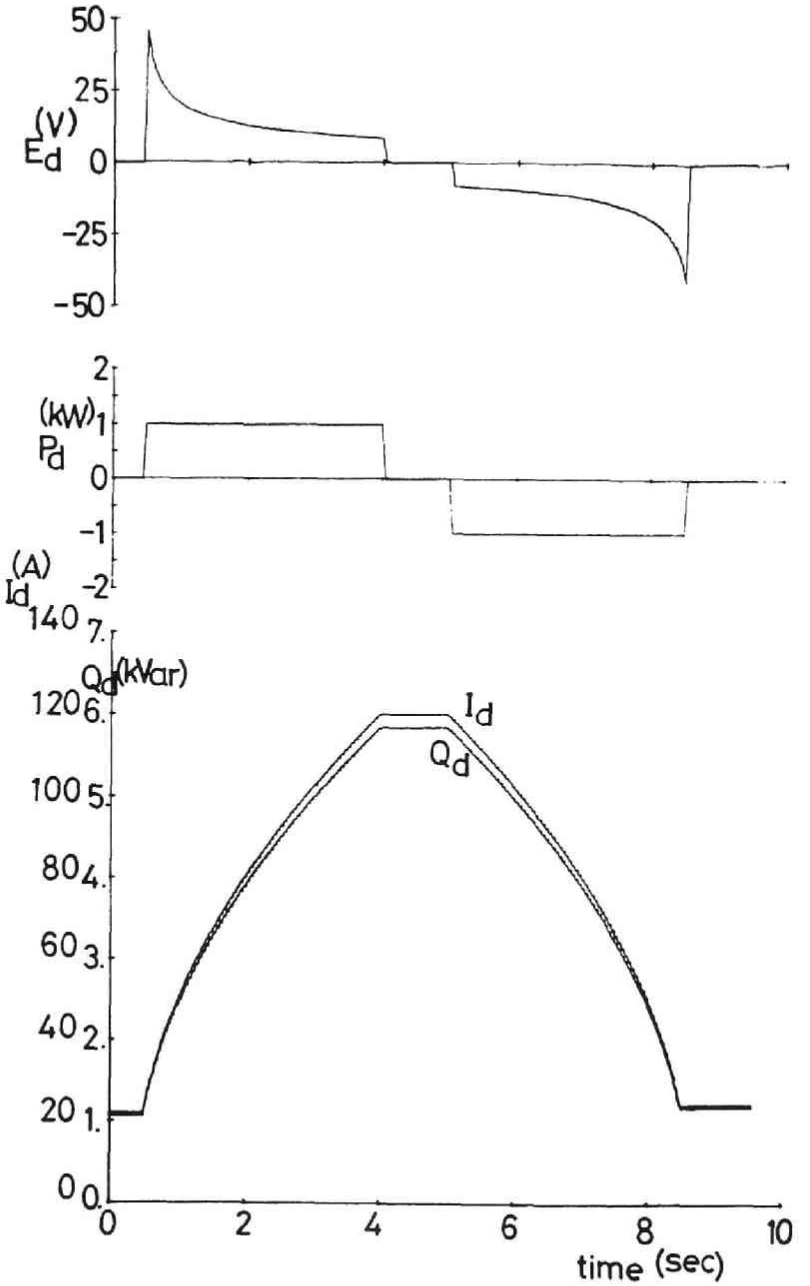

Fig.1-5 Control pattern of constant active power of SMES

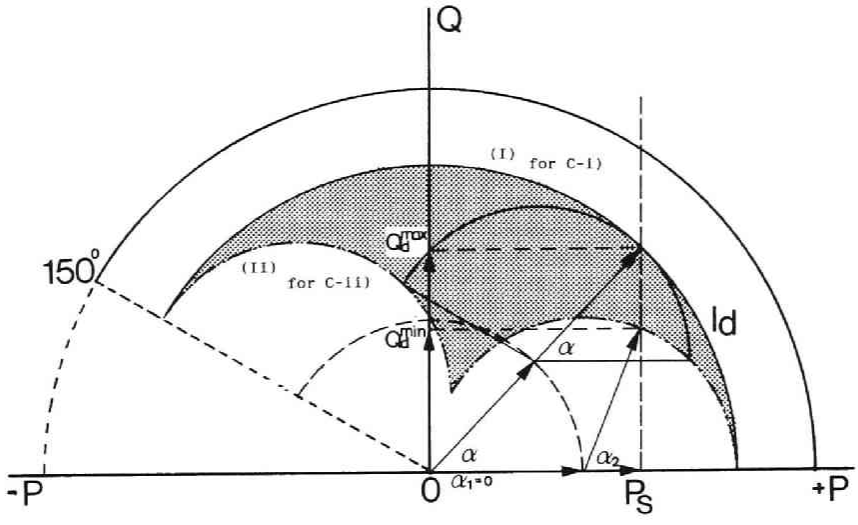

Fig.1-6 Characteristics of active and reactive powers of SMES
for control C-i) $\alpha_1 = \alpha_2$
control C-ii) $|\alpha_1 - \alpha_2|$ max.

Constant active and reactive power control

In the above discussion, the magnet current is assumed to be constant. However, while the superconducting magnet is charged or discharged, the magnet current varies with time. The controllable region of constant active and reactive power also changes with magnet current. Let's consider that the superconducting magnet is charged at a constant power P from a magnet current $Id=I_{A1}$ to $Id=I_{A2}$.

The reactive powers for control patterns C-i) and C-ii) vary with time as shown in Fig.1-7. In the period of the controls, if minimum reactive power in C-i) is greater than maximum reactive power in C-ii), a control of a constant active and reactive power is possible.

In the maximum reactive power-control, the minimum reactive power Q1 is at $Id=I_{A1}$ as shown in Fig.1-7. Then it is obtained as

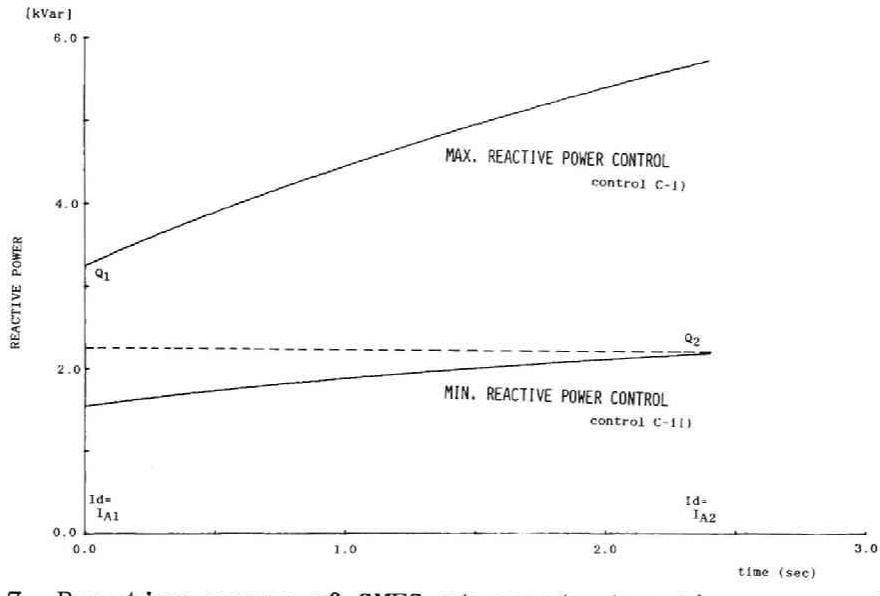

Fig.1-7 Reactive power of SMES at constant active power charging control for control C-i) and C-ii).

$$Q_1 = \{ (EdoI_{A1})^2 - P_A^2 \}^{1/2} \qquad (1\text{-}24)$$

In the minimum reactive power-control, the maximum reactive power Q_2 is obtained for $0° < \alpha_1, \alpha_2 < 150°$ (commutation margin) as

$$\text{for } \frac{2P_A}{EdoI_{A2}} \geq \left(1+\frac{\sqrt{3}}{2}\right)$$

$$Q_2 = \left\{ \left(\frac{EdoId}{2}\right)^2 - \left(P_A - \frac{EdoI_{A2}}{2} \right)^2 \right\}^{1/2} \qquad (1\text{-}25)$$

$$\text{for } \frac{2P_A}{EdoI_{A2}} < \left(1+\frac{\sqrt{3}}{2}\right)$$

$$Q_2 = \left\{ \left(\frac{EdoId}{2}\right)^2 - \left(P_A + \frac{\sqrt{3}EdoI_{A2}}{4} \right)^2 \right\}^{1/2} \qquad (1\text{-}26)$$

The above relations are illustrated in Fig.1-8 for a constant current, where the dotted line is for Eq.(1-24), that is, Q_1, and the thick solid lines are for Eq.(1-25) and (1-26).

Here we consider a control for a constant charging power when magnet current increases from $Id=I_{A1}$ to $Id=I_{A2}$ and a control for a constant discharging power when the current decreases from

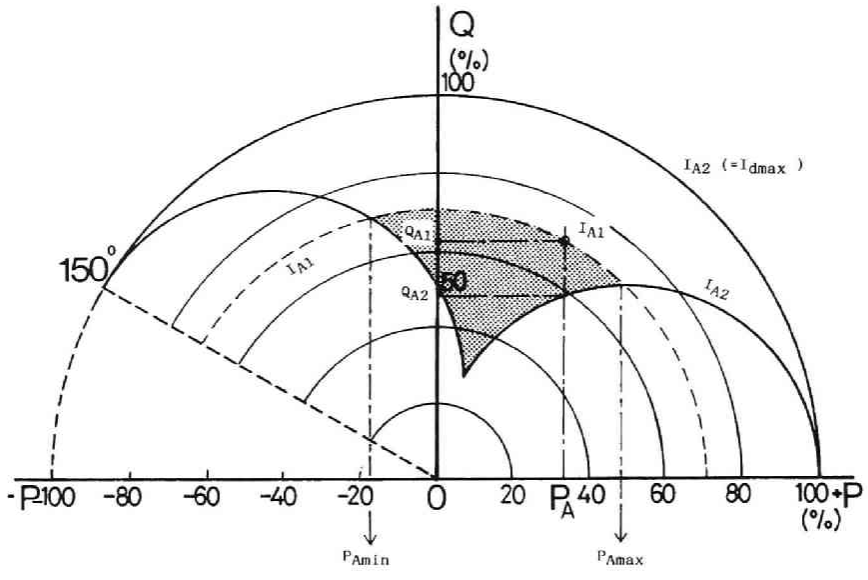

Fig.1-8 Possible region for constant P-Q simultaneous control

Id=I_{A2} to Id=I_{A1}. Figure 1-8 shows that, for a current $I_{A1} \leqq Id \leqq I_{A2}$, the constant power P_A and constant reactive power simultaneous control is possible for $PA_{min} \leqq P_A \leqq PA_{max}$. For a given P_A, a constant reactive power (Q) control is possible for $Q_{A1} \leqq Q \leqq Q_{A2}$.

If a set of active and reactive powers is in the shaded region shown in Fig.1-8, the constant active and reactive power simultaneous control can be performed for a magnet current $I_{A1} \leqq Id \leqq I_{A2}$. We call the shaded region a constant P-Q simultaneous controllable region.

Let's consider how to determine the firing angles for the constant active and reactive powers simultaneous control. From Eq.(1-15) and Eq.(1-16), we define values like powers P_{ro} and Q_{ro}.

$$P_{ro} = Pd + \frac{3(X1+X2)}{\pi} Id^2 \qquad (1-27)$$

$$Q_{ro} = \left\{ \left(\frac{EdoId}{2}\right)^2 - \left(Pd_1 + \frac{3X_1}{\pi} Id^2\right)^2 \right\}^{1/2} + \left\{ \left(\frac{EdoId}{2}\right)^2 - \left(Pd_2 + \frac{3X_2}{\pi} Id^2\right)^2 \right\}^{1/2} \qquad (1-28)$$

When a set of P_{ro} and Q_{ro} are in the simultaneous controllable region of constant active and reactive powers for magnet current Id, voltages of both bridges are given as

$$\frac{Edo}{2}\cos\alpha_1 \quad (\alpha_2) = \frac{P_{ro}}{2Id} + \frac{Q_{ro}}{2Id}\underset{(-)}{\left[\frac{(EdoId)^2}{P_{ro}^2+Q_{ro}^2} - 1\right]^{1/2}} \qquad (1-29)$$

$$: 0^\circ \leqq \alpha_1, \alpha_2 \leqq 150^\circ$$

The first term of the right hand in Eq.(1-29) is given by active power. The second one given by active and reactive powers determines reactive power. If the apparent power derived from P_{ro} and Q_{ro} is less than EdoId, which is an apparent power in $\alpha_1 = \alpha_2$ control, then the term in the bracket is positive. Then an active and reactive power simultaneous control can be done.

Figure 1-9 shows an example of wave forms of magnet voltage, magnet current, active and reactive powers for a constant P-Q simultaneous control. The magnet(inductance of 0.5[H]) is charged and discharged with constant active power $\pm$ 1.0[kW]. The specified reactive power is set to be 4.0[kVar]. During the magnet current Id is between 82[A] and 120[A], the active and reactive power simultaneous control can be done. The terminal voltage of each converter Ed_1 and Ed_2 has different value each other, however, a sum of them is equal to the magnet terminal voltage Ed.

Sinusoidal wave of charging and discharging power and constant reactive power controls.(2),(3)

Quick responsibility is one of the advantages of SMES in power systems. SMES may be controlled to charge and discharge alternatively power with a certain speed. It is necessary to investigate a sinusoidal power and constant reactive power simultaneous control of SMES as a typical case of such a control.

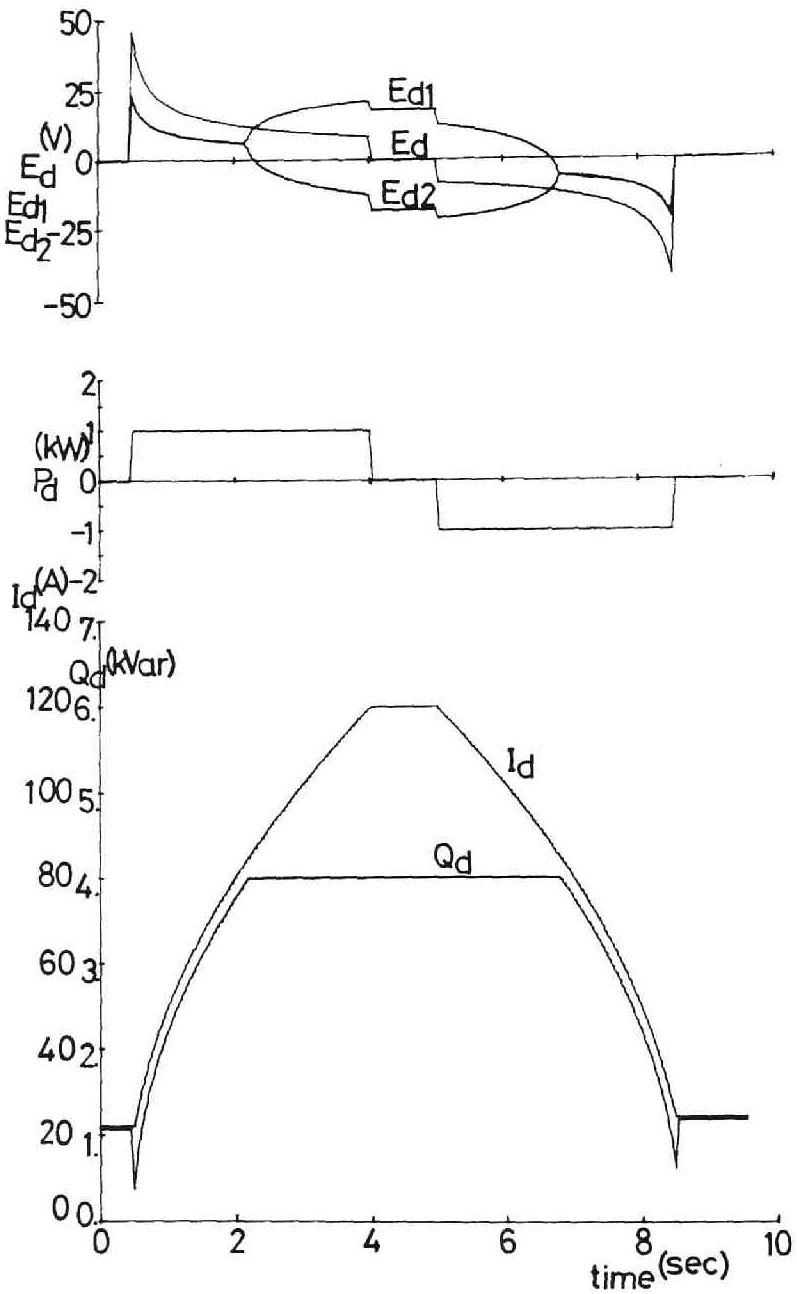

FIg.1-9 Control pattern of constant P-Q simultaneous control

It may be of a basic control where SMES is used for improving the power system stability which is introduced in Background. For the previous step, let us consider only sinusoidal power control of SMES.

A required sinusoidal power Pd is written by frequency f and amplitude of power P_O as

$$Pd=P_O \cdot \cos(2\pi ft) \tag{1-30}$$

Then, the magnet current Id and the magnet terminal voltage Ed are given, respectively, as

$$Id = \left[\frac{P_O}{\pi\ fL} \sin(2\pi ft) + I_O^2 \right]^{1/2} \tag{1-31}$$

$$Ed=Pd/Id$$

$$=P_O\cos(2\pi ft) \left[\frac{P_O}{\pi\ fL} \sin(2\pi ft)+I_O^2 \right]^{-1/2} \tag{1-32}$$

where L ;inductance of magnet

I_O;initial magnet current

In the above relations, the parameters which determine an operating condition are the amplitude P_O, the frequency f of required power and the initial magnet current I_O.

They must satisfy the following two constraints.

(1) The current through the magnet is less than the rating current as

$$0 \leqq Id \leqq Id_{max} \tag{1-33}$$

Then the initial magnet current I_O must satisfy the inequality as

$$\left[\frac{P_o}{\pi\ fL}\right] \leqq I_o \leqq \left[Id_{max}^2 - \frac{P_o}{\pi\ fL}\right]^{1/2} \qquad (1\text{-}34)$$

(2) The firing angles must satisfy the condition $0° \leqq \alpha_1, \alpha_2 \leqq 150°$ for commutation margins, then the voltage Ed across the magnet must satisfy the conditions as

$$-\frac{\sqrt{3}}{2} Edo \leqq Ed \leqq Edo \qquad (1\text{-}35)$$

From Eq.(1-33), the magnet initial current I_o also satisfy the following inequality.

$$I_o^2 \geqq \frac{4P_o^2}{3Edo^2} \cos^2(2\pi ft) - \frac{P_o}{fL\pi} \sin(2\pi ft) \qquad (1\text{-}36)$$

The maximum value of the right hand term of Ineq.(1-36) as a function of time is obtained as

i) for $Po \geqq \frac{3Edo^2}{8fL\pi}$

$$I_o \geqq \left[\frac{4P_o^2}{3Edo^2} + \frac{3}{16}\left(\frac{Edo^2}{fL\pi}\right)\right]^{1/2}$$

$$\text{when } t = \frac{1}{2\pi f} \sin^{-1}\left[-\frac{3}{8}\frac{fL\pi\ Edo^2}{P_o}\right]$$

ii) for $Po < \frac{3Edo^2}{8fL\pi}$

$$I_o \geqq \left[\frac{P_o}{fL\pi}\right]^{1/2} \qquad \text{when } t = \frac{3}{4f} \qquad (1\text{-}37)$$

When a set of (P_O, I_O, f) is in a region determined by Ineq.(1-35) and (1-37), the control of the sinusoidal wave of powers (Eq.(1-30)) can be performed.

For example, a controllable region of the sinusoidal wave of powers are shown on P_O-I_O plane in Fig.1-10 for the frequency f=0.3[Hz], magnet inductance L=0.505[H] and Id_{max}=140[A]. The frequency f=0.3[Hz] of power may be a typical frequency of non-damping power oscillations in power systems.

Here let us consider a simultaneous control for not only sinusoidal active power but also constant reactive power. When the constant reactive power controls are added to the above mentioned control, a reference value of reactive power Qs must satisfy the following conditions.

(3)The apparent power must be less than EdoId. Then, we obtain

$$Q_S \leqq Q_{min} \mid_{\alpha 1=\alpha 2} \qquad \text{i.e. } EdoId-(Pd^2+ Qd^2)\geqq 0 \quad (1\text{-}38)$$

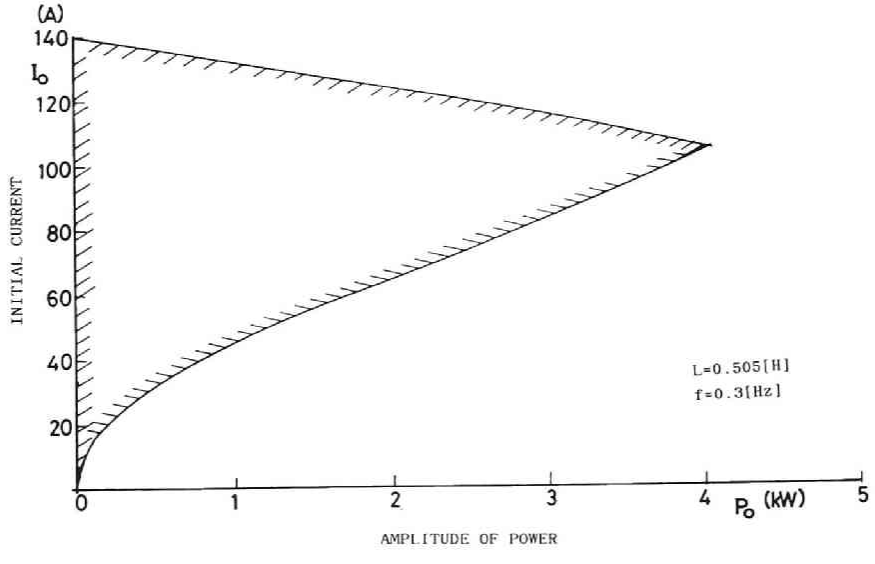

Fig.1-10 Possible region for sinusoidal wave of active power on Po-Io plane (calculated with f=0.3[Hz], L=0.505[H])

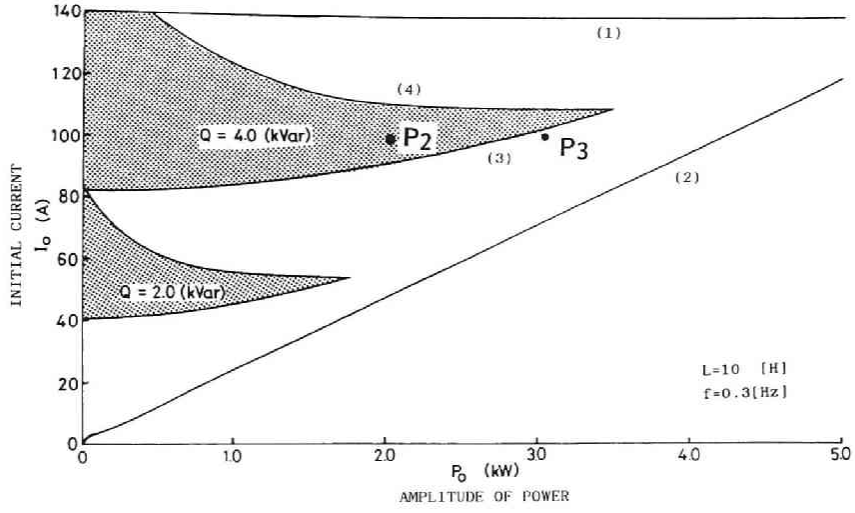

Fig.1-11 Possible region for simultaneous control of sinusoidal active and constant reactive powers on Po-Io plane (calculated with f=0.3[Hz], L=10[H] and Qd=2.0, 4.0[kVar])

where Qmin| $\alpha_1=\alpha_2$ is the minimum reactive power in the controls of $\alpha_1=\alpha_2$.

(4)The firing angles must be between 0° and 150° . Then we obtain

$$Q_S \leqq Q_{max}|\ |\alpha 1=\alpha 2| \rightarrow \max. \qquad (1\text{-}39)$$

$$\text{i.e. } \frac{Edo}{2} \geqq Ed_1 \geqq Ed_2 \geqq -\frac{\sqrt{3}}{4} Edo$$

where Qmax| $|\alpha_1-\alpha_2|$ ->max is the maximum reactive power in the controls of $|\alpha_1-\alpha_2|$ ->max.

The controllable regions of such control on a Po-Io plane are shown as shaded area with reactive power Qd(2.0[kVar] and 4.0[kVar]) in Fig.1-11, where the frequency f is 0.3 Hz. The magnet inductance is 10 H and the maximum current is 140 A.

The examples of Wave forms of voltages, current and powers for the control of sinusoidal wave of active power and constant reactive power are shown in Fig.1-12 and Fig.1-13. A set of (Po,Io,f) is chosen as (2.0[kW],100[A].0.3[Hz]) and (3.0[kW],100[A].0.3[Hz]), respectively. The magnet inductance

L is of 10[H]. The condition is pointed by P_2 and P_3 in Fig.1-11. In Fig.1-12, sinusoidal power and constant reactive power simultaneous control is successfully performed. In Fig.1-13, the active power Pd is controlled to be of sinusoidal wave. However, the condition does not satisfy Ineq.(1-38). Therefore the reactive power Qd can not be kept constant throughout the operation.

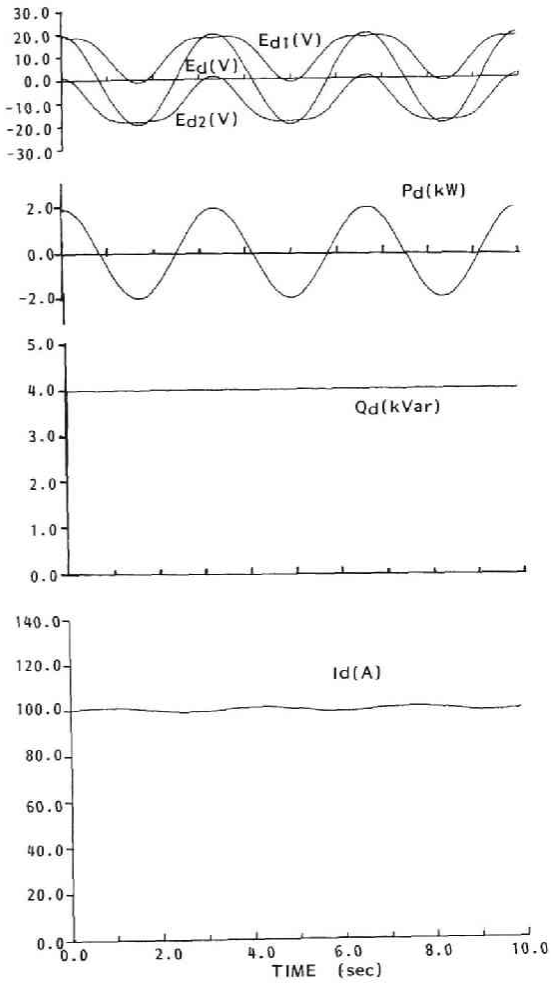

Fig.1-12 Control pattern of sinusoidal active power and constant reactive power P_O = 2.0[kW]

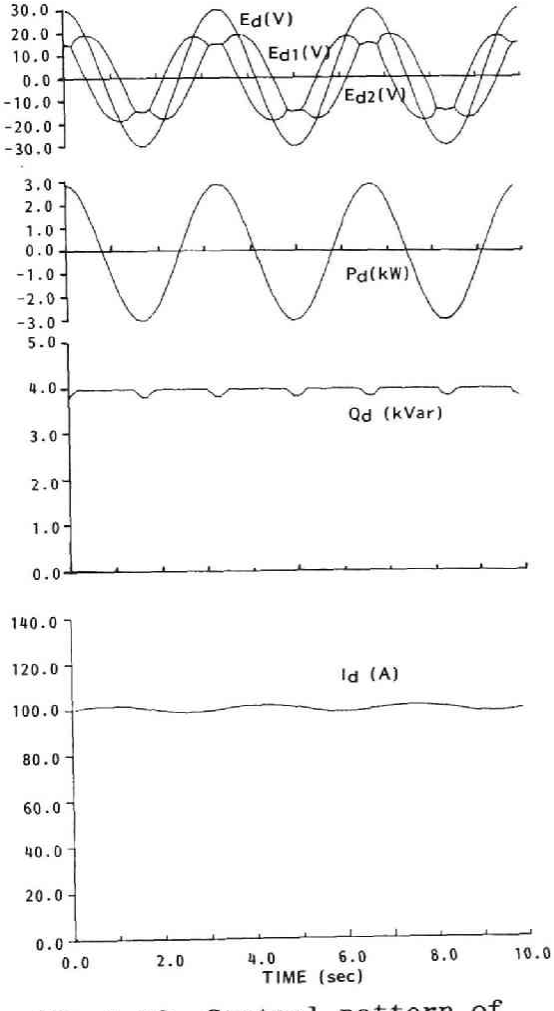

Fig.1-13 Control pattern of sinusoidal active power and constant reactive power P_O = 3.0[kW]

(calculated with f=0.3[Hz], L=10[H] and Qd=4.0 [kVar])

1-5. BASIC DESIGN OF SMES FOR POWER SYSTEM

1-5-1. DESIGN CONCEPT

Main components of SMES system are transformers, converters and superconducting magnet. The important values to be designed are turn ratio of transformers, rated current of magnet (i.e. on-state rated current of thyristors), and inductance of magnet which is related to stored capacity.

The given values are a capacity of power system to which SMES is installed (which is related to capacity of converters and transformers), a maximum charging or discharging power, resistance of circuit of SMES, operating time at the maximum power and total efficiency.

Control schemes of SMES has many variations for utilization. However, when SMES is installed to power systems, a basic control scheme is power control. In power control operation, it is not easy to define efficiency of SMES system uniquely because magnet current and voltage across magnet are varying during the operation. For example, when magnet current is kept constant at its maximum value, active power flowing into SMES is all the losses, which is maximum. The efficiency is considered to be zero.

Then, let us consider a parameter of efficiency. A parameter β which represents a ratio of the losses to the controllable maximum power at a maximum magnet current Id_{max} is introduced.

$$\beta = \frac{Id_{max}^2 \, R}{P_{max}} \qquad (1\text{-}40)$$

Where a symbol R is a total resistance of the circuit through which the magnet current flows.

The ratio of the maximum operating power P_{max} (+:charging, -:discharging) to capacity of transformer may be one of parameters for design of SMES. A parameter γ is defined as

$$\gamma = \frac{P_{max}}{W} \tag{1-41}$$

where W denotes the capacity of the transformer (which is less than the capacity of the power system). For line to line voltage E_2 at low voltage terminal of transformers, an maximum instant power W is given as

$$W = \sqrt{2} E_2 Id_{max} \tag{1-42}$$

On the other hand, a maximum averaging apparent power Pa_{max} is defined as

$$Pa_{max} = (\sqrt{3} E_2)\ (\frac{\sqrt{6}}{\pi} Id_{max}) = EdoId_{max} \tag{1-43}$$

The deference between W and Pa_{max} is

$$\frac{W}{Pa_{max}} = \frac{\pi}{3} \tag{1-44}$$

In order to charge the magnet at P_{max}, the initial current I_o which satisfy the following inequality.

$$P_{max} \leqq EdoI_o \tag{1-45}$$

The maximum charging time T_{max} at the maximum power P_{max} is given by charging the magnet from Io=(P_{max}/Edo) to Id_{max}.

The maximum stored energy W_J can be written as

$$W_J = \frac{1}{2} L Id_{max}^2$$

$$= P_{max} T_{max} + \frac{1}{2} L (\frac{P_{max}}{Edo})^2 \tag{1-46}$$

where L is an inductance of the magnet.

$$L = \frac{2Edo^2(P_{max}T_{max})}{Edo^2Id_{max}^2 - P_{max}^2} \tag{1-47}$$

Finally, Id_{max}, E_2, L and W_J can be written by use of the defined parameters γ and β, and the given parameters P_{max}, T_{max} and R followingly.

$$Id_{max} = \left(\frac{P_{max}\beta}{R}\right)^{1/2} \tag{1-48}$$

$$E_2 = \frac{1}{\sqrt{2}\gamma}\left(\frac{P_{max}R}{\beta}\right)^{1/2} \tag{1-49}$$

$$L = \frac{2\ R\ T_{max}}{\beta\ \left(1-\left(\frac{\pi}{3}\gamma\right)^2\right)} \tag{1-50}$$

$$W_J = \frac{P_{max}T_{max}}{\beta\ \left(1-\left(\frac{\pi}{3}\gamma\right)^2\right)} \tag{1-51}$$

1-5-2.EXAMPLE

By use of the above mentioned design concept, two model type SMES were designed for an artificial transmission systems (capacity : 6[kVA]) used in experiments described in Chap.4 or 5. The conditions are :

a)The maximum power P_{max} is chosen to be a half of the power system capacity.

b)The resistance of thyristors is set to be 0.01(Ω).

c)The efficiency is 95[%].

d)The maximum operating time T_{max} is chosen 1.0[sec] for Magnet-1 and 20.0[sec] for Magnet-2.

P_{max} = 3.0[kW], γ = 0.5, R = 0.01(Ω)
β = 0.05(Efficiency ; 95[%])

	Magnet-1 T_{max} = 1[sec]	Magnet-2 T_{max} = 20[sec]
Id_{max}[A]	122.5	122.5
E_2 [V]	34.6	34.6
L [H]	0.55	11.0
W_J [kJ]	4.13	82.66

From the above designs, the superconducting magnets which are used in the experiments are made.

1-6. CONCLUDING REMARKS

Superconducting Magnetic Energy Storage for an electric power system is introduced and discussed.

In Section 1-2, general considerations on a basic structure of SMES for a power system is discussed. As a result, the main control variables should be powers flow into or out of SMES. For the first step, converters should be of two Graetz bridges in series(12pulses) and consists of normal type thyristors for efficiency and reliability.

In Section 1-3, the terminal characteristics of SMES connected to power systems is discussed. The power characteristics of SMES with single and double bridge converters are studied. By use of power vector diagram, the superiority of

double bridge converters on control of active and reactive powers to single bridge converters is indicated. The effects of leakage reactances of transformers on the power vector diagram are shown.

In Section 1-4, power control scheme of SMES are studied in case of single and double bridge converters. For single bridge converter, constant active power control is discussed, for example. The relations among magnet voltage, magnet current and charging powers are described. For double bridge converters, constant active and reactive powers simultaneous controls are examined. The possible region for such control is obtained. The sinusoidal wave of active and constant reactive powers simultaneous control are also investigated. The possible region for such controls is discussed and obtained.

In Section 1-5, under the consideration in the former Sections, a basic design concept of SMES is introduced. The SMES system was designed, for example, for artificial transmission line system.

CHAPTER.2

EXPERIMENT FOR BASIC CHARACTERISTICS OF SMES[1],[4],[5]

2-1. INTRODUCTION

As is mentioned in Chapter 1, the characteristics of SMES is quite different from other conventional power system apparatus. That is,

a)SMES is consist of a large magnet with little loss.

b)SMES behaves as a large current source in power systems.

c)SMES behaves as a controllable load and, at the same time, a quick response generator without inertia.

Therefore it is necessary to investigate characteristics of SMES in power systems experimentally in order to reveal problems on operating SMES and utilities of SMES in power systems.

When we study interaction between SMES and power systems, it is significant problems where SMES is installed and what capacity of SMES is needed in a certain power system. In this chapter, before investigating power system characteristics of SMES, we consider that SMES is connected to a bus of large capacity.

In order to approach the problems experimentally, model SMES system for an artificial transmission line system(6[kVA], 220[V] base) was designed and made. Superconducting magnets were made for the artificial transmission line system in accordance with the designed parameters mentioned in Section 1-5-2. It is a basic concept to design SMES for a certain power system. A control equipment to control active power and/or reactive power of SMES was also designed and made.

Before studying power system characteristics of SMES, it is necessary to investigate fundamental characteristics of exchanging powers between a superconducting magnet and an infinite bus (power source) by use of the model SMES system experimentally.

characteristics of exchanging powers between a superconducting magnet and an infinite bus (power source) by use of the model SMES system experimentally.

In Section 2-2, model SMES system for the artificial transmission line system is introduced and described.

In Section 2-3, basic tests for fundamental characteristics of SMES are written.

In Section 2-4, fundamental characteristics of SMES is studied by use of computer simulation. A controller was designed and made from the simulation results.

2-2. EXPERIMENTAL SYSTEM

A schema of the experimental system is shown in Fig.2-1. A small superconducting magnet is connected to the commercial three phase power source (voltage 220[V] :assumed as an infinite bus) through two transformers and thyristor bridge converters. Here Superconducting magnets, converters(transformers) and controller designed for the power system(6[kVA],220[V]) are described.

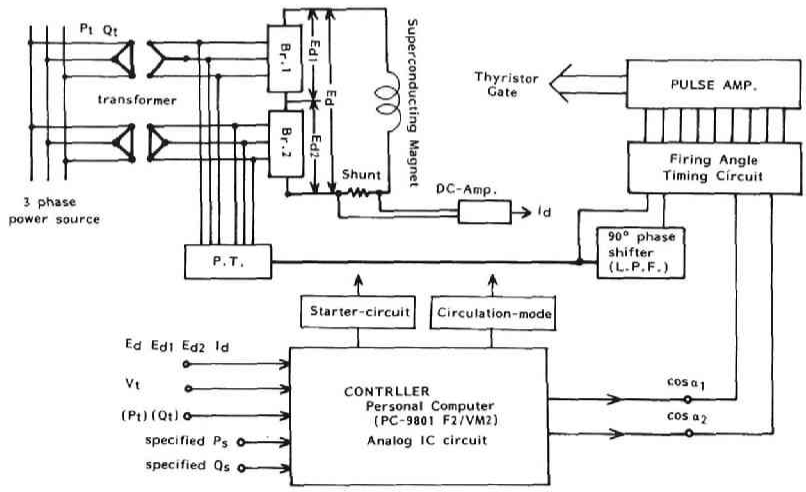

Fig.2-1 Schema of experimental system

2-2-1. SUPERCONDUCTING MAGNET

Two superconducting magnets were designed and made for the experiment. Specifications of these magnets are shown in Table 2-1. Structural drawings are shown in Fig.2-2. Both are fabricated with multi-filament Nb-Ti twisted wire. The smaller one is of inductance 0.505[H], rated current 125[A] and stored energy 3.95[kJ]. The magnet can be charged for 1[sec] at active power 3[kW] (half of power system capacity). It is

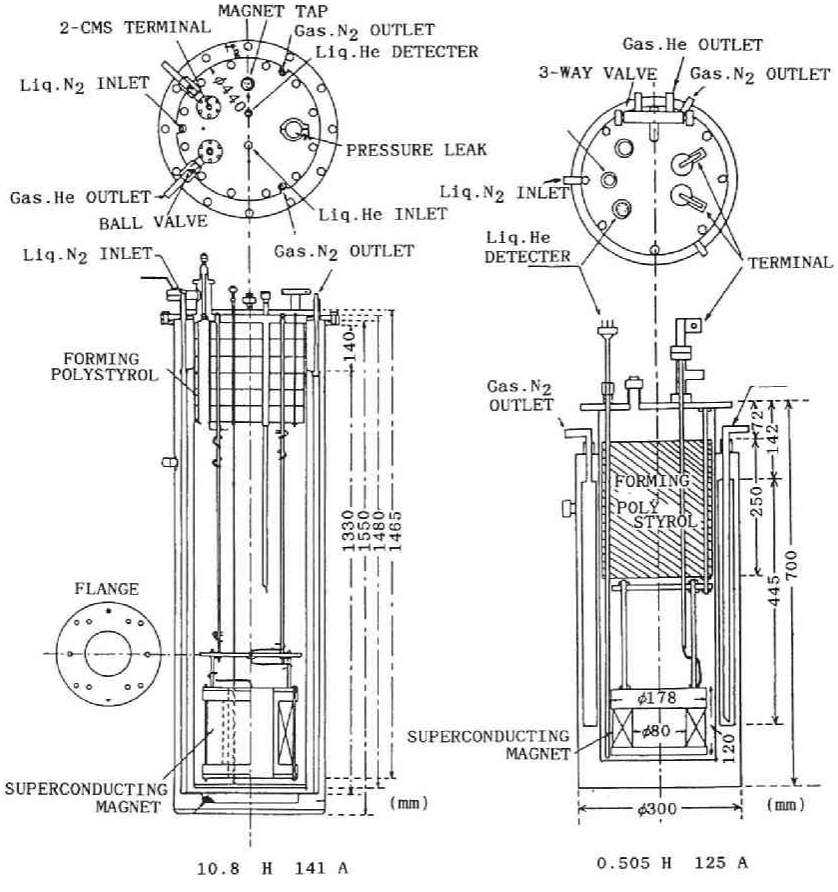

Fig.2-2 Superconducting magnet and cryostat

corresponding to the characteristic frequency (about 0.7[Hz]) of swing of generator of the experimental system. The larger one is of inductance 10.8[H], rated current 141[A] and stored energy 107[kJ]. The charging time is 20 times of that of the smaller one.

Table 2-1 Specification of superconducting magnets

	Magnet-1	Magnet-2
Performance:		
effective inner diameter	80mm	140mm
rated magnetic field at center	2.3T	5.5T
rated current	125A	141A
mag. field constant	0.01881T/A	0.03907T/A
inductance	0.505H	10.8H
rated stored energy	3.95kJ	107kJ
Structure:		
wire	Nb-Ti square 0.65x1.035	
dimensions of coil		
inner diameter	99.87	174.05
outer diameter	167.32	258.6
height	69.77	199.8
turn	2218	9091
layer	36	65

The magnet is immersed deep enough in liquid helium bath in order to keep low temperature for maintaining superconductivity of the magnet. It is suspended in the cryostat (as shown in Fig.2-2) which is made of stainless-steel to insulate thermally from outside. The cryostat has four layers, that is, from outside, vacuum space, Liq.N_2 space and then vacuum space and Liq.He bath. Foaming polystyrol is set in the upper space of

the Liq.He bath as a heat insulator to keep thermal gradient. The superconducting magnet is lead to terminals on the top of the cryostat. The wire between the terminals and the magnet in liquid helium is called "power-lead". The power-lead do not have superconductivity. The characteristics of power-lead affect the control of SMES.

The main difference of these two cryostats is design of Gas.He outlet. The smaller cryostat have two Gas.He paths, that is, main Gas.He outlet and sub-outlet for power-lead cooling. Almost all the evaporated He-gas is recovered through the main Gas.He outlet. Therefore the power-leads can not be cooled down sufficiently. On the other hand, the larger one has Gas.He outlet along the power-lead through which all the evaporated He-gas is used for cooling the power-lead and then recovered. Power-lead losses are reduced compared with the former design. Since the total losses of the superconducting magnet is quite small, the losses of power-lead become to be problem on performance of controller of SMES. Because it depends on the thermal condition in Liq.He bath, it varies during operation of SMES. It is experimentally confirmed as described in section 2-2-4.

2-2-2. CONVERTER

Transformers and AC-DC converters are designed and made in order to connect the superconducting magnet to AC power system. The specifications of the transformers and the thyristorized converter are shown in Table 2-2. The three-phase Graetz connection thyristorized bridges which are connected in series(double-bridge) are chosen as an AC-DC converter.

Thyristors of normal type are chosen as valves of converters mainly because superconducting magnet is operated similar to a large scale current source so that open-circuit is one of the most dangerous accident. The natural commutation is considered to be better for safety than forced commutation.

A rated capacity of the transformer and the converter is decided to be 6[kVA] equal to rated capacity of the artificial transmission line system. One is of D-Y connection and another one is of D-D connection. In order to eliminate harmonics of the 3rd order, delta connection of transformer is necessary.

Table 2-2 Specification of transformer and thyristor.

TRANSFORMER:	
Rated Capacity	6kVA
Turn ratio	220V/(18V,36V)
Connection	D-D, D-Y
THYRISTOR:	
Inverse voltage	400V
Off-state voltage	400V
Average current	500A

2-2-3. CONTROLLER

By use of the above experimental apparatus, in order to control powers flowing into or out of the superconducting magnet according to the control scheme as described in Section 1-4, controller is designed and made.

Block diagram for P-Q simultaneous control

Figure 2-3 shows the block diagram of controller used in experiments. It is designed based on the active and reactive power control described in Section 1-4. By only integral based control, rising and overshoots of SMES's power appear in our experimental results which may be due to the time delay of

controller. They are mainly due to the converter voltage drop. It is considered that they can be reduced by control considering the compensations of the converter voltage drops.

The characteristics of the voltage drop can be obtained by loss-test as described in Section 2-3-4. It has non-linear characteristics for the magnet current. While it is estimated, on the whole, by tests of transformer and technical data of thyristors. Results of the estimation almost agree with those obtained by loss-test.

Therefore we can design a controller considering compensation of the voltage drops without loss-test. The voltage drops are assumed to be approximately expressed by sum of a constant term (E_{th}) and a term proportional to magnet current ($Z \cdot Id$). Constants Eth and Z can be determined by the estimated characteristics of the voltage drops.(see Sec.2-3-4) Experimental results show that performance of the power control is improved by the compensator.

The reference signals of active and reactive powers (Pr,Qr) are given by use of specified powers (Ps,Qs) in accordance with the block diagram of the controller as shown in Fig.2-3.

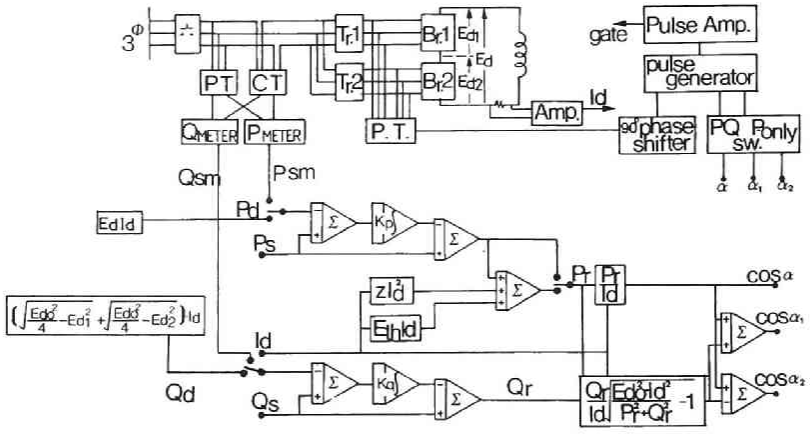

Fig.2-3 Block diagram of P-Q simultaneous control

$$Pr=Ps+K_{pp}(Ps-Pd)+K_{ip}\int (Ps-Pd)+ZId^2+E_{th}Id \qquad (2\text{-}1)$$

$$Qr=Qs+K_{pq}(Qs-Qd)+K_{iq}\int (Qs-Qd) \qquad (2\text{-}2)$$

Kpp:proportional gain for active power
Kip:integral gain for active power
Kpq:proportional gain for reactive power
Kiq:integral gain for active power

The control performance is discussed by use of experiments and simulation studies described in Section 2-3 and Section 2-5, respectively.

When a set of Pr and Qr is in the controllable region described in Section 1-4, the voltages across each converter is set by

$$\cos\alpha_1 \atop (\alpha_2) = \frac{P_{ro}}{EdoId} + \frac{Q_{ro}}{EdoId_{(-)}}\left[\frac{(EdoId)^2}{P_{ro}^2+Q_{ro}^2}-1\right]^{1/2} \qquad (2\text{-}3)$$

$$: 0^\circ \leqq \alpha_1, \alpha_2 \leqq 150^\circ$$

which determine the firing angles of the converters.

Control equipment

Control equipments is designed and made to achieve the above control. It is divided into four major parts;

1]Setting or Changing the operating conditions, that is; the specified powers Ps, Qs, the region of operating magnet current Idmin, Idmax, the control gains, the operating mode(only-P, P-Q simultaneous, Id-hold, Start, Emergency discharge) and so on.

2]Detecting the signals from the system, that is; powers Pt, Qt of SMES, the terminal voltage of the converters Ed(Ed_1,Ed_2), the magnet current Id.

3]Main controller; The firing angles α_1, α_2 are calculated according to Eq.(2-1),(2-2) and (2-3) using the detected data.

4]Firing pulse generator; The firing pulses are generated with delay time corresponding to the α_1 and α_2. The control circuit and converters are insulated each other by the photo-couplers.

We made two controllers;one is composed of analogue ICs and another is of a personal computer. The flow chart of the controller is shown in Fig.2-4.

2-3. BASIC EXPERIMENT FOR POWER CHARGING AND DISCHARGING OF SMES[19],[20]

First of all, the superconducting magnet should be cooled down to have and keep superconductivity by Liq.N_2 and Liq.He. Then the converters start up and the magnet is charged to a certain current by use of a starter circuit mentioned in Section 2-3-2. The magnet current is maintained by the controller. Circulation mode which means isolation of magnet and power systems is discussed and tested. Loss test was carried out and discuss how to compensate the losses in Section 2-3-4. Power charging and discharging tests are shown in Section 2-3-5. Constant active and reactive power simultaneous control tests were done. Sinusoidal active and constant reactive power simultaneous control tests were also performed in accordance with the control schemes described in Section 1-4.

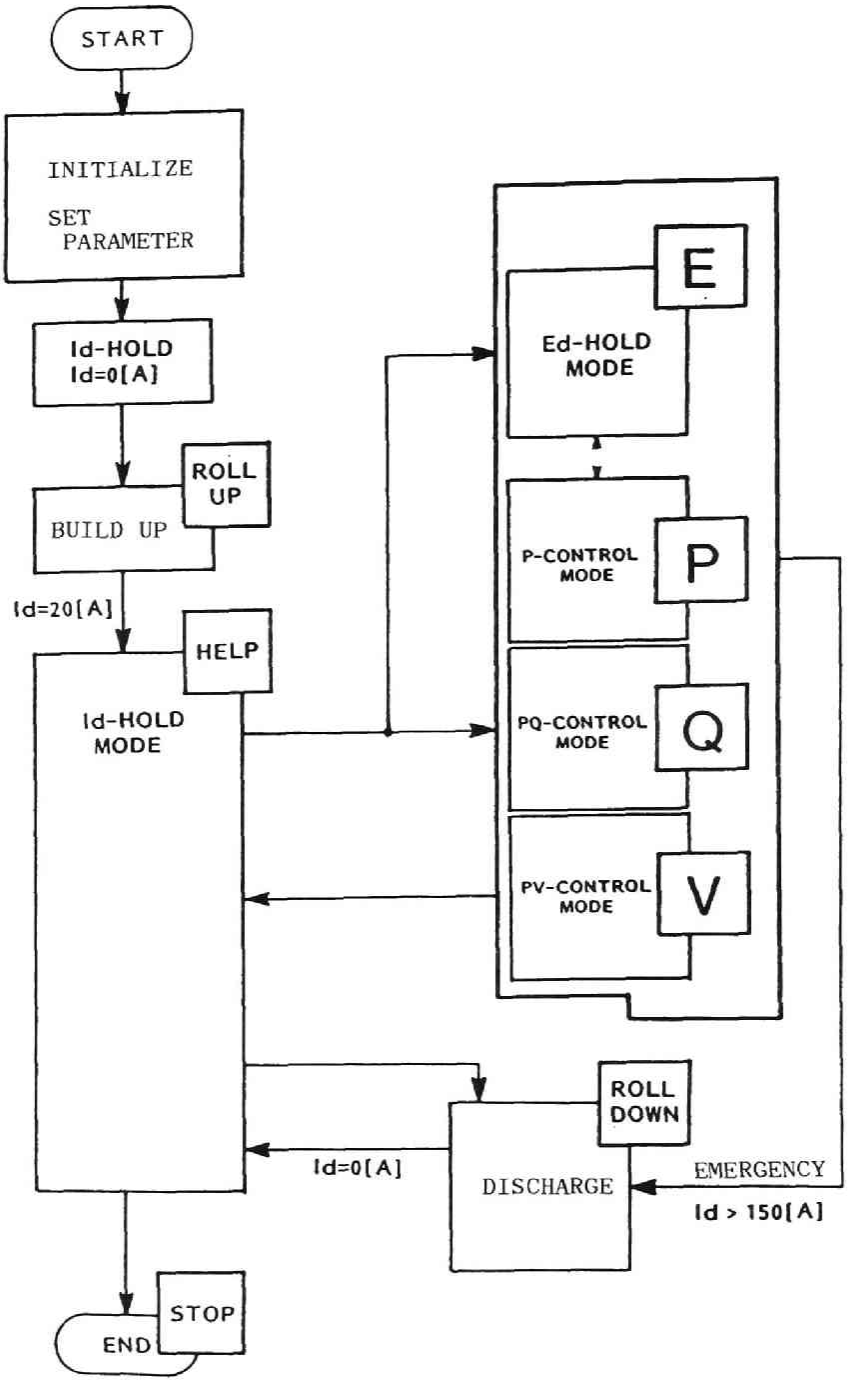

Fig.2-4 Flow chart for controller

2-3-1. PROCEDURE

The superconducting magnet is pre-cooled by liquid Nitrogen(Liq.N_2) a few days before experiment starts. After Liq.N_2 is purged out by gas helium(Gas-He), Liq-He is transferred from the Liq-He vessel to the cryostat for the superconducting magnet. During the operation, Liq-He is continuously supplied to keep the superconductivity of the magnet.

2-3-2. Starter Circuit

A current through magnet is made to rise from 0[A] by giving trigger pulses to all thyristors of the converter. The magnet current, however, may not become greater than latching current of thyristors while the trigger pulses are given. Then thyristors are not turned on. It may occur when inductance of a magnet is large and rated current of converter thyristor are large. SMES is the exact case. Because of the above reason, converter did not start in the first experiment. It is necessary to discuss how to build up the magnet current.

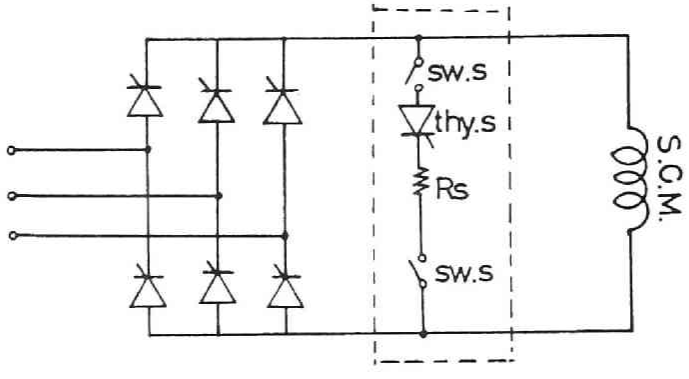

Fig.2-5 Starter-circuit

A method to turn on converters is to give wider pulses to thyristors initially so that a current through thyristors exceeds the latching current while the firing pulses served. However, pulse amplifiers for the method must be large.

Here, a simple method for turning on converters when a load has large inductance and less resistance is proposed. Fig.2-5 shows a circuit to turn on the converter (which is called a starter-circuit). Single bridge converter is used for discussions and tests. The starter-circuit is composed of a small thyristor(Thy.s), a resistor(Rs) and switches(Sw.s).

The procedure to build up the magnet current by use of the starter-circuit is described as follows. Constant-power-charging operation mode of the controller is chosen. The switches are closed and the trigger pulses are served to all thyristors of the converters and the small thyristor of the starter-circuit.

At first, the starter circuit current I_{stt} flows through the resistor R_S. The converter starts up easily. As the terminal voltage Ed of the magnet is positive ($=I_{stt} \cdot R_S$), the magnet current Id become larger and larger gradually ($Id=[1/L]\int Ed\,dt$). Since the charging power is controlled to be constant, the terminal voltage of the magnet becomes smaller (firing angle is getting larger) as the magnet current increases. At the moment that instantaneous voltage is zero (that is, firing angle is nearly equal to $\pi/3$), the current I_{stt} flowing through Thy.s becomes zero and Thy.s turns off. Before this moment, the magnet current becomes larger than the latching current of converter thyristors so that the converter does not turn off. Then switches(Sw.s) are opened. The procedure of the starter-circuit ends.

Let us consider how to decide values of each elements. The resistor R_S and the small thyristor Thy.s must be chosen to keep converter thyristors on-state after firing pulses served. The current I_{stt} is, at the beginning, equal to E/R_S (E is a little smaller than Edo:maximum terminal voltage at no-load). The resistor R_S is chosen such that E/R_S can be greater than a

latching current (I_{lat}) of converter thyristors. A rated on-state current of Thy.s should be larger than I_{lat}.

A work time T_s of the starter-circuit is obtained as follows. Superconducting magnet and starter-circuit are excited by the maximum voltage(Edo: α =0) for a certain time since the first firing pulses are given to converter thyristors. Then power control comes into operation and the firing angle increases up to π /3. Here T_1 denotes the time while the angle α is 0, that is, the time before the constant power control become possible. T_2 denotes the time during α vary from 0 to π /3, that is, instantaneous voltage becomes zero in the constant power control.

During the first stage, the magnet is charged as

$$Id = \frac{Edo}{L} t \qquad (2\text{-}4)$$

where L is the inductance of the magnet. At the time T_1, the magnet current Id is reached Id1.

$$Id_1 = \frac{Ps}{Edo} = \frac{Edo}{L} T_1 \qquad (2\text{-}5)$$

Where Ps denotes a specified power for constant power control. Therefore the T_1 can be given as

$$T_1 = \frac{LPs}{Edo^2} \qquad (2\text{-}6)$$

After the power control comes into operation, the voltage across the magnet Ed changed with time as (obtained from Eq.(1-21))

$$Ed = \left\{ \frac{2}{PsL} t + \left(\frac{1}{Edo} \right)^2 \right\}^{-1/2} \qquad (2\text{-}7)$$

At the time when the firing angle is $\pi/3$, the voltage Ed is equal to Edo/2. Therefore the time T_2 is obtained as follows.

$$T_2 = \frac{3}{2} \frac{LPs}{Edo^2} \qquad (2\text{-}8)$$

The time T_S for the specified reference power Ps is given as

$$T_S = T_1 + T_2 = \frac{5LPs}{2Edo^2} \qquad (2\text{-}9)$$

We carried out tests of the starter circuit. Rated current of each converter-thyristor we used is 500[A] and latching current may be less than 1[A].(which is not found in the technical data) Therefore the small thyristor(Thy.s) whose rated current is of 3[A] is chosen. The resistor R_S is of 50[Ω] since the maximum voltage across the converter is about 49[V].

Figure 2-6 shows one of the test results of the starter-circuit. Current through the starter-circuit(I_{stt}) is recorded by photo-recorder. Specified power Ps is 100[W]. Inductance of the magnet is 0.505[H]. At first, the current I_{stt} is almost 1[A] and then is gradually shunted to the superconducting magnet. About 51[msec] later, firing angle α is reached $\pi/3$, the small thyristor(Thy.s) is turned off.

The working time T_S of the starter-circuit is calculated to be 53[msec] using Eq.(2-9). The experimental value T_S=51[msec] is almost agree with calculated one.

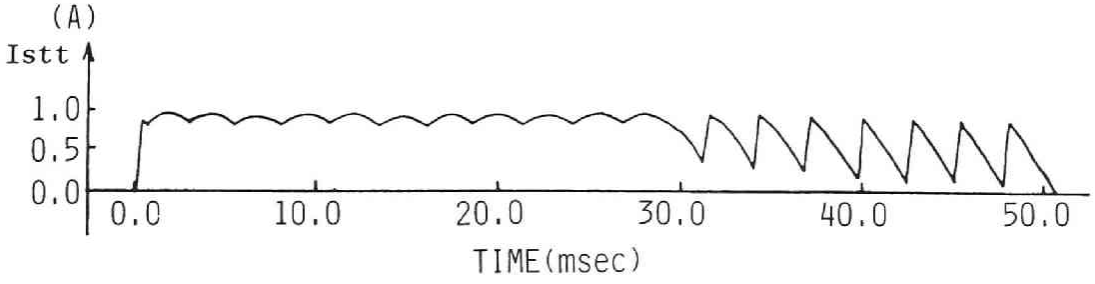

Fig.2-6 Instantaneous current I_{stt} through Starter-Circuit with specified power Ps is 100[W].
(:magnet inductance L=0.505[H])

However, the current through the starter-circuit leads to heat loss. It cannot be neglected for a large scale SMES. In order to reduce the heat loss, the working time T_s is the smaller, the better. The minimum starting time T_{min} can be obtained as follows. T_{min} can be given on conditions that the magnet current is larger than the latching current of the thyristors(I_{lat}) and the magnet voltage is $Ed=Edo\cdot\cos(\pi/3) = Edo/2$ at the end of the starting operation. Therefore reference power for the minimum starting time is

$$P_{so} = EdoI_{lat}/2 \qquad (2\text{-}10)$$

When a magnet is charged at a constant power (P_{so}), the magnet current Id changes in accordance with following equations.

$$\left.\begin{aligned} &\text{i)}\quad Id = \frac{Edo}{L}t && (0 \leqq t \leqq T_1)\\ &\text{ii)}\quad Id = \left[\frac{2Pso}{L}t + Ido^2\right] && (T_1 < t \leqq T_2) \end{aligned}\right\} \qquad (2\text{-}11)$$

where $Ido = Ps/Edo = EdoT_1/L = I_{lat}/2$

The magnet current Id reached the current I_{lat} at the time T_2.

$$T_2 = \frac{L}{2Pso}\left(I_{lat}^2 - Ido^2\right)$$

$$= \frac{3}{4}\frac{LI_{lat}}{Edo} \qquad (2\text{-}12)$$

Then T_{min} is written as

$$T_{min}=T_1+T_2 = \frac{5}{4}\frac{LI_{lat}}{Edo^2} \qquad (2\text{-}13)$$

2-3-3. CIRCULATION MODE

Magnet current flows also through converters and transformers even when the magnet need not to be charged or discharged. The circuit has heat loss by the magnet current. A circuit to short the superconducting magnet is necessary to maintain stored energy without loss or with a little loss. (Circulation Mode)

To short the magnet means isolation of the magnet from power systems. It is useful for safety of superconducting magnet at faults in power systems.

Some study and experimental data are reported on circulation mode, for example, by use of superconducting thermal switch.

In this section, circulation mode by use of a thyristor is studied. A flow-chart for Circulation mode is shown in Fig.2-7. Because of using a thyristor(Thy.C) to short magnet, it cannot be turned on at an arbitrary time. Instantaneous terminal voltage of magnet must be below zero for turning on Thy.C. Therefore when Circulation mode switch is turned on, the control mode is changed

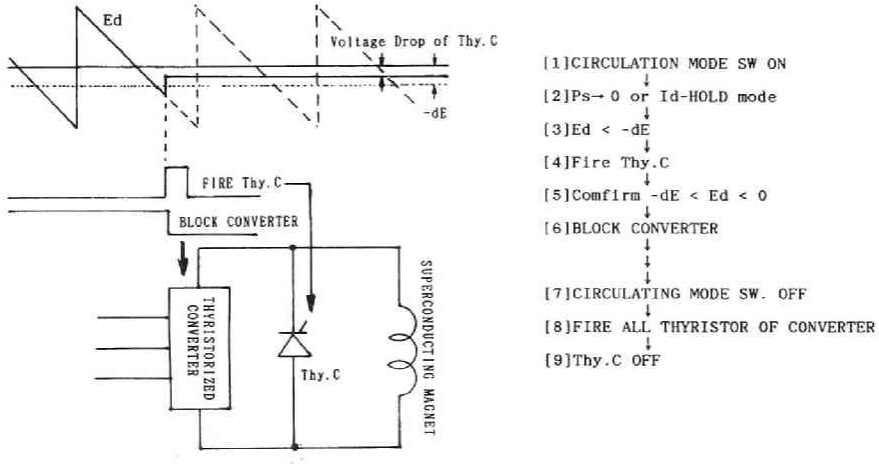

Fig.2-7 Flow chart for Circulation-mode by use of thyristor

to an active power zero control mode or an Id-HOLD control mode so that the magnet voltage has a negative value. A triangular wave in Fig.2-7 shows the magnet voltage Ed at the control. When Ed is smaller than a certain negative value -dE which is set to be larger than a voltage drop of Thy.C in absolute value, a firing pulse is served to thyristor Thy.C. If Thy.C turned on, magnet voltage Ed is between -dE and zero. After confirming that, a converter is blocked. Superconducting magnet is isolated from power systems. In order to return the normal operation mode, all the thyristors of converter are fired on. Then thyristor Thy.C has a inverse voltage and turned off. The Circulation mode ends.

One of experimental results is shown in Fig.2-8. On the way of charging operation with Ps=500[W], the magnet is shorted by the thyristor at Id=51.8[A]. During Circulation mode, the power Pd and the voltage Ed are constant to be a little below zero due to the voltage drop of the thyristor. Therefore the current Id decreases with time, the magnet is re-connected to power system at Id =29.8[A] and back to constant power charging mode. Circulation mode operation was successfully performed.

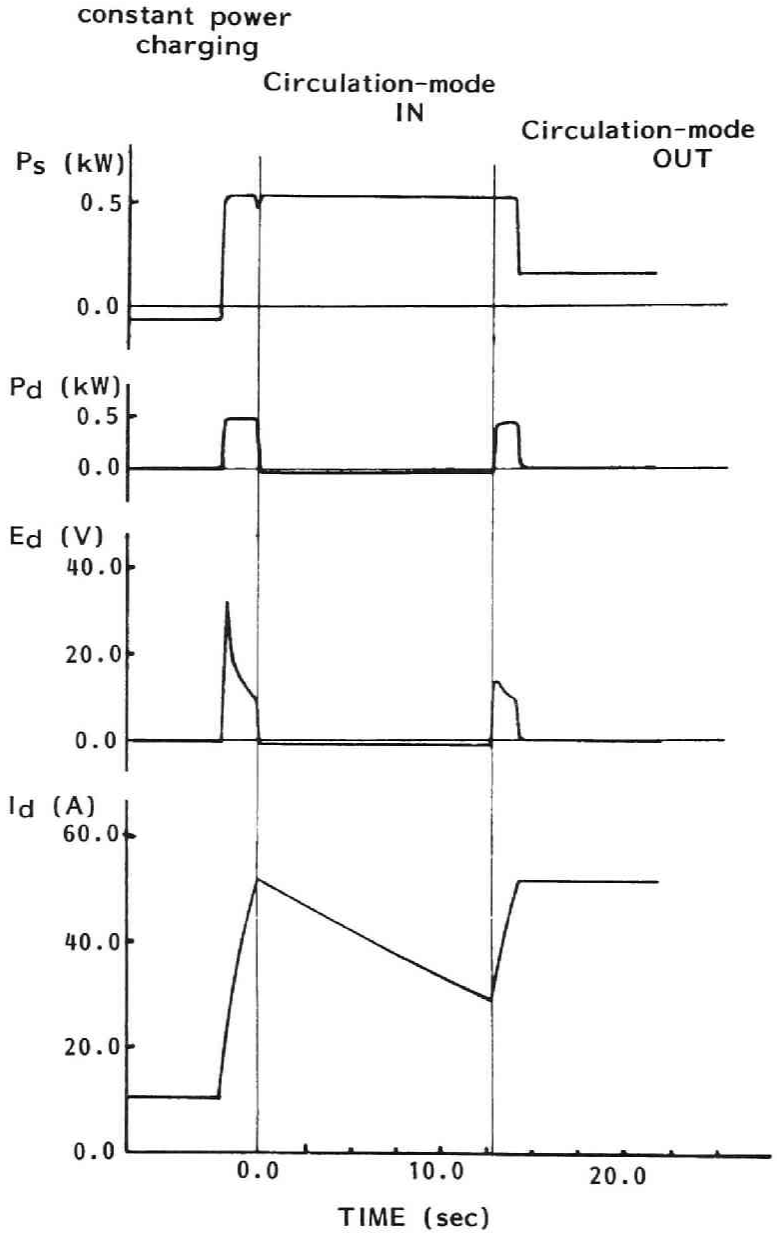

Fig.2-8 Test result of Circulation-mode

2-3-4. LOSS ESTIMATION AND COMPENSATION

In order to design the controller of SMES, losses of SMES circuit were estimated and experimentally measured.

Magnet current circulate also through the power-lead, thyristors and transformers. Resistance of the circuit leads to losses. Voltage drop of the magnet is also caused by leakage reactances of the transformers. Among these components, resistance and leakage reactances of transformers can be obtained from test results and voltage drop of thyristor is given in technical data.

The leakage reactances X_1, X_2 and the resistance R_1, R_2 per phase of the transformers (1:trans.1[D-Y connection], 2:trans.2 [D-D connection]) are measured as

Trans.1(D-Y)	X1 = 1.49[mΩ]	R1 = 0.70[mΩ]
Trans.2(D-D)	X2 = 1.50[mΩ]	R2 = 0.73[mΩ]

at the low-voltage terminal.

Therefore the total resistance R_{th} of the transformers is given as

$$R_{th}= \frac{3}{\pi}(X_1+X_2) + 2(R_1+R_2) \qquad (2\text{-}14)$$

which is considered to be of a resistance 5.72[mΩ]. The voltage drop E_{drop} of the whole circuit is estimated as

$$E_{drop}(Id)=4E_{thy}(Id) + R_{th}Id \qquad (2\text{-}15)$$

Figure 2-9 shows the voltage drop E_{drop} as a function of Id. E_{drop} is given by use of technical data of the thyristor ($E_{thy}(Id)$) and the above test data (R_{th}) of the transformers.

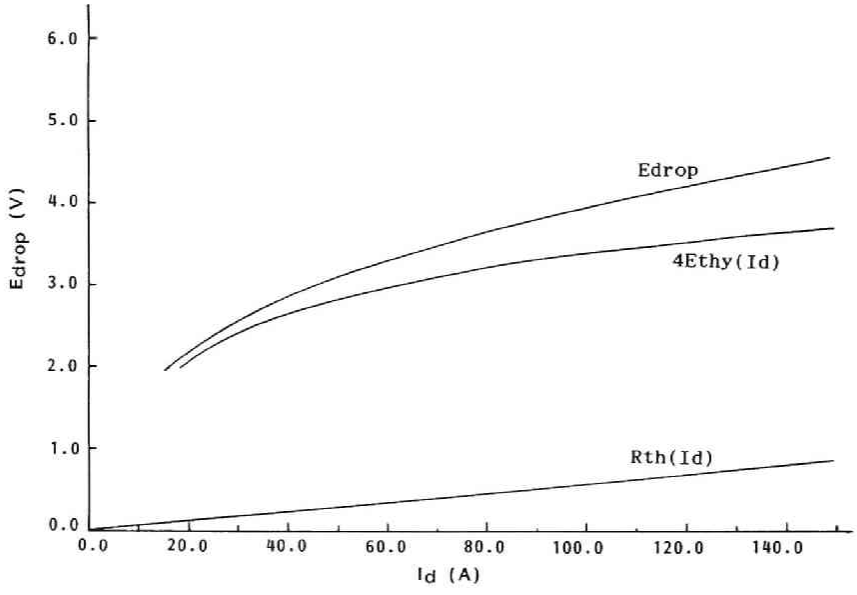

Fig.2-9 E_{drop} as a function of magnet current Id
:E_{drop}= $4E_{thy}(Id) + R_{th}Id$
;given by test result of transformer and technical data of thyristor

A loss-test of SMES is performed as described below. Only the constant positive signal Ps is put into the controller without feedback control, that is, the open-loop control. The thyristors are fired with delay angle α given by

$$Edo \cos\alpha = \frac{Ps}{Id} \qquad (2\text{-}16)$$

However, the magnet voltage Ed is reduced by $E_{dr}(Id)$.

$$Ed = Edo \cos\alpha - E_{dr}(Id) \qquad (2\text{-}17)$$

When the voltage Ed is positive, the current Id increases and the voltage $E_{dr}(Id)$ also increases. The voltage Ed reduced to be

zero. When the voltage Ed is negative, the current Id decreases and the voltage $E_{dr}(Id)$ also decreases. Then Ed increases to be zero.

Therefore after a sufficient time, Eq.(2-18) should hold.

$$Pd = EdId = Ps - E_{dr}(Id)Id = 0 \qquad (2\text{-}18)$$

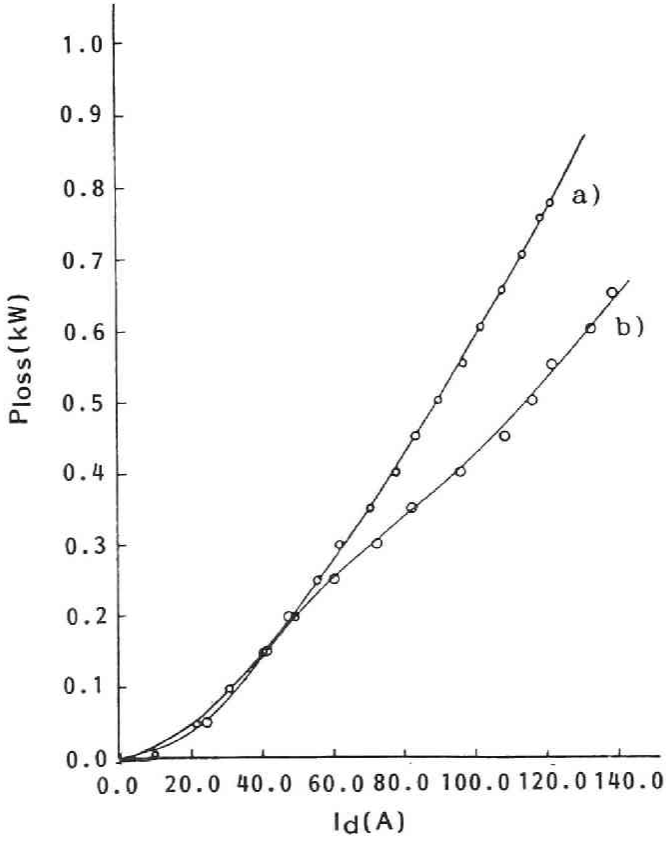

Fig.2-10 Loss of SMES as a function of Id :(P_{loss}-Id)
a) MAGNET-1 : L=0.505[H]
b) MAGNET-2 : L=10.8[H]

Magnet current becomes to be kept constant at Id which satisfy the above equation. The loss of SMES (E_{dr}(Id)Id) at the magnet current Id equal to the specified power Ps .

By changing Ps, loss characteristics (P_{loss}-Id) are obtained as shown in Fig.2-10. The voltage drop E_{dr} is also obtained as shown in Fig.2-11. The dotted line indicates E_{drop}(Id) estimated before. The difference between E_{dr} and E_{drop} means the voltage drop due to the power-lead resistance which is indicated by one-point chain line.

In the cryostat for magnet-2, vapored Gas-He is recovered through pipes along the power-leads in order to cool down it. Therefore the power-lead loss does not become large as the magnet current Id increases.

Control parameters E_{th} and Z are determined by the results of the loss test as shown in Fig.2-12 for magnet-1 and magnet-2, respectively. The characteristics of the power control are improved by the voltage drop compensator using the parameters in experiments. The same discussions are done for SMES of single bridge converter. The test results are shown in Fig.2-16 and Fig.2-17.(see Section 2-3-5)

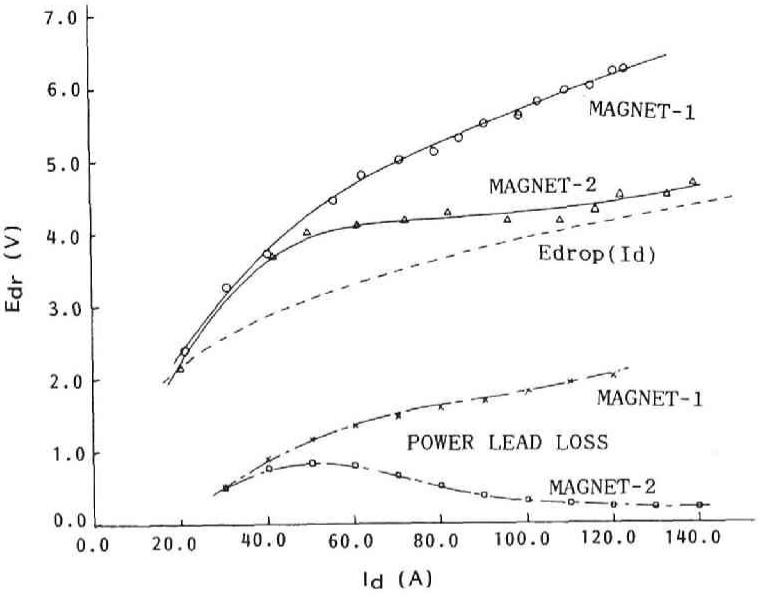

Fig.2-11 Voltage drop E_{dr} given by P_{loss}
dotted line : $E_{drop}(Id)$
one-point chain line : power-lead loss
MAGNET-1 : 0.505[H] MAGNET-2 : 10.8[H]

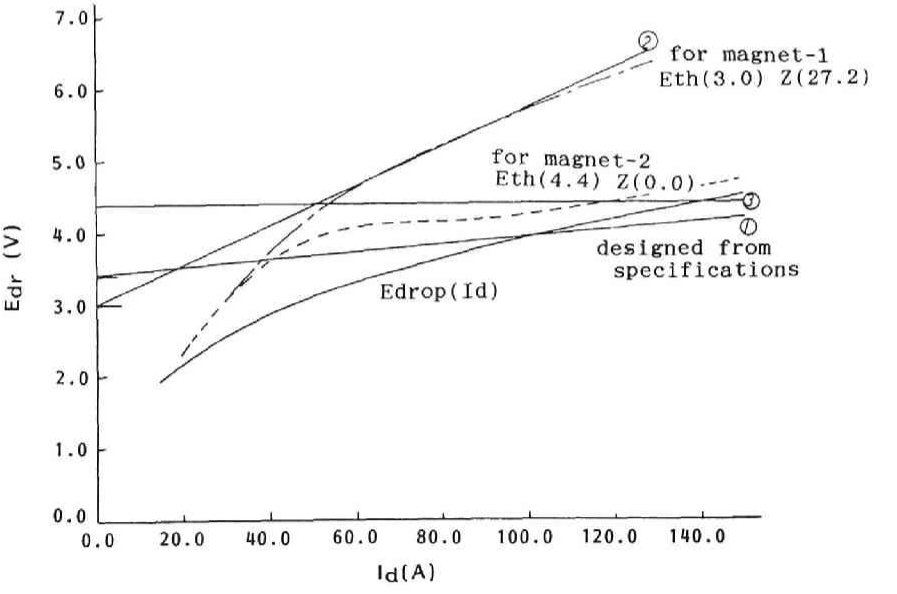

Fig.2-12 Parameters E_{th} and Z of voltage drop compensator

2-3-5. CHARGING AND DISCHARGING CONTROL

In this section, powers to be controlled are given by DC currents and voltages measured at the terminal of SMES, in order to investigate fundamental characteristics of SMES.

In constant active power control, magnet voltage and magnet current vary with time. Therefore, SMES system is not in steady state in power control. It is not easy to obtain optimum power control. For the first step, experiments for only constant active power control are performed. The purposes of the experiments are;

1]to investigate the characteristics of superconducting magnet.

2]to study the power control of SMES.

Simulation studies for the above purposes are also done. (see Chap.2-4.) The superconducting magnets (inductance L=0.505[H] and 10.8[H]) are charged or discharged with magnet current Id between (Ps/Edo) and Id_{rate} for specified power Ps up to 4[kW].

Figure 2-13 and 2-14 show the experimental results of constant active power control by integral-control with gain K_{ip}=1 and 10, respectively.(see Eq.(2-1) and Eq.(2-2)) They are recorded by pen recorders. An integral of power error (Ps-Pd), that is, error energy is denoted by C_p. The active power control is improved by choosing proper integral gain K_{ip}. The rising of the power has overshoot in discharging mode. It may be due to time delay of integral control.

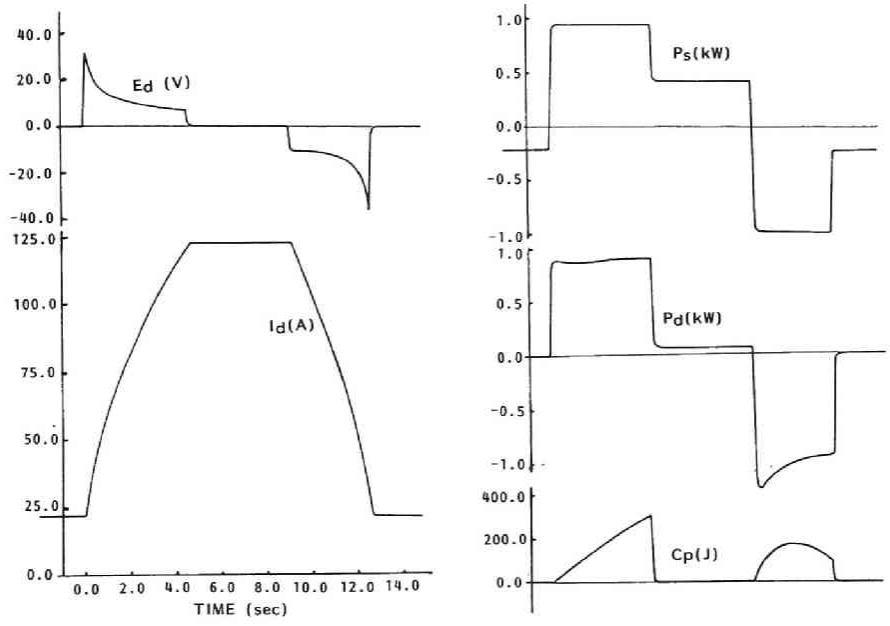

Fig.2-13 Test result of constant active power control by I-control with integral gain K_{ip} is 1.

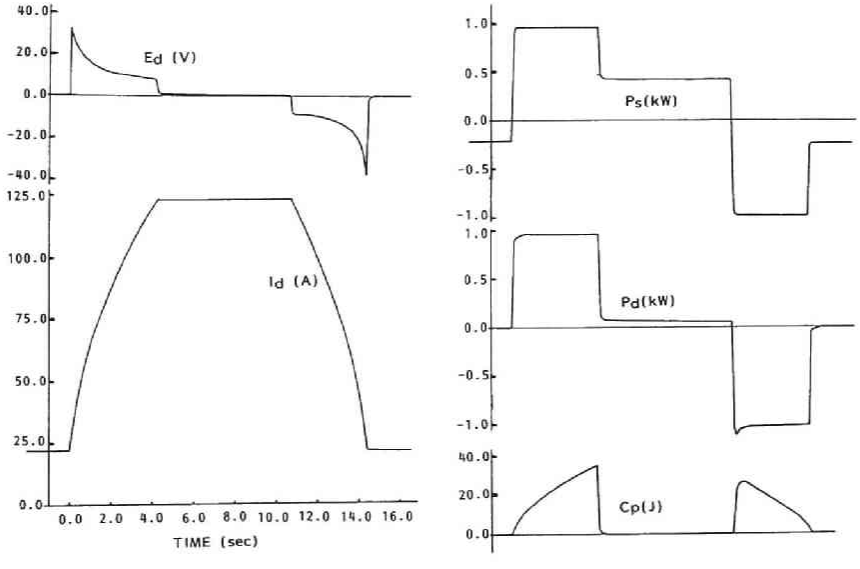

Fig.2-14 Test result of constant active power control by I-control with integral gain K_{ip} is 10.

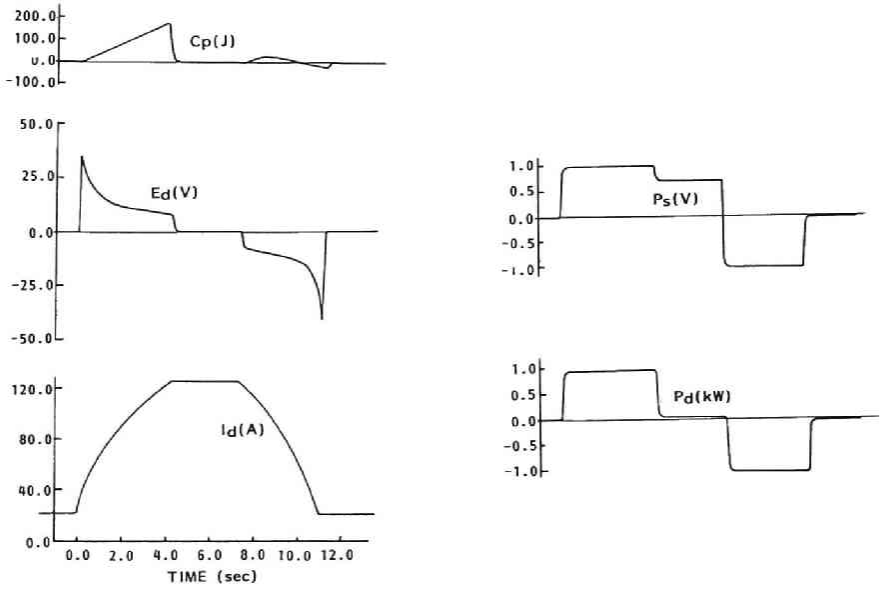

Fig.2-15 Test result of constant active power control by PI-control with integral gain K_{ip} is 1 and proportional gain K_{pp} is 0.075(charging), 0.138(discharging).

The experimental result of constant active power control by PI-control with gains K_{ip}=1 and K_{pp}=0.075 (for charging mode), K_{pp}=0.138 (for discharging mode) are shown in Fig.2-15. The control performance can be improved by adding the proportional factor(the 4-th and the 5-th term of Eq.(2-1)). The optimum gain K_{pp} need to be changed for the specified power Ps.

The voltage drops of the converter and the transformers mainly causes the power error. Therefore the factor of compensating the voltage drop is added to the integral-control. Test results are shown in Fig.2-16(K_{ip}=50) and Fig.2-17(K_{ip}=100). The error energy Cp is fairly small both in charging and in discharging.

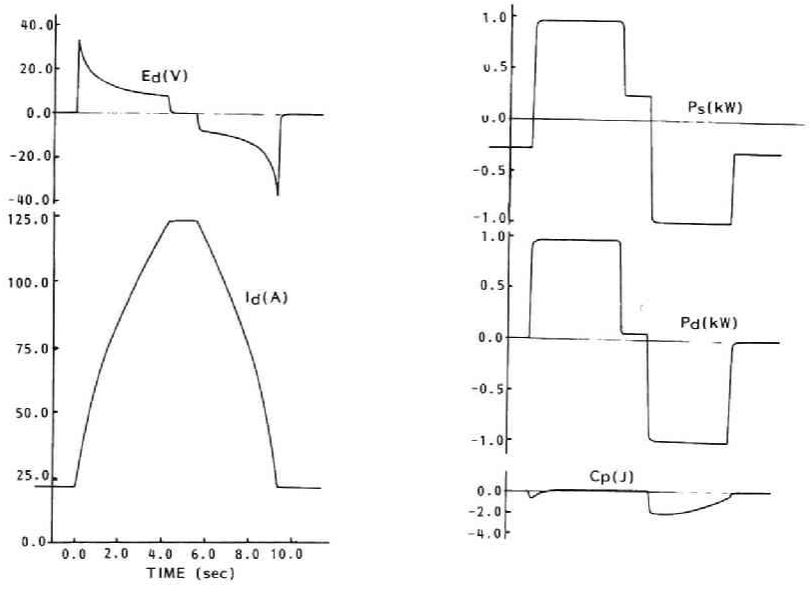

Fig.2-16 Test result of constant active power control by $I+E_{drop}$ compensation control with integral gain K_{ip} is 50, compensating parameter E_{th} is 1.6[V] and Z is 11[mΩ] (for single bridge converter).

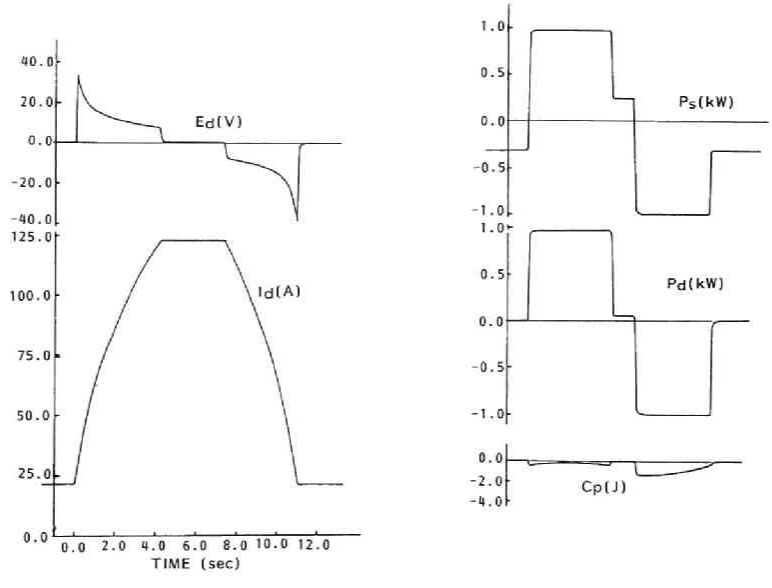

Fig.2-17 Test result of constant active power control by $I+E_{drop}$ compensation control with integral gain K_{ip} is 100, compensating parameter E_{th} is 1.6[V] and Z is 11[mΩ].

2-3-6. ACTIVE AND REACTIVE POWER SIMULTANEOUS CONTROL (6),(7),[21]

A)Constant active and reactive power simultaneous control

Experiments for constant active and reactive power simultaneous controls were carried out. Two examples of the are shown in Fig.2-18 and 2-19. In Fig.2-18, the operating conditions are;

1]specified active power Ps=± 1.0[kW] (the sign + denotes the charging mode and - denotes the discharging mode) and specified

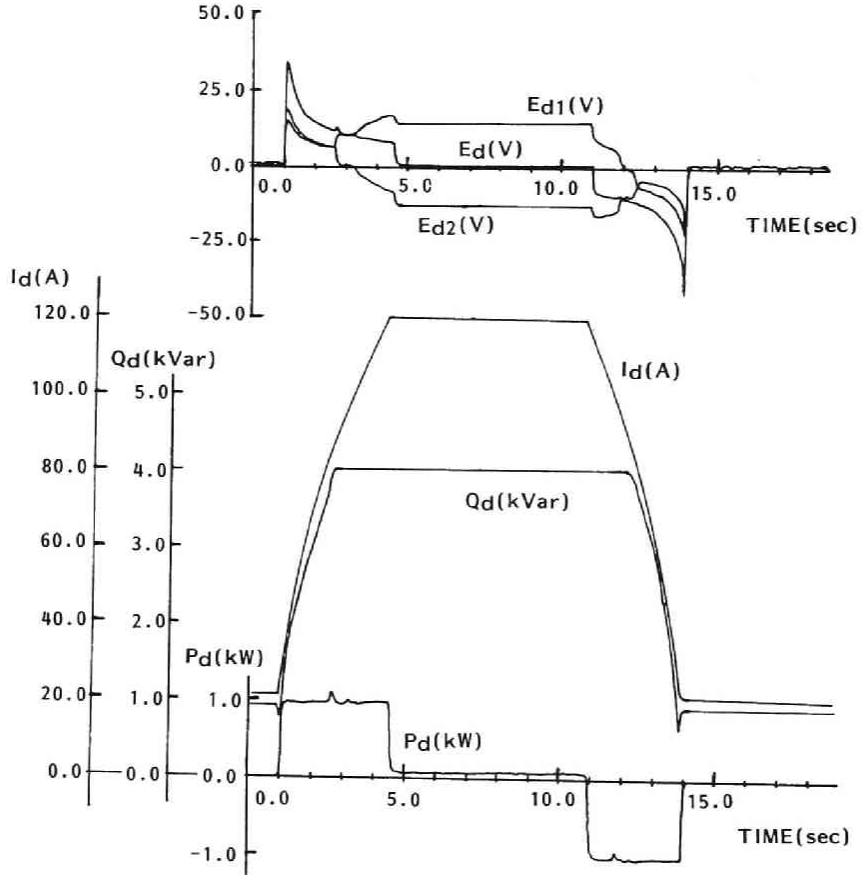

Fig.2-18 Test result for constant active and reactive power control (Ps = ± 1.0[kW], Qs = 4.0[kVar], L = 0.505[H])

reactive power Qs=4.0[kVar].

2]upper limited current is 120[A] and lower limited current is 22[A].

When the current Id is less than 85[A], only active power is controlled. This shows that the state is out of the possible

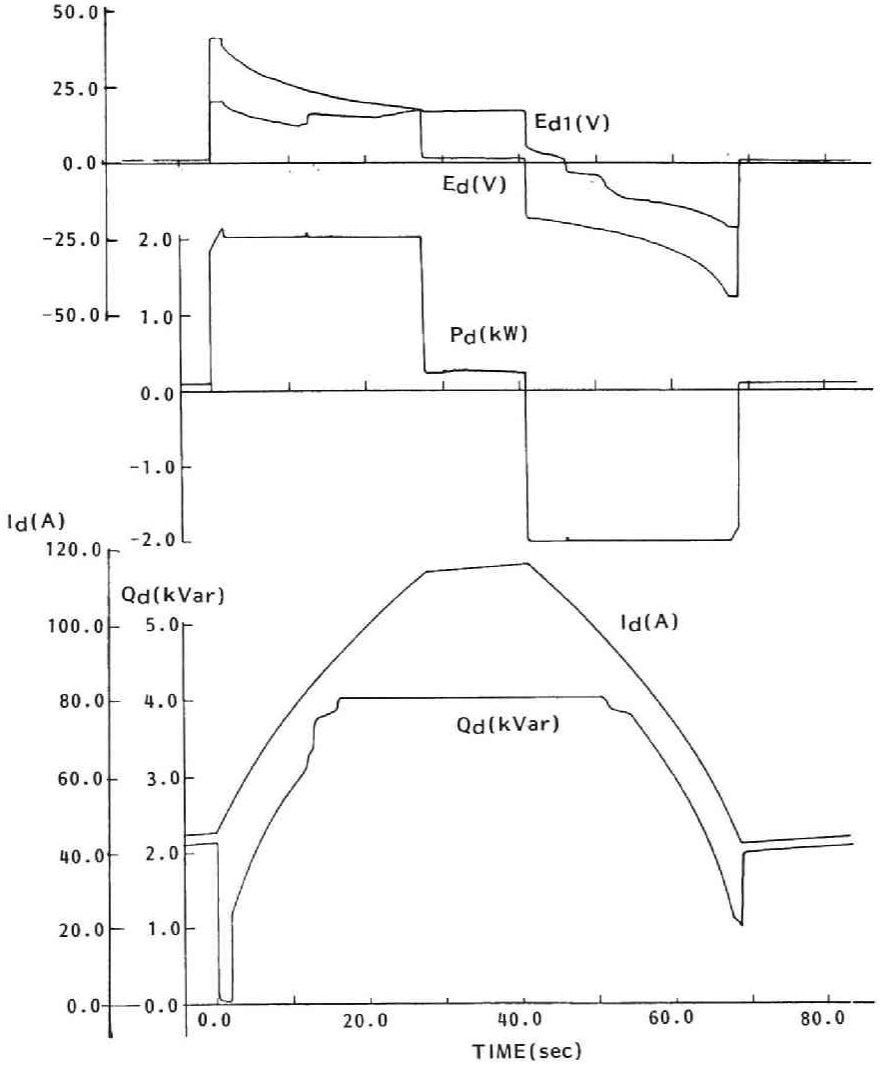

Fig.2-19 Test result for constant active and reactive power control (Ps = ± 2.0[kW], Qs = 4.0[kVar], L = 10.8[H])

region for the P-Q simultaneous control. When the current becomes greater than 85[A] the simultaneous control begins. Converter voltages Ed_1 and Ed_2 become to have different values each other to keep the reactive power constant.

Figure 2-19 shows the result of the experiment where Ps=} 2.0[kW] and Qs=4.0[kVar], the magnet inductance is 10.8[H].

From the results of the experiments for several sets of Ps and Qs, we obtain the characteristics of the constant active and reactive power simultaneous controls as shown in Fig.2-20. It is corresponding to Fig.1-8. It is confirmed that constant active and reactive power simultaneous controls can be done if specified powers Ps and Qs are in the controllable region shown in Fig.2-20. It is similar to the power characteristics shown in Fig.1-8. The difference is due to whether the loss of SMES system is considered or not. For example, if a set of Ps and Qs is in the shaded region, the constant active and reactive power control is possible for 100[A]<Id<120[A].

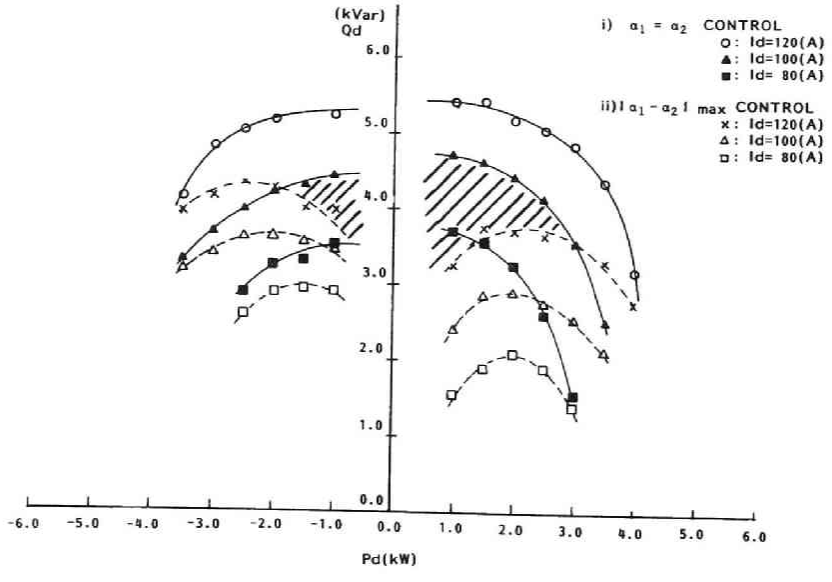

Fig.2-20 Active and reactive power characteristics of SMES (experimental result)

B)Simultaneous control of sinusoidal wave active power and constant reactive power

A sinusoidal wave active power and constant reactive power control tests were carried out. One of the results is shown in Fig.2-21 on a condition that P_O=2.0[kW], Qs=4.0[kVar], I_O=100[A] and f=0.3[Hz]. This case is in the controllable region in Fig.1-11. Then the reactive power is kept constant at the beginning of the control. However, as time passes the average value of current Id decreases due to losses of the circuit. The state are out of possible region of the simultaneous control. The reactive power can not maintain constant. It occurs at the time t satisfying the following equation. Active power P and magnet current Id do not satisfy the condition (3) shown in section 2-3.

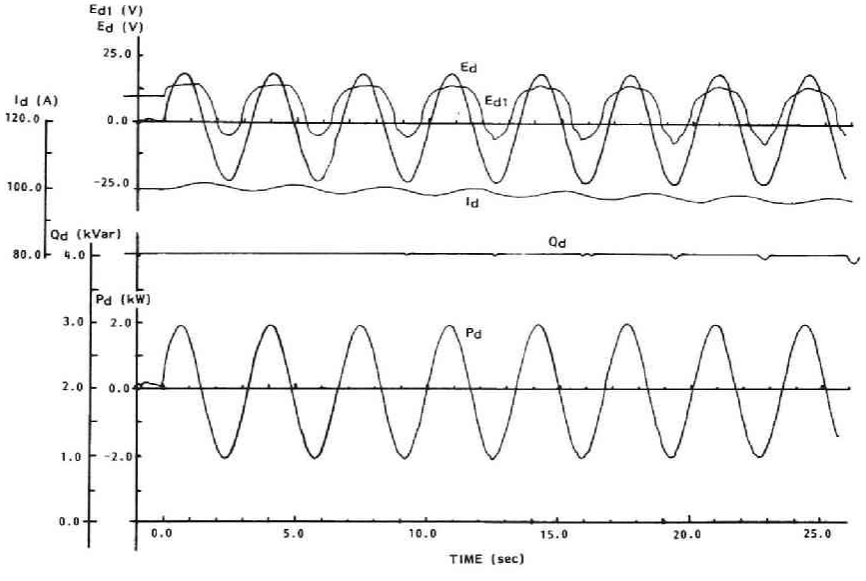

Fig.2-21 Test result for simultaneous control of sinusoidal active and constant reactive power
(Po = 2.0[kW], Qs = 4.0[kVar], f = 0.3[Hz], Io = 100[A], L = 10.8[H])

$$\sin(2\pi ft) \geqq -\frac{Edo^2}{2\pi ftP_o} \qquad (2\text{-}19)$$

Figure 2-22 shows one of the experimental results where the conditions are different from the above case in the amplitude of power Po=3.0[kW]. The case is out of the controllable region shown in Fig.1-11. Therefore the reactive power Qd can not be maintained constant.

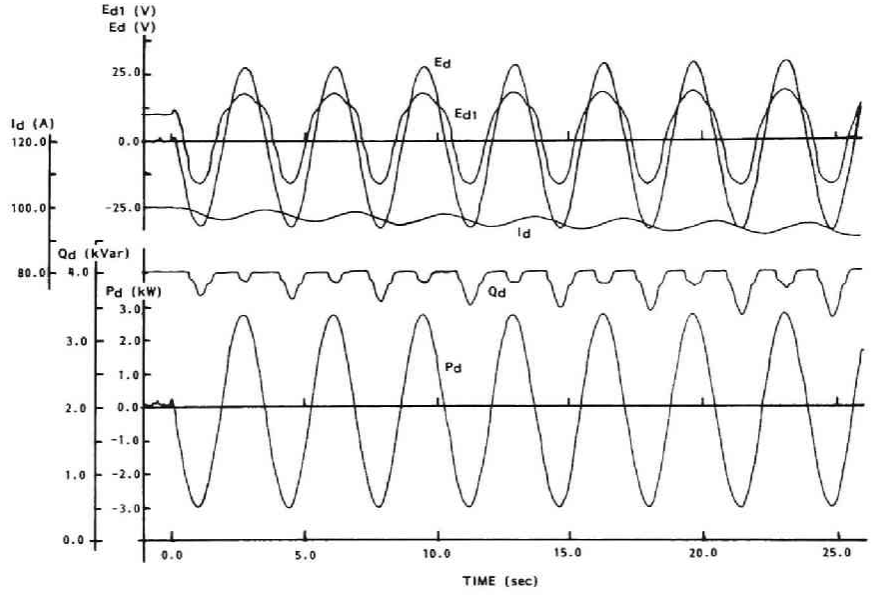

Fig.2-22 Test result for simultaneous control of sinusoidal active and constant reactive power
(Po = 3.0[kW], Qs = 4.0[kVar], f = 0.3[Hz], Io = 100[A], L = 10.8[H])

2-4. SIMULATION STUDY OF POWER CONTROL

It is one of the problems to design power controller because active power is controlled by changing both terminal voltage and magnet current. SMES does not have steady state in power control operation. Therefore control schemes are studied by use of computer simulation.

In computer simulations, exciting circuits of transformers are neglected and voltage drops across converter thyristors are assumed to be constant for simplifications. Differential equations are derived considering commutations of converter thyristors.

2-4-1. ACTIVE POWER CONTROL

In order to design a controller, active power controls of SMES using a single thyristorized bridge converter are discussed by computer simulations. Let us consider the following four cases.

1) without feedback control (open-loop control)

Figure 2-23 shows one of the simulation results without feedback control. Difference between the specified power Ps and the charging power Pd is getting larger as the magnet current increases because of the losses of the transformer and the thyristors. In order to reduce the power error(Ps-Pd), integral control are considered in the next place.

2) I-control

Here, new specified power signal Pr is defined using detected power Pd as

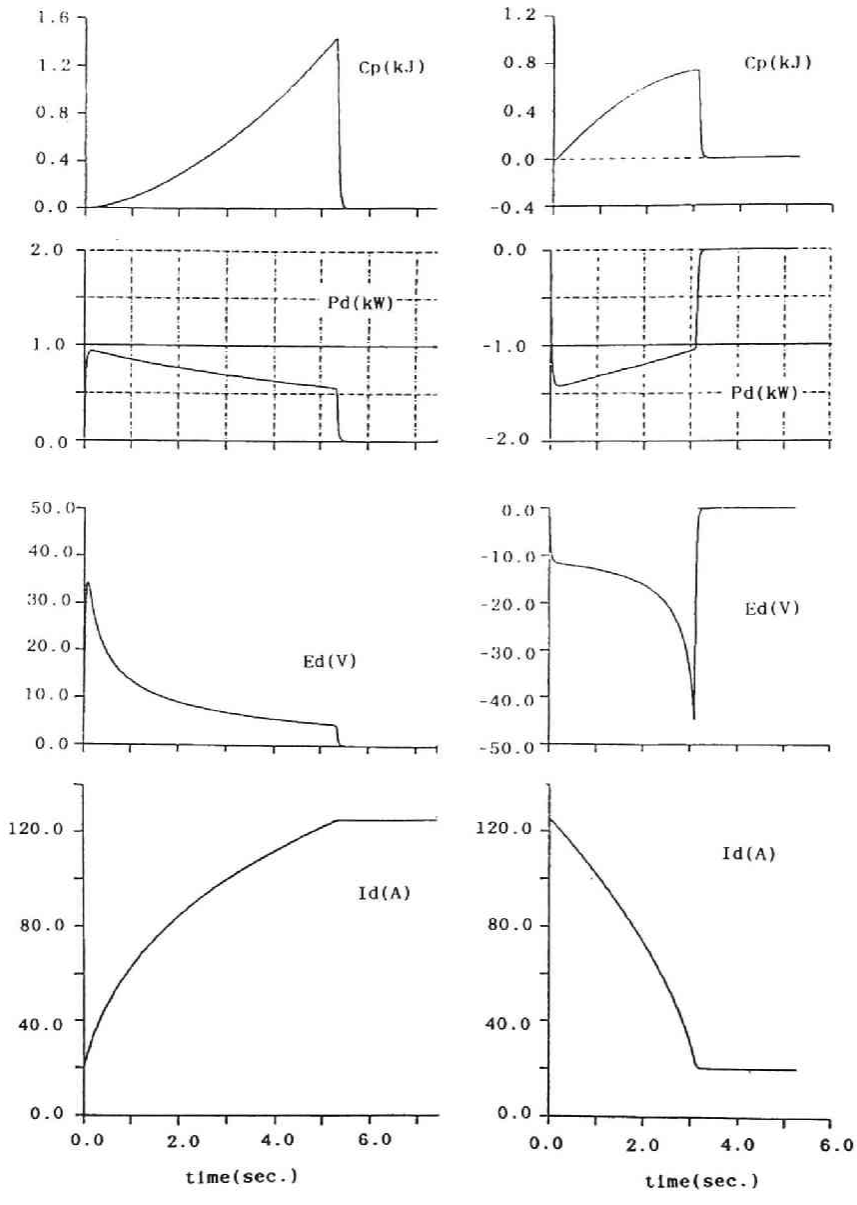

Fig.2-23 Simulation result for constant active power control without feedback control

$$Pr = Ps + K_{ip} \int (Ps-Pd) \qquad (2\text{-}20)$$

When thyristorized converters are used for power converter, we can not control powers during the time between a certain firing pulse and the following firing pulse. The interval time T(sec) between two firing angles is given as

$$T = \frac{1}{p\ 60} \qquad (2\text{-}21)$$

where the p is the number of converter pulses and firing angles are assumed to be constant. Let's consider firing angle at the time T_o since the power control has begun. The integrated power error Cp at time T_o is given as follows.

$$C_p = \int_0^{To} (Ps-Pd)dt \qquad (2\text{-}22)$$

The charging or discharging energy in the next period dW is

$$dW = (Ps+K_{ip}C_p)T \qquad (2\text{-}23)$$

Therefore the power in the next period is determined as

$$Pr = \frac{\dot{dW}}{T} \qquad (2\text{-}24)$$

The integrated power error Cp is considered to be a power which should be corrected within the time $T'=1/K_{ip}$.

Figure 2-24 shows one of simulation results associated with the experimental result shown in Fig.2-13. The integral gain K_{ip} is 1.

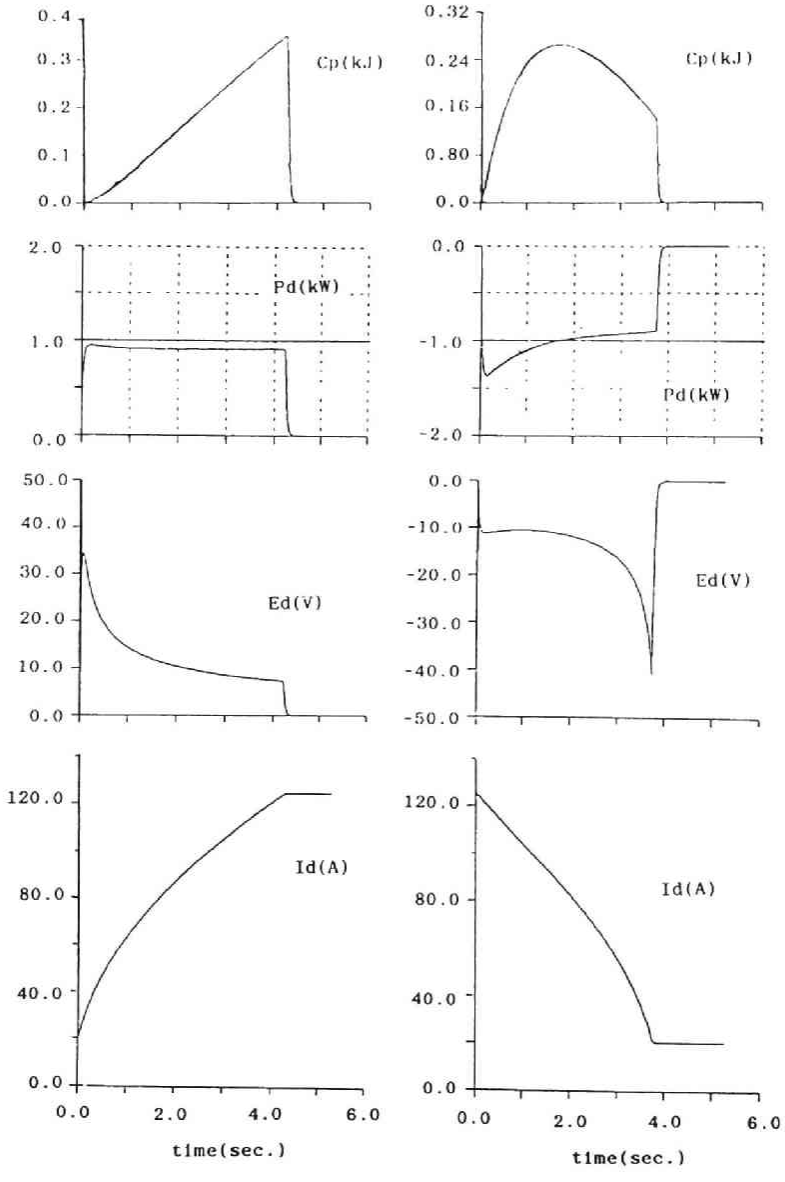

Fig.2-24 Simulation result for constant active power control by I-control of K_{ip}=1. (see Fig.2-13)

The simulation results are shown in Fig.2-25 (K_{ip}=10) and Fig.2-26 (K_{ip}=100). The larger the gain Kip is, the smaller the energy error Cp is. However, the overshoot appears at the starting point for large gain K_{ip}. It may due to the voltage drop at the magnet terminal. The energy error Cp cannot follow step change of power and it cannot compensate the voltage drops.

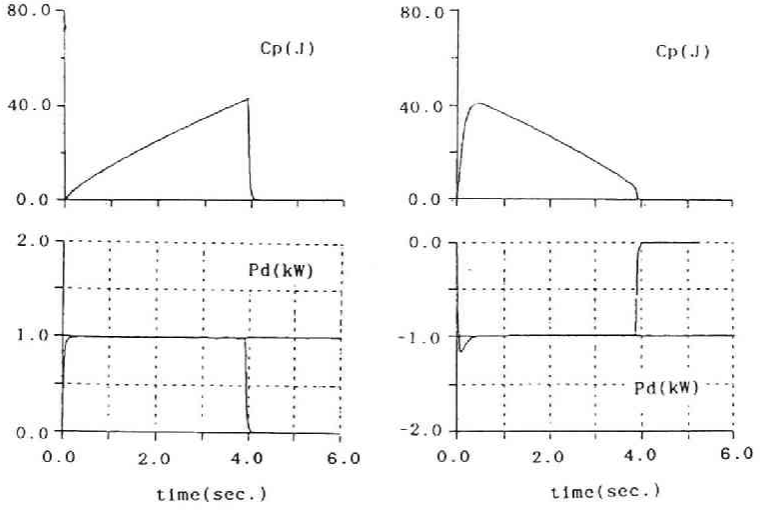

Fig.2-25 Simulation result for constant active power control by I-control of K_{ip}=10. (see Fig.2-14)

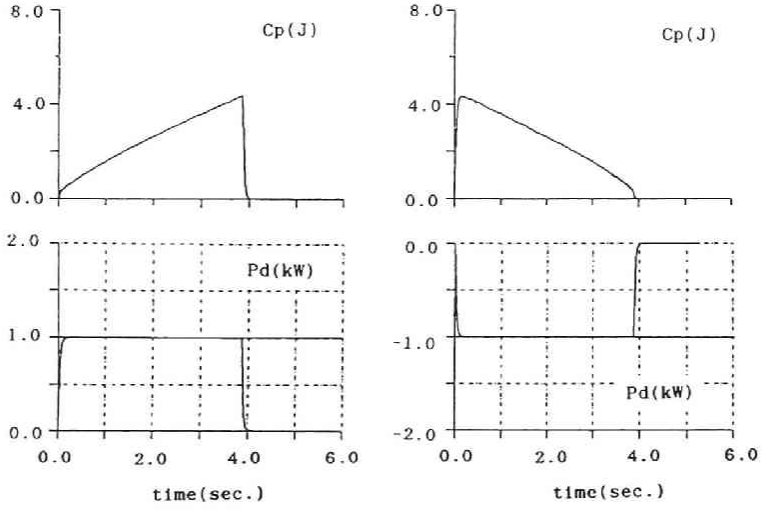

Fig.2-26 Simulation result for constant active power control by I-control of K_{ip}=100.

3) PI-control

Here, a proportional term is added to the integral control. The power control is improved by the proportional term. However, the gain K_{pp} for proper control depends on whether the control is in the charging mode or the discharging mode. The gain K_{pp} should be changed with operating conditions for proper control. Then we consider the Edrop-compensation control.

4) I+Edrop compensating control

As described in Sec.2-3-4, the E_{drop}-compensation is added to the integral control. One of the simulation results is shown in Fig.2-27. Integral gain K_{ip} is 100. The constants E_{th} and Z for the compensator are set to be 1.6 and 11, respectively.($E_{drop}=E_{th}+ZI_d$) The error energy C_p is the smallest among that in the other control.

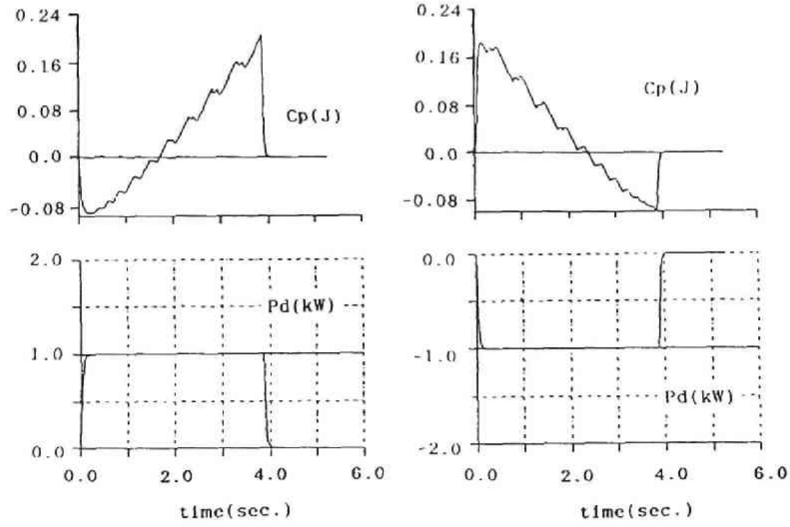

Fig.2-27 Simulation result for constant active power control by I+E_{drop} compensation-control of K_{ip}=100, E_{th}=1.6, Z=11. (see Fig.2-17)

2-4-2. ACTIVE AND REACTIVE POWER CONTROL

In order to design a controller for active and reactive power simultaneous controls, simulation studies for SMES by use of double bridge converter were carried out.

Figure 2-28 shows one of the simulation results. (corresponding to Fig.2-18) The conditions are as follows.

1] The magnet is charged at active power Ps=1.0[kW].

2] The magnet current is held for a while.

3] The magnet is discharged at Ps=-1.0[kW].

During this operation, specified reactive power Qs is set to be 4.0[kVar]. It is confirmed that active power and reactive power can be controlled independently.

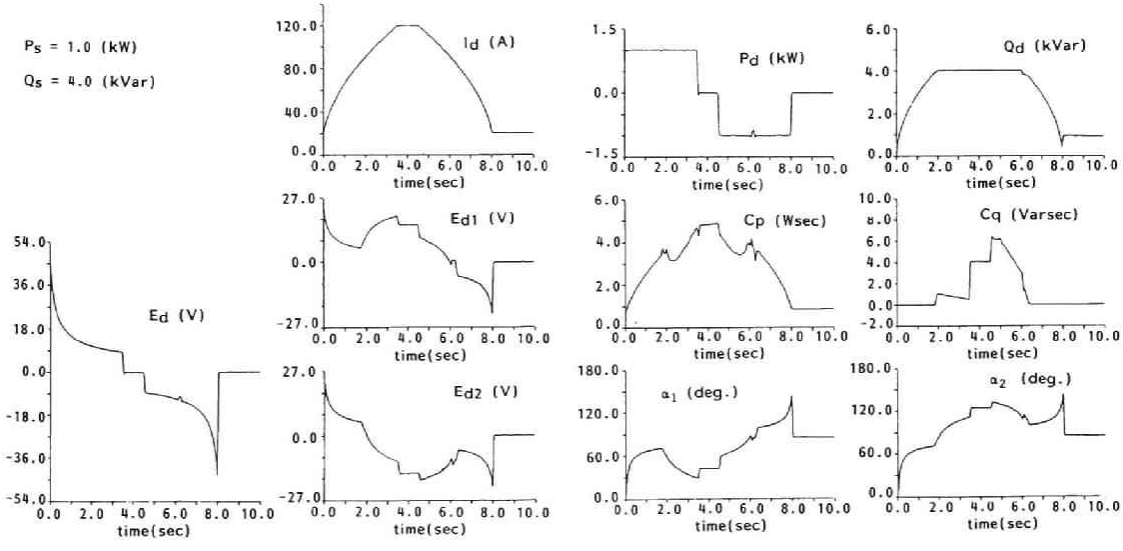

Fig.2-28 Simulation result for constant active and reactive power control (Ps = ± 1.0[kW], Qs = 4.0[kVar], L = 0.505[H]) (see Fig.2-18)

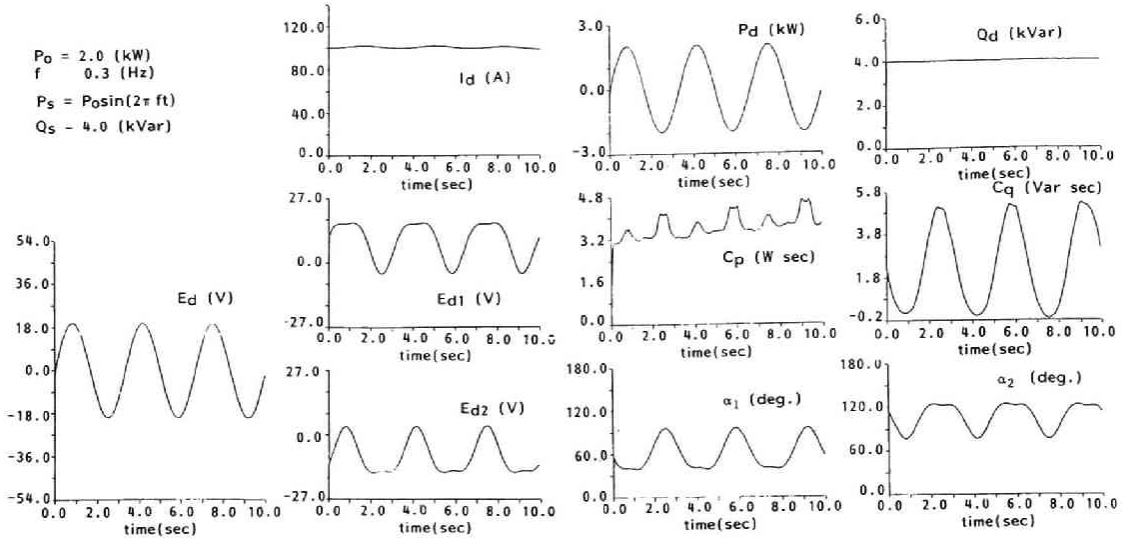

Fig.2-29 Simulation result for simultaneous control of sinusoidal active and constant reactive powers
(Po = 2.0[kW], Qs = 4.0[kVar], f = 0.3[Hz], Io = 100[A], L = 10.8[H]) (see Fig.2-21)

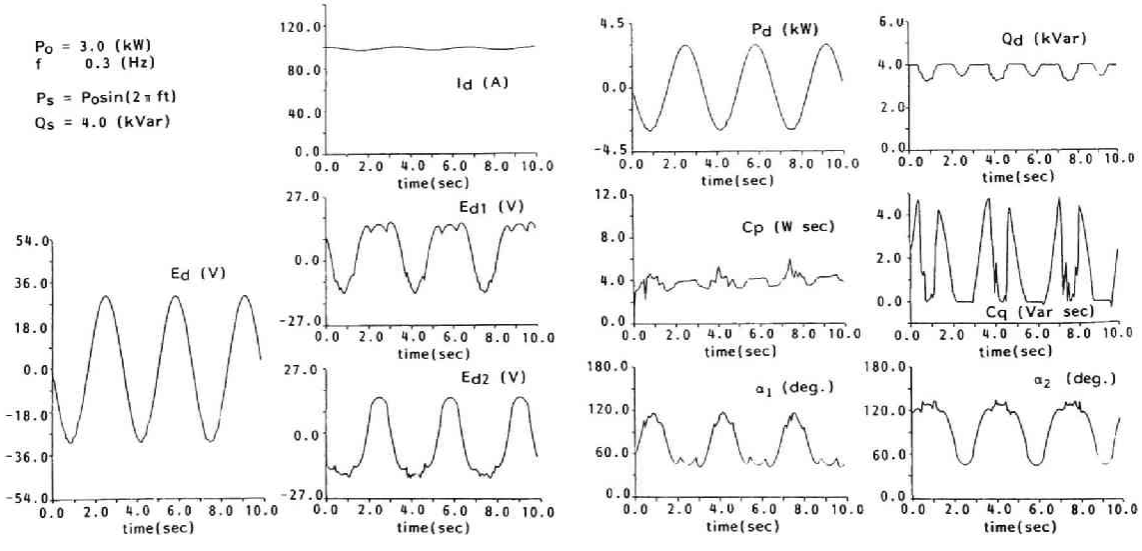

Fig.2-30 Simulation result for simultaneous control of sinusoidal active and constant reactive power
(Po = 3.0[kW], Qs = 4.0[kVar], f = 0.3[Hz], Io = 100[A], L = 10.8[H]) (see Fig.2-22)

The same discussion can be done in the sinusoidal wave of active power and constant reactive power control. Figures 2-29 and 2-30 shows the simulation results corresponding to the test results shown in Fig.2-21 and 2-22, respectively.

2-5. CONCLUDING REMARKS

In this chapter, the experimental system is introduced. We have two superconducting magnets; one is of inductance 0.505[H] and another one is of 10.8[H]. The power control scheme is realized by the analogue ICs and the personal computer.

In the experiments, the circuit for building up the magnet current(Starter-circuit) was proposed and tested.

The circuit to short the superconducting magnet (Circulation mode) for disconnecting it electrically from the power system is studied. Control scheme of Circulation mode by use of thyristor was proposed and examined.

The power charging and discharging test were carried out. By use of the single bridge converter, the characteristics of the active power control was investigated. By use of the double bridge converter, the active and reactive power simultaneous control was performed. The controllable region for P-Q simultaneous control was obtained from the experimental results.

The power controllers were designed and examined by use of computer simulations. The voltage drop compensator is effective in power control.

The fundamental characteristics of SMES was obtained by the experiments and the simulations.

CHAPTER.3

COMPUTER SIMULATION OF POWER SYSTEM INCLUDING SMES[8],[9]

3-1. INTRODUCTION

It is necessary to study problems on power systems including SMES. For example, how the power systems behave during operations of SMES or at faults of SMES. On the other hand, how SMES will respond or should operate when some faults occur in power system.

In order to investigate these problems, simulation study is necessary and effective. In this chapter, a simulation code for such purposes is discussed and made. The simulation code should explain commutations of thyristor converters of SMES. There are many circuit modes for SMES associated with combinations of on-state thyristors. Moreover, when SMES is operated at power control mode, the DC current and the terminal voltage of superconducting magnet vary with time in terms of change of the firing angles of converters. Then the simulation code should give transient solutions. At the same time, it is desirable to be easily changed corresponding to the power system configurations.

It is complicated to derive a set of state equations for the whole power system including generators and other power system apparatus associated with every commutation mode of SMES's converters. We propose a convenient method that a set of the state equations for the whole system is separated into one for the power system and the other for SMES at the magnetic circuit of SMES's transformers. Then we only prepare several set of equations of every commutation modes for SMES and one set of the state equations for the power system. Therefore even when the configuration or situation of power system change, only the equations for power system should be reformed, which are obtained

independently of the commutations of the thyristor converters.

In order to start the simulation at an arbitrary time for saving computation time., the initial values of the state variables should be obtained. However, since operations of SMES are always in transient state, it is not easy to obtain the accurate values of the state variables at an arbitrary time. A method for determining the initial values is introduced.

3-2. SIMULATION METHOD

3-2-1. EQUIVALENT CIRCUIT OF SMES(10)

State equations of SMES are derived as to an equivalent circuit as shown in Fig.3-1. We assumed ; 1] an equivalent circuit of transformer consists of an ideal transformer with linear leakage impedances on the power system side and linear exciting impedances on SMES side. 2]A superconducting magnet is expressed as a pure inductor. 3]Thyristors are considered to be constant resistors at conducting state and to be open circuits at off state.

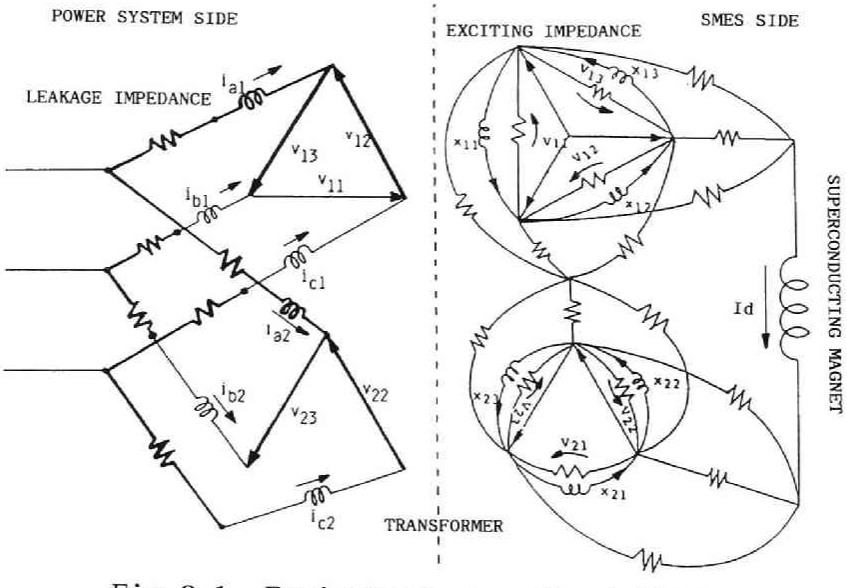

Fig.3-1 Equivalent circuit of SMES

The combinations of conducting thyristors or the firing angle of each thyristor vary with the operating condition of SMES. Therefore proper tree[25] for equivalent circuit varies. It is troublesome to derive a set of state equations for the whole system corresponding to each proper tree. In order to obtain state equations easily, we derive a set of state equations for SMES and for power system individually by separating at the magnetic circuit of the transformers. Solutions of these state equations are connected by voltage and current relations between power system and SMES at the transformers.

Therefore a set of state equations for power system need not change with operating condition of SMES. Switchings of thyristor converters are only expressed in the state equations for SMES.

3-2-2. STATE EQUATIONS FOR SMES

In normal operation, there are 144 circuit modes for commutations of thyristors. These modes are divided into four groups;

A)neither of upper and lower bridges is in commutation mode.
B)only upper bridge is in commutation mode.
C)only lower bridge is in commutation mode.
D)both of upper and lower bridges are in commutation mode.

Figure 3.3 shows a equivalent circuit and a proper tree for each case A), B), C) and D).

The proper tree is decided so that the superconducting magnet current and the transformer exciting inductor current can be selected as state variables in every cases. Then a set of state equations for SMES is obtained as

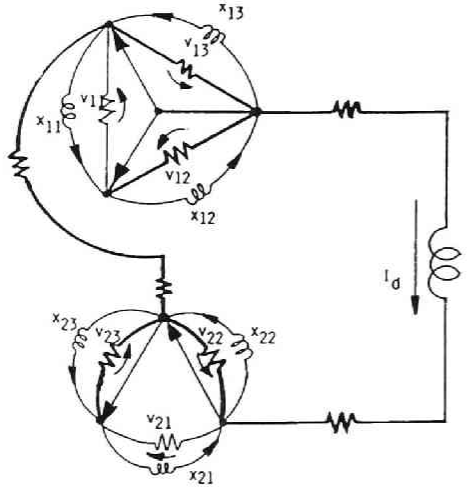

A)Both converters are out of commutation

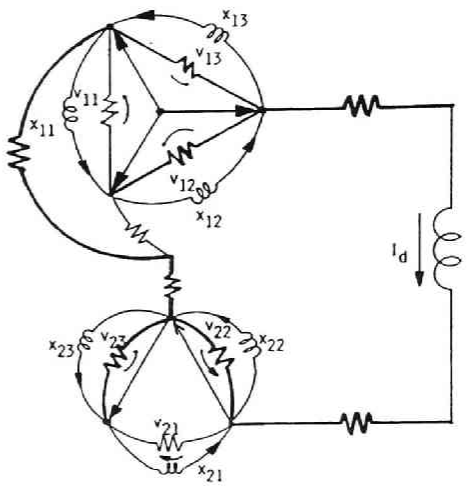

B)Upper is in commutation

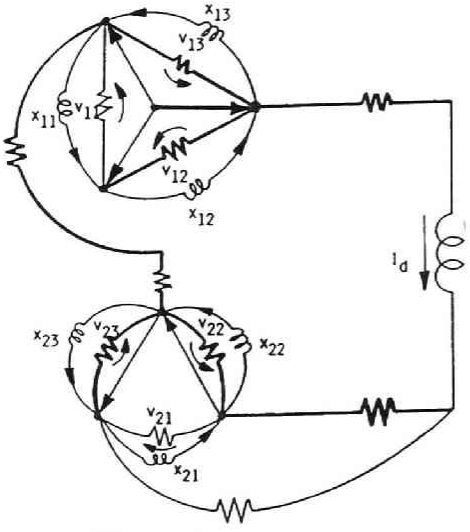

C)Lower is in commutation

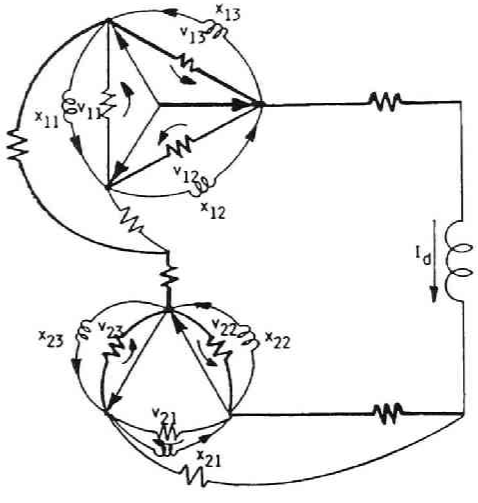

D)Both are in commutation

Fig.3-2 Proper tree at SMES side for case A), B), C) and D)

PROPER TREE : THICK SOLID LINE

$$\frac{d}{dt}\mathbf{x}_S = \mathbf{A}_S \cdot \mathbf{x}_S + \mathbf{B}_S \cdot \mathbf{I}_S \qquad (3\text{-}1)$$

$\mathbf{x}_S$;$[I_d, x_{11}, x_{12}, x_{13}, x_{21}, x_{22}, x_{23}]^t$
$\mathbf{I}_S$;$[I_{C1}, I_{A1}, I_{C2}, I_{A2}]^t$
$\mathbf{A}_S, \mathbf{B}_S$;Matrices for converter mode

where a current vector $\mathbf{I}_S$ is determined by the currents through the leakage inductor of the transformer in the equivalent circuit for power system.

A voltage vector $\mathbf{V}_S$ (V_{ij}: voltage across the exciting impedances) is necessary as an input vector for a set of state equations for power system. It is obtained from the output equation of Eq.(3-1).

$$\mathbf{V}_S = \mathbf{C}_S \cdot \mathbf{x}_S + \mathbf{D}_S \cdot \mathbf{I}_S \qquad (3\text{-}2)$$

$\mathbf{V}_S$;$[V_{11}, V_{12}, V_{13}, V_{22}, V_{23}]^t$:exciting voltage
$\mathbf{C}_S, \mathbf{D}_S$;Matrices for converter mode

The matrices $\mathbf{A}_S$, $\mathbf{B}_S$, $\mathbf{C}_S$ and $\mathbf{D}_S$ corresponding to conducting situations of thyristor converters are prepared. They are independent of configuration of power systems.

3-2-3. STATE EQUATION FOR POWER SYSTEM

In order to express transient phenomena of synchronous generators, Park's equations are adopted. A set of state equations for power system is written as

$$\frac{d}{dt}\mathbf{x}_{p\text{-}dq} = \mathbf{A}_p \cdot \mathbf{x}_{p\text{-}dq} + \mathbf{B}_p \cdot \mathbf{e}_{p\text{-}dq} + \mathbf{C}_p \cdot \mathbf{v}_{p\text{-}dq} \qquad (3\text{-}3)$$

$\mathbf{x}_{p\text{-}dq}$;state vector for power system
$\mathbf{e}_{p\text{-}dq}$;input vector
$\mathbf{v}_{p\text{-}dq}$;$[v_{d1}, v_{q1}, v_{d2}, v_{q2}]^t$
:input vector (line-to-line voltage of transformer given by Eq.(3-7))

The proper tree of transformers at power system side is chosen as indicated in Fig.3-1. Leakage inductor current i_{b1}, i_{b2}, i_{c1} and i_{c2} are chosen as state variables. They are transformed to d-q value i_{d1}, i_{q1}, i_{d2} and i_{q2} which are components of the vector $\mathbf{x}_{p\text{-}dq}$. The vector $\mathbf{v}_{p\text{-}dq}$ consists of line to line voltages of the transformer which is determined by the output equation for SMES, that is Eq.(3-2). A symbol $\mathbf{e}_{p\text{-}dq}$ denotes an external input vector. It consists of the infinite bus voltages and generator field winding voltage.

A swing equation of generator is assumed to be;

$$2M \frac{d^2r}{dt^2} = \omega_0 \cdot (P_m - P_e) \qquad (3\text{-}4)$$

M ;inertia constant
P_m ;mechanical input power
P_e ;generator output power
r ;electrical angle of rotor

$$P_e = \frac{2}{3}(v_{dg} \cdot i_{dg} + v_{qg} \cdot i_{qg})$$

Leakage inductor current vector $\mathbf{i}_t$ is used for the input vector of Eq.(3-1). It is given by the output equation of Eq.(3-4).

$$\mathbf{i}_t = \mathbf{D}_p \cdot \mathbf{x}_{p\text{-}dq} \qquad (3\text{-}5)$$

$$\mathbf{i}_t ; [i_{d1}, i_{q1}, i_{d2}, i_{q2}]^t$$

This current vector $\mathbf{i}_t$ is converted to $\mathbf{I}_s$ in Eq.(3-1) by using voltage and current relations of the transformers. (see Section 3-2-4)

3-2-4. STATE EQUATION FOR WHOLE SYSTEM

The state equations (3-1) and (3-3) are combined to be one state equation by use of the following relations.

$$\left.\begin{aligned} \mathbf{I}_S &= \mathbf{R}\cdot \mathbf{i}_t \\ \mathbf{v}_{p\text{-}dq} &= \mathbf{S}\cdot \mathbf{V}_S \end{aligned}\right\} \qquad (3\text{-}6)$$

$$\mathbf{R}=\begin{bmatrix} \dfrac{1}{\sqrt{3}k_1}\begin{bmatrix} -\sin r_1 & \cos r_1 \\ \sin r & \cos r \end{bmatrix} & \mathbf{0} \\ \mathbf{0} & \dfrac{1}{k_2}\begin{bmatrix} \cos r_1 & \sin r_1 \\ \cos r & \sin r \end{bmatrix} \end{bmatrix}$$

$$\mathbf{S}=\frac{2}{3}\begin{bmatrix} \dfrac{1}{\sqrt{3}k_1}\begin{bmatrix} \sin r & \sin r_2 & \sin r_1 \\ -\cos r & -\cos r_2 & -\cos r_1 \end{bmatrix} & \mathbf{0} \\ \mathbf{0} & -\dfrac{1}{k_2}\begin{bmatrix} \cos r \cos r_2 \cos r_1 \\ \sin r \sin r_2 \sin r_1 \end{bmatrix} \end{bmatrix}$$

$$r_1=(r+\frac{2}{3}\pi) \quad r_2=(r-\frac{2}{3}\pi)$$

k_1, k_2 ;turn ratio of transformer

where **R**, **S** are matrices which explain the the voltage and current relations of ideal transformers. By eliminating the vectors $\mathbf{v}_{p\text{-}dq}$ and $\mathbf{I}_S$ from Eq.(3-1) and Eq.(3-3), we can obtain state equations for the whole system shown as

$$\frac{d}{dt}x_{sp} = A_{sp} \cdot x_{sp} + B_{sp} \cdot e_{p\text{-}dq} \qquad (3\text{-}7)$$

x_{sp} ;state vector for whole system $[x_s , x_{p\text{-}dq}]^t$

A_{sp} ;transfer matrix

$$\begin{bmatrix} A_s & B_s \cdot R \cdot D_p \\ C_p \cdot S \cdot C_s & A_p + C_p \cdot S \cdot D_s \cdot R \cdot D_p \end{bmatrix}$$

B_{sp} ; $[0 , B_p]^t$

To solve this state equation is equivalent to solve two state equation in accordance with the block diagram given in Fig.3-3-(a).

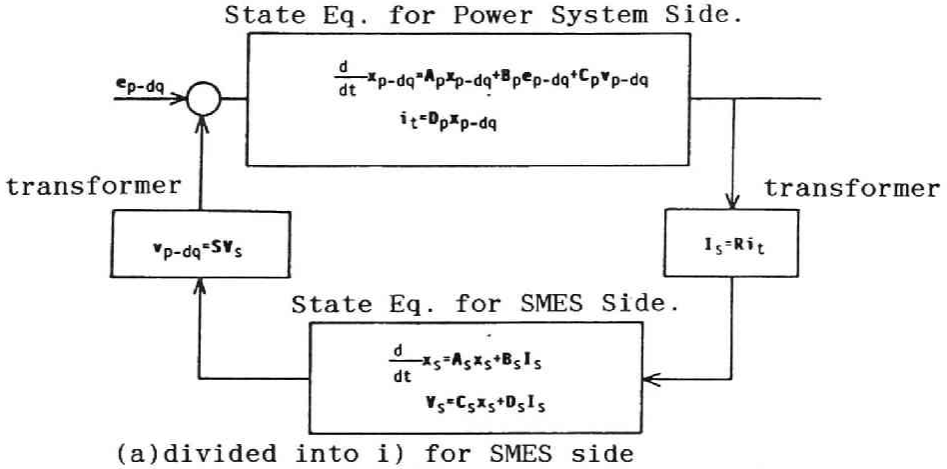

(a)divided into i) for SMES side and ii)for power system side.

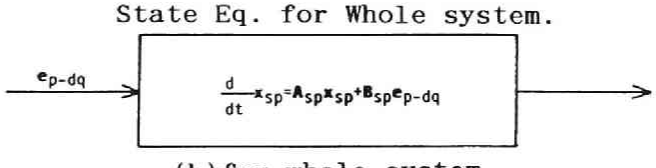

(b)for whole system.

Fig.3-3 State equations
(a)divided into i) for SMES side and ii)for power system side
(b)for whole system.

This method has following advantages;

1] When we use a set of state equations for whole system, we must handle the large transfer matrices $\mathbf{A}_{sp}$ and $\mathbf{B}_{sp}$. The matrices should be changed with switchings of thyristor converter. On the other hand, using this method, several sets of matrices $\mathbf{A}_S$, $\mathbf{B}_S$, $\mathbf{C}_S$ and $\mathbf{D}_S$ are to be prepared for switchings of converters.

2] When conditions of power system change, state equations for SMES need not to be changed. Only a set of state equations for power system is to be changed. It is easy because state equations for power system are obtained independently of commutations of thyristor converters.

3-3. INITIAL STATE FOR SIMULATION(11),(12)

3-3-1. INITIAL SITUATION OF SYSTEM FOR SIMULATION

The simulation method mentioned above can analyze systems in detail. However, it takes much calculation time if it simulates from the start of operations. Therefore initial values of state variables should be obtained in order that it can start at an arbitrary time. However, since operation of SMES is always in transient state, it is not easy to obtain accurate values of state variables at an arbitrary time.

Given parameters in the system at a certain operation are as follows;

1]Voltage source in power system $e_{p\text{-}dq}$ (the infinite bus voltage, the generator field winding voltage and so on.) in Eq.(3-3).

2]Mechanical input power P_m in Eq.(3-4).

3]Superconducting magnet current Id and specified powers (Ps,Qs) for SMES.

Firing angles of double thyristorized converters and combinations of conducting thyristors are determined by operating

conditions of SMES. Initial values of state variables should be obtained by the given parameters.

SMES generates higher harmonic currents whose orders or amplitudes are functions of firing angles of two thyristorized converters and a superconducting magnet current. Moreover when SMES is operated at a power control mode, the magnet current and the firing angles are vary with time. Therefore in order to obtain initial values, we must take the higher harmonic currents generated by SMES into account.

In order to meet the problems, a superconducting magnet is assumed to have infinite inductance so that an operation of SMES may be considered to be in a steady state. Superconducting magnet and converters are replaced by harmonic current sources of fundamental and higher order components associated with firing angles of converters and magnet current. The fundamental component is obtained by power flow analysis. The initial values can be obtained by superposing solutions of steady state analysis for each order of harmonics.

Before we describe a proposed method for obtaining the initial values for each set of state equations, we prepare steady state equations and harmonic current sources of fundamental and higher order components as mentioned above.

3-3-2. STEADY STATE EQUATION

In a steady state condition, we replace d/dt to $j\omega$ and dr/dt to ω_o in the Eq.(3-3). Then we can get a set of equations;

$$(j\omega E - \mathbf{A'}_p)\cdot \hat{\mathbf{x}}_{p\text{-}dq} = \mathbf{B'}_p \cdot \hat{\mathbf{e}}_{p\text{-}dq} + \mathbf{C'}_p \cdot \hat{\mathbf{v}}_{p\text{-}dq} \qquad (3\text{-}8)$$

$\hat{}$;phaser

$'$;dr/dt --> ω_o in each matrix

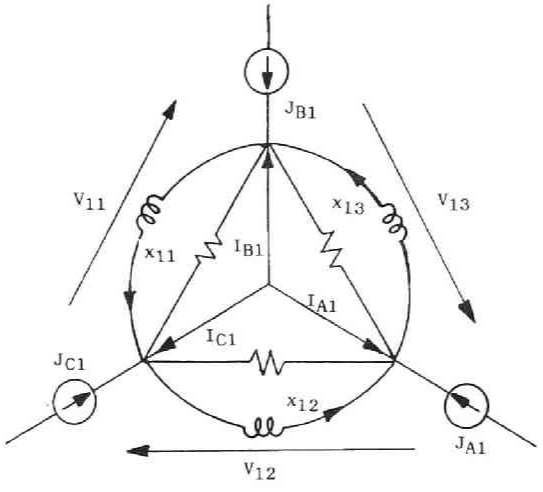

$J_{A1} \sim J_{C1}$:harmonic current source
$I_{A1} \sim I_{C1}$:current given from P wer System side
$x_{11} \sim x_{13}$:exciting inductor current
$V_{11} \sim V_{13}$:exciting voltage

Fig.3-4 Equivalent circuit of transformer for SMES side with SMES as current sources JA_1, JB_1 and JC_1. (Y-connection)

When SMES's superconducting magnet current is assumed to be a harmonic current source of the fundamental and the higher orders, an equivalent circuit for SMES is given as shown in Fig.3-4.(only for upper transformer) The equivalent circuit gives us;

$$\begin{bmatrix} J_{di} \\ J_{qi} \end{bmatrix} + \begin{bmatrix} I_{di} \\ I_{qi} \end{bmatrix} + \sqrt{3} \begin{bmatrix} -x_{qi} \\ x_{di} \end{bmatrix} + \frac{\sqrt{3}}{R_{si}} \begin{bmatrix} -V_{qi} \\ V_{di} \end{bmatrix} = \mathbf{0} \qquad (3\text{-}9)$$

$i=1,2$

On the other hand, the transformer exciting circuit voltages V_{di} and V_{qi} can be expressed by the exciting inductor currents x_{di} and x_{qi} as

$$\begin{bmatrix} V_{di} \\ V_{qi} \end{bmatrix} = L_{si} \left[\frac{d}{dt} \begin{bmatrix} x_{di} \\ x_{qi} \end{bmatrix} - \frac{dr}{dt} \begin{bmatrix} -x_{qi} \\ x_{di} \end{bmatrix} \right] \qquad i=1,2 \tag{3-10}$$

From Eq.(3-9) and (3-10), we can get

$$L_i \cdot \hat{x}_{dq-i} + \hat{I}_{dq-i} + \hat{J}_{dq-i} = 0 \tag{3-11}$$

$$L_i = \frac{\sqrt{3}}{R_{si}} \begin{bmatrix} \omega_o L_{si} & -(R_{si} + j\omega L_{si}) \\ R_{si} + j\omega L_{si} & \omega_o L_{si} \end{bmatrix}$$

$$\hat{x}_{dq-i} = [\hat{x}_{di}, \hat{x}_{qi}]^t \quad , \quad \hat{I}_{dq-i} = [\hat{I}_{di}, \hat{I}_{qi}]^t$$
$$\hat{J}_{dq-i} = [\hat{J}_{di}, \hat{J}_{qi}]^t \qquad i=1,2$$

Therefore the voltage vectors v_{p-dq} of the transformer at power system side are given as

$$\begin{bmatrix} -\hat{v}_{q1} \\ \hat{v}_{d1} \end{bmatrix} = \frac{R_{s1}}{3k_1} M_1^{-1} \left[\begin{bmatrix} \hat{J}_{d1} \\ \hat{J}_{q1} \end{bmatrix} + \frac{1}{\sqrt{3}k_1} \begin{bmatrix} \hat{i}_{q1} \\ -\hat{i}_{d1} \end{bmatrix} \right] \tag{3-12-a}$$

$$\begin{bmatrix} \hat{v}_{d2} \\ \hat{v}_{q2} \end{bmatrix} = \frac{-R_{s2}}{\sqrt{3}k_2} M_2^{-1} \left[\begin{bmatrix} \hat{J}_{d2} \\ \hat{J}_{q2} \end{bmatrix} + \frac{1}{k_2} \begin{bmatrix} \hat{i}_{d2} \\ \hat{i}_{q2} \end{bmatrix} \right] \tag{3-12-b}$$

$$M_i = \begin{bmatrix} (R_{si}/L_{si})h_1 & 1+j(R_{si}/L_{si})h_2 \\ -[1+j(R_{si}/L_{si})h_2] & (R_{si}/L_{si})h_1 \end{bmatrix}$$

$$h_1 = \frac{\omega_o}{\omega_o^2 - \omega^2} \qquad h_2 = \frac{\omega}{\omega_o^2 - \omega^2} \qquad i=1,2$$

By substituting Eq.(3-12) into Eq.(3-8), we can obtain a basic

equation to get initial values as

$$\mathbf{P}\cdot\hat{\mathbf{x}}_{p\text{-}dq} = \mathbf{Q}\cdot\hat{\mathbf{e}}_{p\text{-}dq} + \mathbf{V}\cdot\hat{\mathbf{J}}_{dq} \qquad (3\text{-}13)$$

$$\hat{\mathbf{J}}_{dq}=[\hat{\mathbf{J}}_{dq\text{-}1},\ \hat{\mathbf{J}}_{dq\text{-}2}]^t$$

3-3-3. SMES AS A HARMONIC CURRENT SOURCE

In this section, we decide J_{dq} in Eq.(3-13), that is, amplitudes and phase angles of harmonic current sources of the fundamental and the higher orders which represents the superconducting magnet and the converters. These are functions of the firing angles α_1, α_2 of thyristor converters and the superconducting magnet current Id.

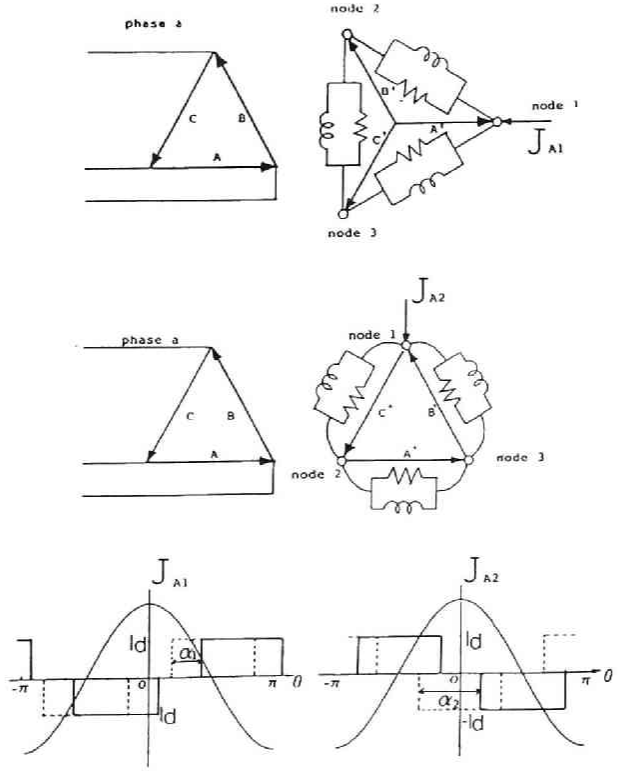

Fig.3-5 Current through transformers J_{A1} and J_{A2} of square wave shape with firing angles α_1 and α_2.

In order to simplify harmonic analysis, it is assumed as;

1]commutating period is neglected.

2]currents through the transformers have ideal square shape shown in Fig.3-5.

The symbols J_{A1} and J_{A2} denote a current source set on the upper transformer and the lower one, respectively. In Fig.3-5, a sinusoidal wave is the a-phase voltage of transformer at power system side. The current sources J_{A1} and J_{A2} can be illustrated in the solid lines with the firing angles α_1 and α_2. An amplitude and a phase of the current sources for each order are given by Fourier series of these square shape currents $J_1=\{J_{A1},J_{B1},J_{C1}\}$, $J_2=\{J_{A2},J_{B2},J_{C2}\}$. For example, Fourier series of the current J_{A2} is given as

$$J_{A2} \sim \sum_{n=1}^{\infty} a_n \cdot \cos n\theta \cdot I_d \qquad (3\text{-}14)$$

$$a_n = \frac{2}{n\pi} \sin \frac{n\pi}{3} [(-1)^{-1}] \qquad n=1,2,...$$

The fundamental component of the current source J_1, J_2(1,2 ; for each transformer) are illustrated in a vector diagram Fig.3-6. The firing angles are decided based on the infinite bus voltage V^{∞}. Then the n-th order harmonic current source J_{2n} is expressed as follows from Eq.(3-14).

$$J_{2n} = Id \cdot a_n \begin{bmatrix} \cos n[r-(\alpha_2+r_o)] \\ \cos n[(r-2\pi/3)-(\alpha_2+r_o)] \\ \cos n[(r+2\pi/3)-(\alpha_2+r_o)] \end{bmatrix} \qquad (3\text{-}15)$$

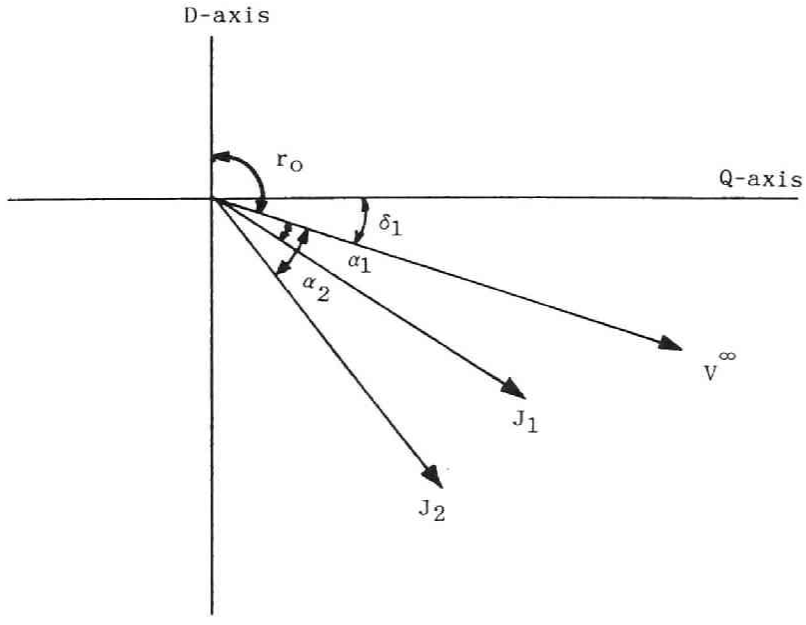

Fig.3-6 Phaser diagram of current source(SMES) for fundamental component.

The electrical angle r is given as $r=\omega_o t + r_o$ in a steady state. The current source J_{2n} is transformed into d-q value as

i) n=3m;

$$\mathbf{J}_{dq2n} = \begin{bmatrix} J_{d2n} \\ J_{q2n} \end{bmatrix} = \mathbf{0} \qquad (3\text{-}16\text{-}a)$$

ii) $n=3m\pm 1$

$$\mathbf{J}_{dq2n} = \begin{bmatrix} J_{d2n} \\ J_{q2n} \end{bmatrix} = I_d \cdot a_n \begin{bmatrix} \cos[(n\mp 1)r - n(\alpha_2+r_o)] \\ \sin[(n\mp 1)r - n(\alpha_2+r_o)] \end{bmatrix} \qquad (3\text{-}16\text{-}b)$$

SMES produce the $6k\pm1$ (k=1,2,..) current theoretical harmonics. Therefore the phase velocity ω appeared in Eq.(3-13) is substituted by $0\cdot\omega_o$(the fundamental), $6\cdot\omega_o$, $12\cdot\omega_o$, …… . Then the input current source $\mathbf{J}_{dq2n}$ (for transformer

No.2) in Eq.(3-13) is obtained as

$$\begin{bmatrix} J_{d2n} \\ J_{q2n} \end{bmatrix} = \frac{1}{\sqrt{2}} Id \cdot a_n \begin{bmatrix} \exp\{j[(n\mp 1)r - n(\alpha_2+r_o)]\} \\ \pm \exp\{j[(n\mp 1)r - n(\alpha_2+r_o)]\} \end{bmatrix} \quad (3\text{-}17)$$

$$n=3m\pm 1$$

The input current source J_{dq1n} (for transformer No.1) leads J_{dq2n} by $\pi/2$ in phase. The input voltage source $e_{p\text{-}dq}$ is considered only for the fundamental component.

3-3-4. CALCULATION FLOW FOR INITIAL VALUE

Figure 3-7 shows a flow chart for calculating initial values.

A] POWER FLOW CALCULATION

In order to get the first approximated values, we calculate the power flows by Newton-Raphson method. It is assumed that SMES is a state load for specified active and reactive powers(Ps,Qs). Commutations of the converters are neglected. The generator is indicated by a internal electromotive voltage V_g (determined by an exciter voltage E_f) and the generator output power $P_e(=P_m)$. The infinite bus is selected as a standard node. By power flow calculation, the terminal voltage vector of SMES is obtained. The phase deference δ_1 between the voltage vector V_g and the infinite bus voltage vector V^∞ is also determined.

When the simulation starts at the time when a-phase voltage of the infinite bus has the maximum value, the initial value of the electrical angle of the generator rotor r is obtained as

$$r_o = \delta_1 + \pi/2 \quad (3\text{-}18)$$

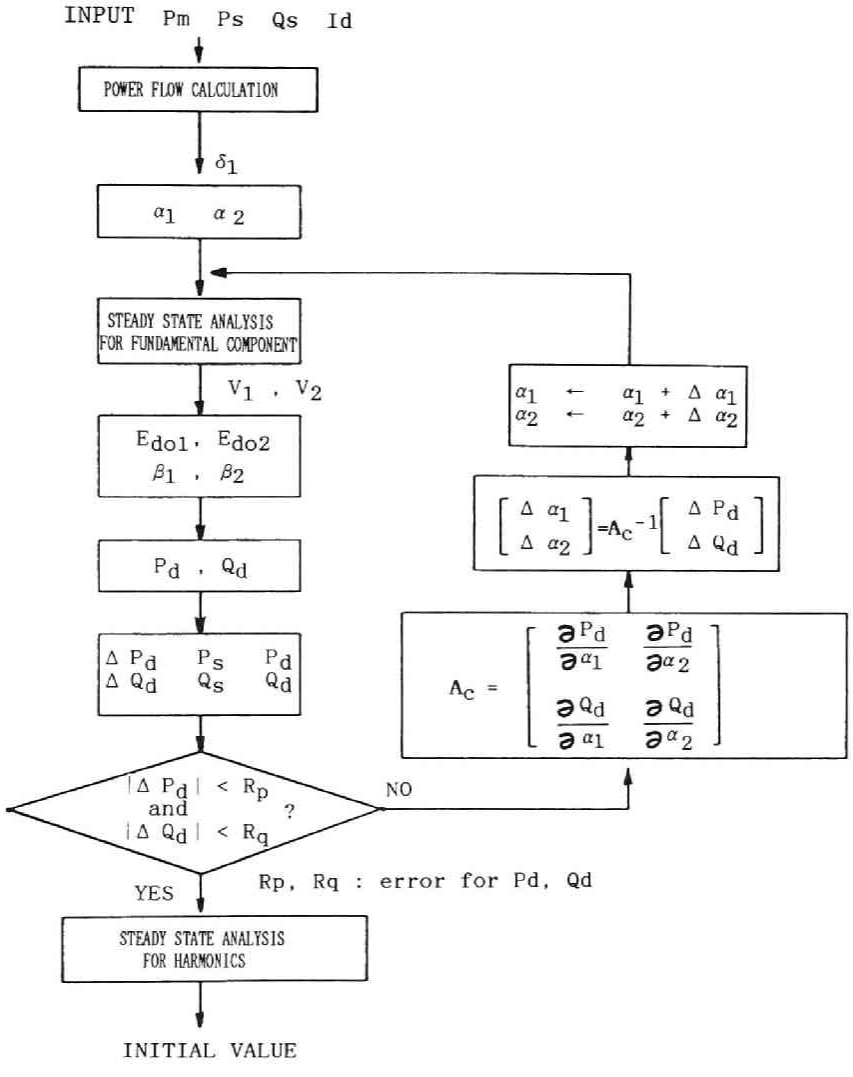

Fig.3-7 Flow chart for initial value calculation.

B] STEADY STATE ANALYSIS FOR FUNDAMENTAL COMPONENT

For the second step, the accurate value of firing angles α_1 and α_2 are determined by the steady state analysis only for the fundamental component.

By use of the rotor angle r_o given by Eq.(3-18) and the current source J_{dq} given by Eq.(3-17), the steady state equation (3-13) is solved for the fundamental component. The r.m.s. value and the phase of line-to-line voltage of the transformer of SMES side (V_i, β_i) can be obtained(i=1,2). When the standard voltage for the firing angle is defined to be the terminal voltage of the transformer of SMES side, the firing angles of each converter are determined as ($\alpha_1+\beta_1$) and ($\alpha_2+\beta_2$), respectively. Since the average direct voltage at no-load Edo_i is written as

$$Edo_i = \frac{3\sqrt{2}}{\pi} V_i \qquad (3\text{-}19)$$

The active power Pd and the reactive power Qd (calculated at the DC side) are given as

$$Pd=P_{d1}+P_{d2} \quad ;P_{di}=[Edo_i \cos(\alpha_i+\beta_i)-R_{th}Id]Id \qquad (3\text{-}20)$$

$$Qd=Q_{d1}+Q_{d2} \quad ;Q_{di}=[(Edo_i Id/2)^2 - Pd_i^2]^{1/2} \qquad (3\text{-}21)$$

The powers Pd and Qd obtained by Eq.(3-20) and (3-21) are not equal to those of the power flow calculation. It is because;

1]voltage drop and phase shift at the SMES terminal are not taken into consideration in the power flow calculation

2]feedback loop of the SMES's controller are not taken into consideration in the power flow calculation.

Then we should re-correct the firing angles so that the active power Pd become equal to the specified power Ps and, at the same time, the reactive power Qd become equal to the specified value Qs.

From Eq.(3-20),(3-21), new firing angles α_i are obtained as follow. For simplification, Edo_i and β_i are assumed to be independent from firing angle α_i. The derivatives of active and reactive powers with the firing angles α_i are

$$A_c = \begin{bmatrix} \frac{\partial Pd}{\partial \alpha_1} & \frac{\partial Pd}{\partial \alpha_2} \\ \frac{\partial Qd}{\partial \alpha_1} & \frac{\partial Qd}{\partial \alpha_2} \end{bmatrix} = \begin{bmatrix} -Edo_1 Idsin(\alpha_1+\beta_1) & -Edo_2 Idsin(\alpha_2+\beta_2) \\ \frac{Pd}{Qd} Edo_1 Idsin(\alpha_1+\beta_1) & \frac{Pd}{Qd} Edo_2 Idsin(\alpha_2+\beta_2) \end{bmatrix} \quad \ldots(3\text{-}22)$$

By neglecting the higher order terms, the deviation of Pd, Qd, α_1 and α_2 are written as

$$\begin{bmatrix} \Delta \alpha_1 \\ \Delta \alpha_2 \end{bmatrix} = A_c^{-1} \begin{bmatrix} \Delta P_d \\ \Delta Q_d \end{bmatrix} \quad (3\text{-}23)$$

The new firing angles are obtained by power errors (Ps-Pd) and (Qs-Qd) from Eq.(3-23).

The steady state analysis for the fundamental component are performed again using the new firing angles. The re-correcting loop are repeated in order to diminish the errors of the powers to a certain rate.

C] STEADY STATE CALCULATION FOR HIGHER HARMONICS

When the firing angles α_1 and α_2 are obtained by this algorithm, the current sources J_{dq} of each order of harmonics can be determined. The steady state solutions for each order of

harmonics is obtained from Eq.(3-13).

The simulation can begin at an arbitrary time without large jump in state variables by using this initial values. Here, however, one should note that it is better to start the simulation at the time when each converter are not in a commutating state.

3-4. SIMULATION ANALYSIS OF ONE GENERATOR-INFINITE BUS SYSTEM WITH SMES

3-4-1. EQUIVALENT CIRCUIT FOR EXPERIMENTAL SYSTEM

The equivalent circuit for the experimental circuit(shown in Fig.5-1) is shown in Fig.3-8. For simplification, the transformers in the transmission line 3300/220 are assumed to be the ideal transformers. The transmission lines are represented as resistors and reactors. The generator does not have the damper winding. The specified values used in the simulation are shown in Table 3-1. Under the above conditions,

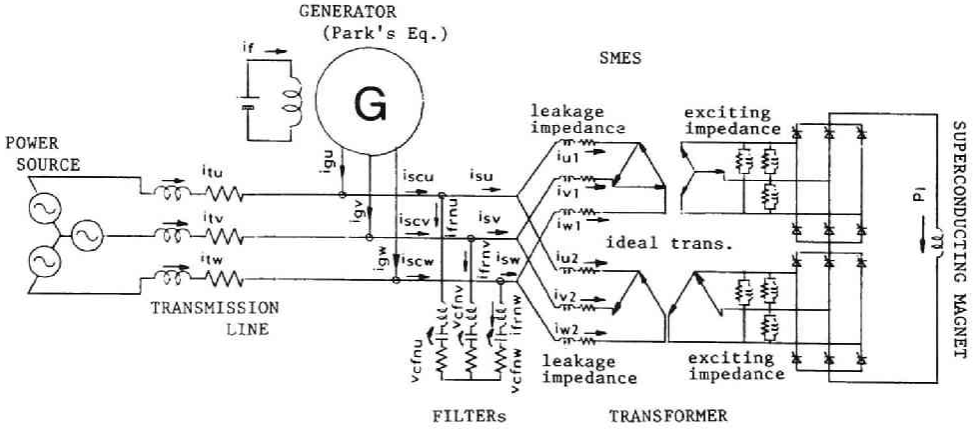

Fig.3-8 Equivalent circuit for experimental system
(corresponding to experimental system as shown in Fig.5-1)

Table 3-1 Specified values for simulation.

GENERATOR:			
SYNCHRONOUS INDUCTANCE	L_d	3.96×10^{-2}	[H]
ARMATURE RESISTANCE	R_a	3.45×10^{-1}	[Ω]
SELF INDUCTANCE OF FIELD WINDING	L_{ffd}	6.87×10^{-2}	[H]
MUTUAL INDUCTANCE OF ARMATURE AND FIELD	M_{afd}	3.97×10^{-2}	[H]
FIELD RESISTANCE	R_f	6.87×10^{-1}	[Ω]
INERTIA CONSTANT	M	23.2	[kWsec]
TRANSFORMER:			
LEAKAGE INDUCTANCE(upper)	L_1	5.89×10^{-4}	[H]
LEAKAGE INDUCTANCE(lower)	L_2	5.95×10^{-4}	[H]
WINDING RESISTANCE(upper)	R_1	1.04×10^{-1}	[Ω]
WINDING RESISTANCE(lower)	R_2	1.08×10^{-1}	[Ω]
EXCITING INDUCTANCE(upper)	L_{s1}	5.02×10^{-4}	[H]
EXCITING INDUCTANCE(lower)	L_{s2}	6.50×10^{-4}	[H]
EXCITING RESISTANCE(upper)	R_{s1}	4.42×10^{-1}	[Ω]
EXCITING RESISTANCE(lower)	R_{s2}	6.89×10^{-1}	[Ω]
INDUCTANCE OF SUPERCONDUCTING MAGNET	L_{scm}	10.8	[H]
RESISTANCE OF THYRISTOR(CONDUCTING)	R_{thy}	1.0	[mΩ]

PASSIVE FILTER:

ORDER	L_F[mH]	C_F[μF]	R_F[Ω]
5	2.814	100	0.379
7	2.872	50	0.474
11	2.908	20	0.496
13	2.082	20	0.392

the state variable vector $\mathbf{x}_{p-dq}$ of power system in Eq.(3-3) are $[i_{dg}, i_{d1}, i_{d2}, i_{dfrn}, i_f, i_{qg}, i_{q1}, i_{q2}, i_{qfrn}, v_{dcfn}, v_{qcfn}]^t$. The current i_{dg} and i_{qg} are the generator armature current. The current i_{d1}, i_{d2}, i_{q1} and i_{q2} are the leakage inductor current of the SMES's transformers, the current i_{dfrn}, i_{qfrn} and the voltage v_{dcfrn}, v_{qcfrn} are the inductor current and the capacitor voltage of the n-th order passive filters. The current i_f is the field current of the generator. The voltage source vector $\mathbf{e}_{p-dq}$ is $[V^{\infty}{}_d, V^{\infty}{}_q, E_f]^t$. The voltage $V^{\infty}{}_d$, $V^{\infty}{}_q$ are the infinite bus voltage and the voltage E_f is the exciting voltage. The voltage source vector $\mathbf{v}_{p-dq}$ which is decided by the solutions of the state equations for SMES is $[v_{d1}, v_{d2}, v_{q1}, v_{q2}]^t$.

3-4-2. EXAMPLE OF INITIAL VALUE CALCULATION

One of the results of the calculation for the initial values is shown in Fig.3-9. The output active power of the generator is 1.0[kW], the field current i_f is 12[A], the active power Ps and the reactive power Qs of SMES are 1.0[kW] and 3.7[kVar], respectively. The wave forms are shown when the superconducting magnet current Id is 100[A]. The symbols i_{u1}, i_{u2} are the transformer leakage inductor currents, i_{gu} is the generator armature winding current. The passive filter is not installed. The solutions for the fundamental and the 5-th, 7-th, 11-th, 13-th order harmonics components are superposed together. The harmonic currents generated by SMES flow into the generator. The field current i_f has distortion.

3-4-3. SIMULATION RESULTS AND DISCUSSIONS

Figure 3-10 shows one of the simulation results. The conditions are ; the generator output power is 1.0[kW] and the field current i_f=12.0[A]. The transmission line reactance is 10[%] (6[kVA],220[V]). SMES is operated by the power control

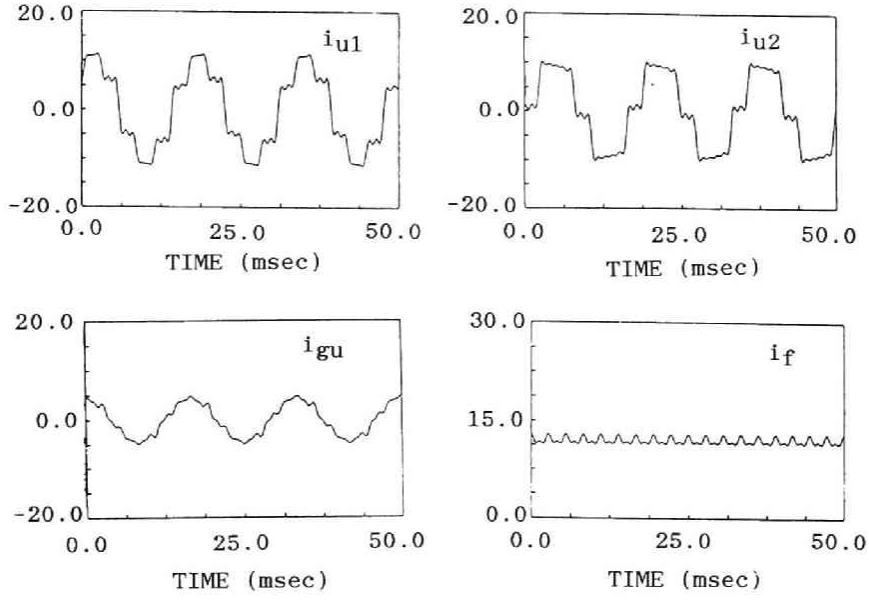

Fig.3-9 Result of steady state analysis for initial values assuming SMES as current source.
i_{u1}:leakage inductor current of upper transformer
i_{u2}:leakage inductor current of lower transformer
i_{gu}:generator armature current
i_f :generator field current

with (Ps,Qs)=(1.0[kW],3.5[kVar]). The wave forms of the voltages and the currents are at the magnet current Id=100[A]. The commutation process is clearly expressed in the wave form of the superconducting magnet voltage and the AC terminal voltage. The wave form of field current i_f shows that it is affected by commutation of SMES's converters.

The result of the harmonic analysis is shown in Fig.3-11. The current of SMES i_{su} contains the theoretical harmonics. The harmonic current distributed to the generator and the infinite bus through the transmission line. The field current i_f contains the ripples of the 6-th and the 12-th components. They are caused by the harmonics of the armature current i_{gu}. The 6-th is caused by the 5-th and the 7-th components and the 12-th is caused by the 11-th and the 13-th components.

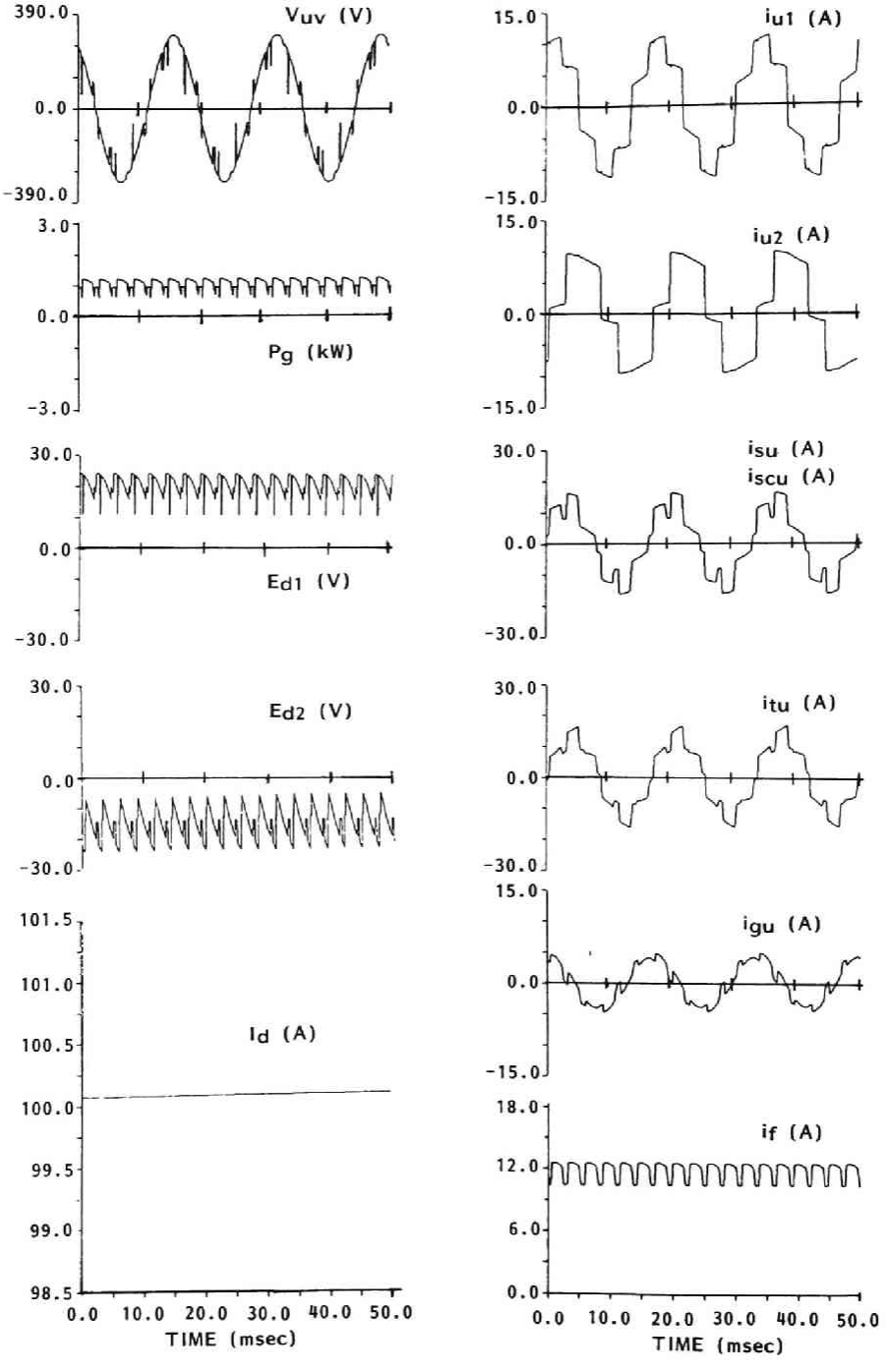

Fig.3-10 Simulation result without filters
P_g = 1.0[kW], i_f = 12.0[A]
Ps = 1.0[kW](charging), Qs = 3.5[kVar]
X_L = 10[%]

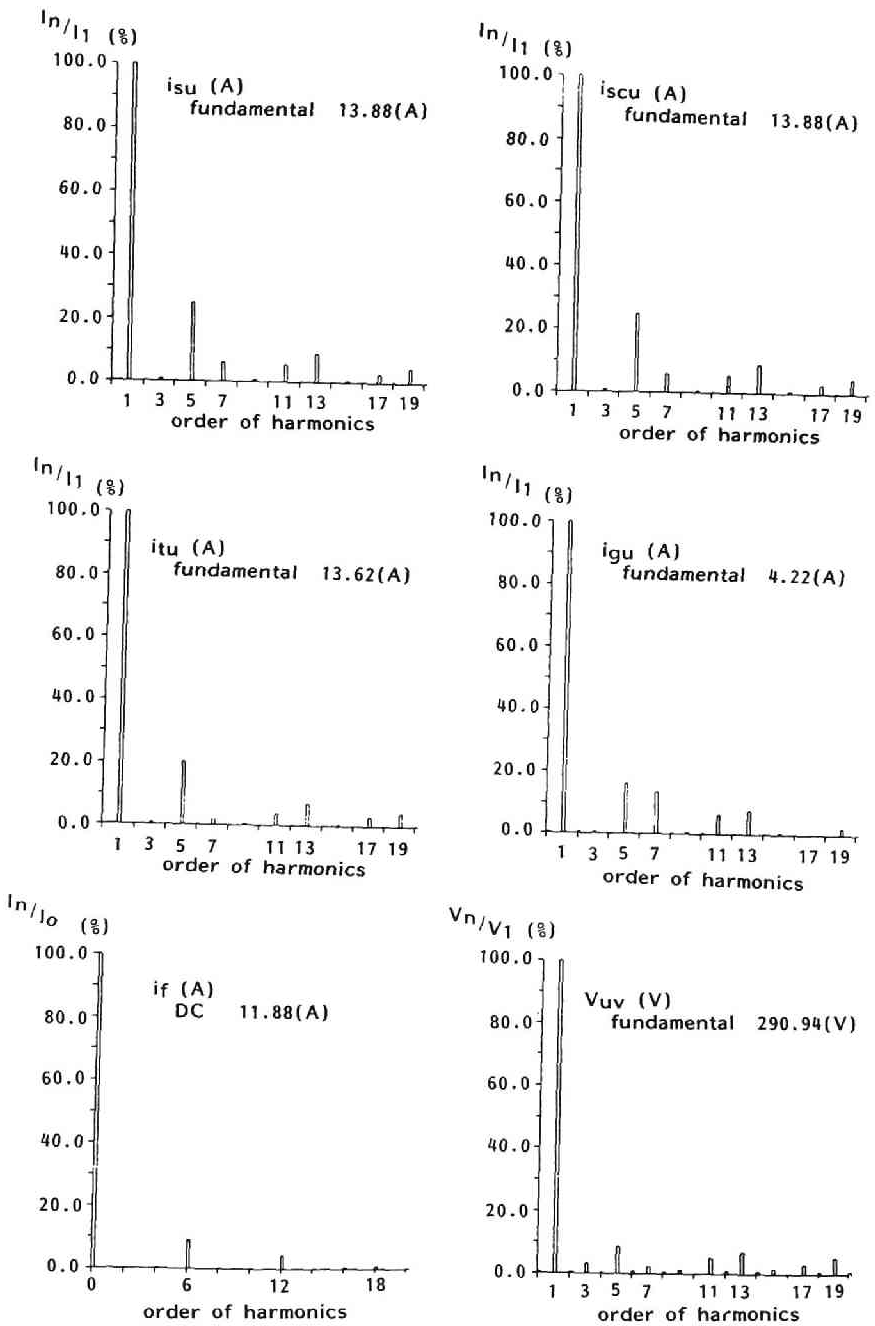

Fig.3-11 Harmonic component of voltages and currents in Fig.3-10.

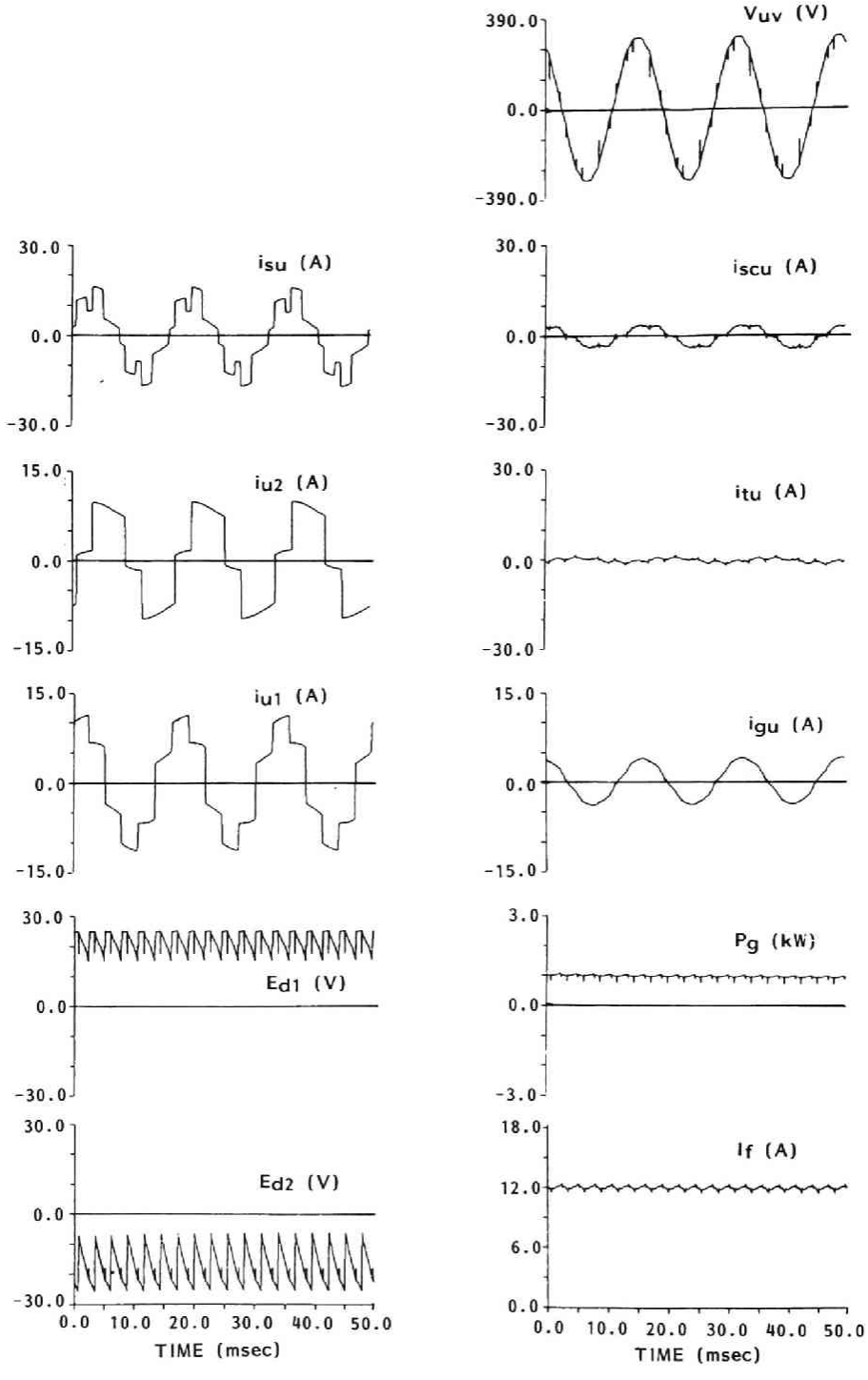

Fig.3-12 Simulation result with filters (a)
P_g = 1.0[kW], i_f = 12.0[A]
Ps = 1.0[kW](charging), Qs = 0.0[kVar]
X_L = 10[%]

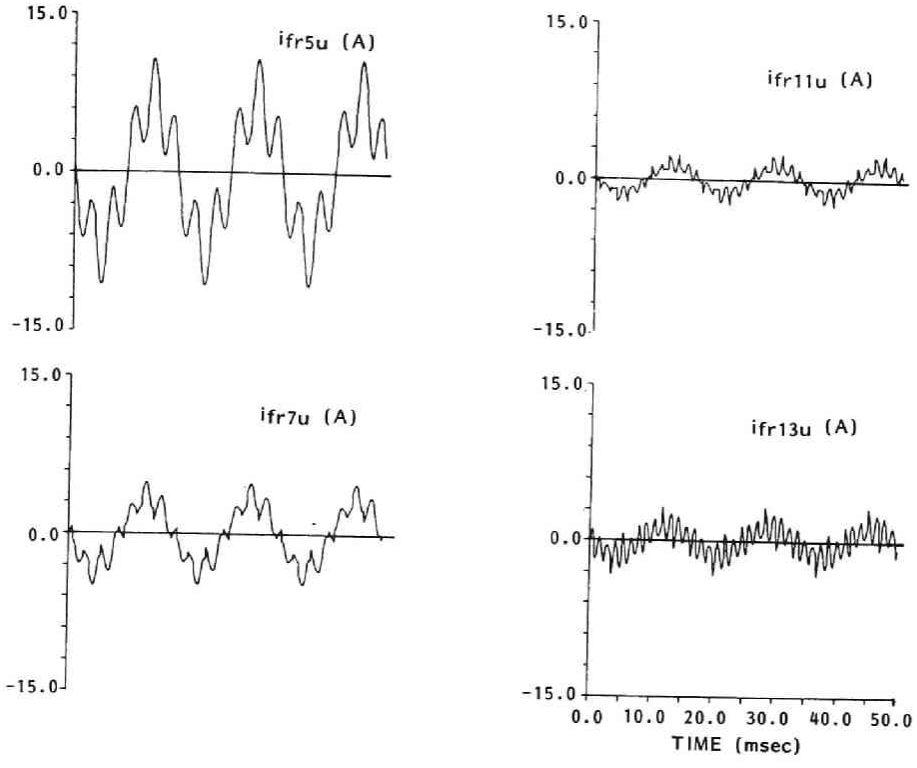

Fig.3-12 Simulation result with filters (b) filter currents
P_g = 1.0[kW], i_f = 12.0[A]
Ps = 1.0[kW](charging), Qs = 0.0[kVar]
X_L = 10[%]

The passive filters are set in order to remove distortions. One of the simulation results is shown in Fig.3-12. Harmonics of generator armature current i_{gu} appeared in Fig.3-10 are reduced as shown in the figure. The fluctuation of generator field current i_f is also reduced. Each filter current is shown in Fig.3-12 (b). The performance of the filters is clearly expressed. Harmonic components of each voltages and currents are shown in Fig.3-13 (a) and (b). It is found that each filter current has fundamental component (corresponding to the reactive power it produces) and each order component.

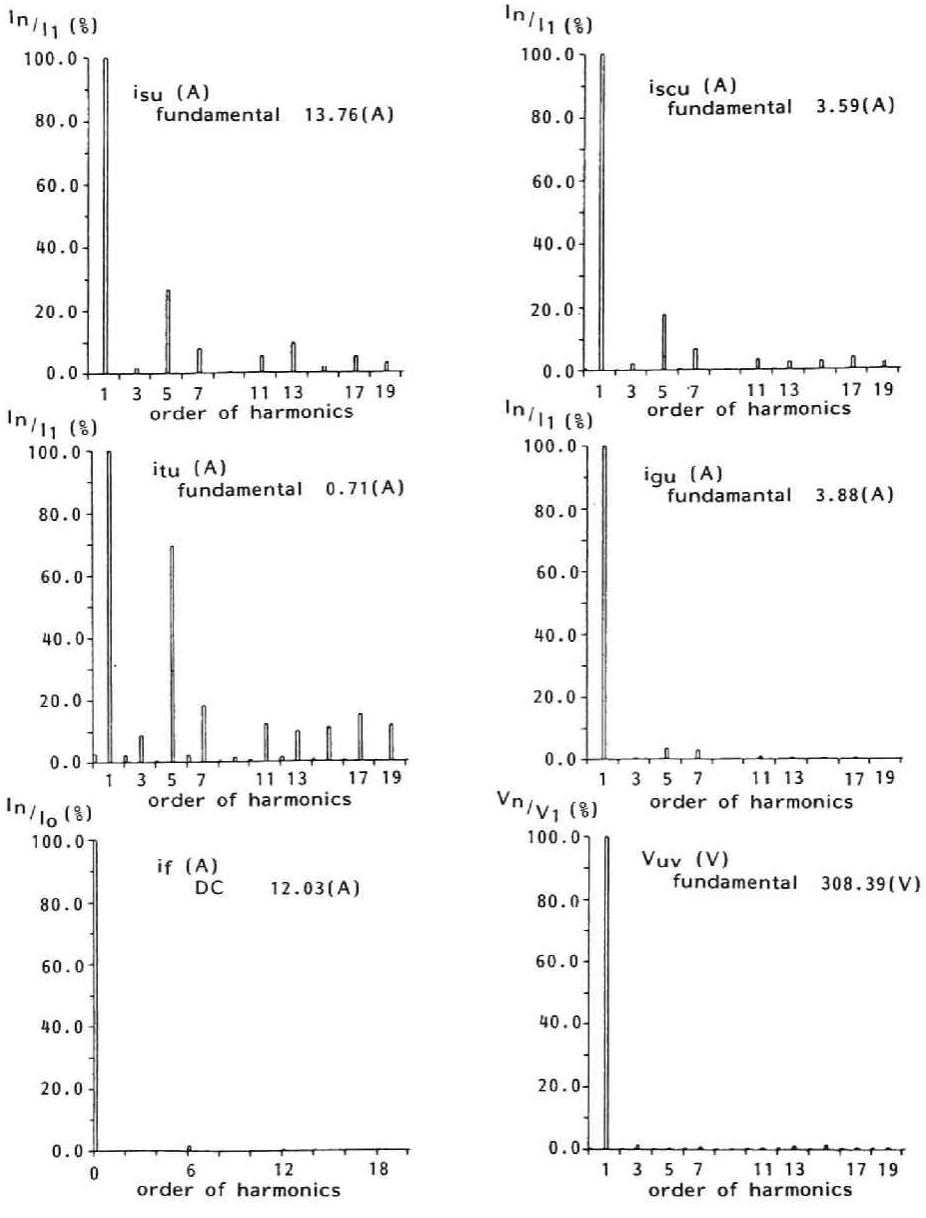

Fig.3-13 Harmonic component of voltages and currents in Fig.3-12 (a)

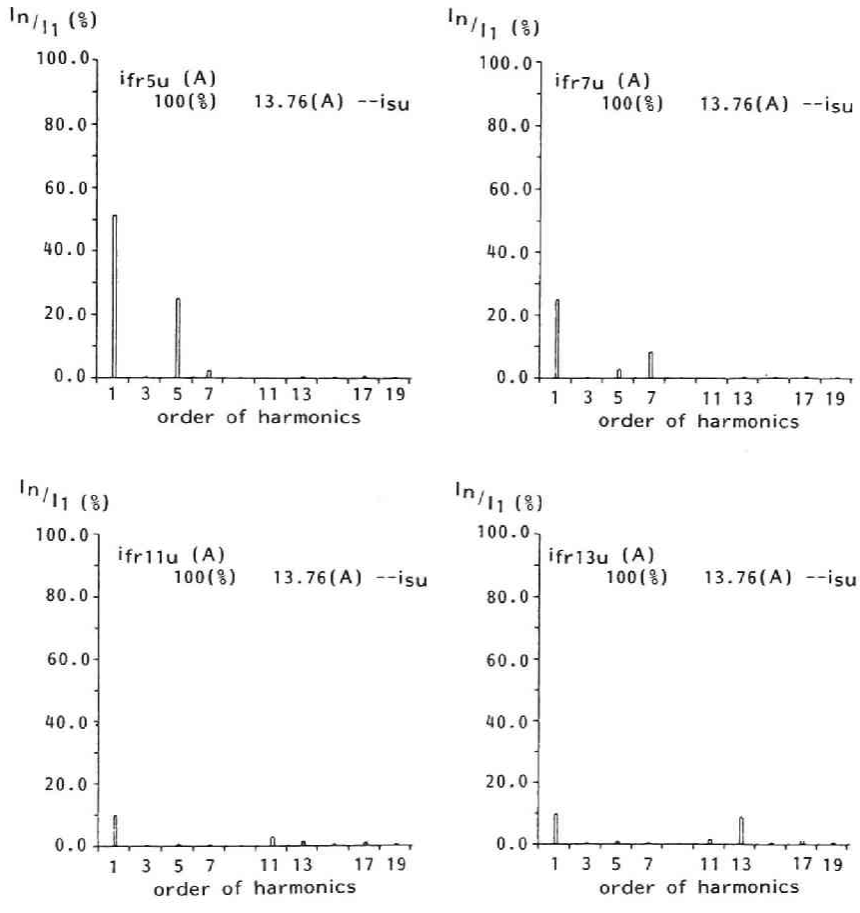

Fig.3-13 Harmonic component of voltages and currents in Fig.3-12 (b)

The simulation code can demonstrate in a long time range. For example, the power flows of the generator and SMES are shown in Fig.3-14. The active power of SMES is controlled to be a sinusoidal wave of frequency (a)2.0[Hz], (b)0.7[Hz]. The output power of generator becomes to swing drawn by SMES.

It is confirmed that the simulation results agree well with those of experiments described in Chapter 4 and 5.

By use of the simulation code, the problems on the power system including SMES is studied in Chapter 4 and Chapter 5.

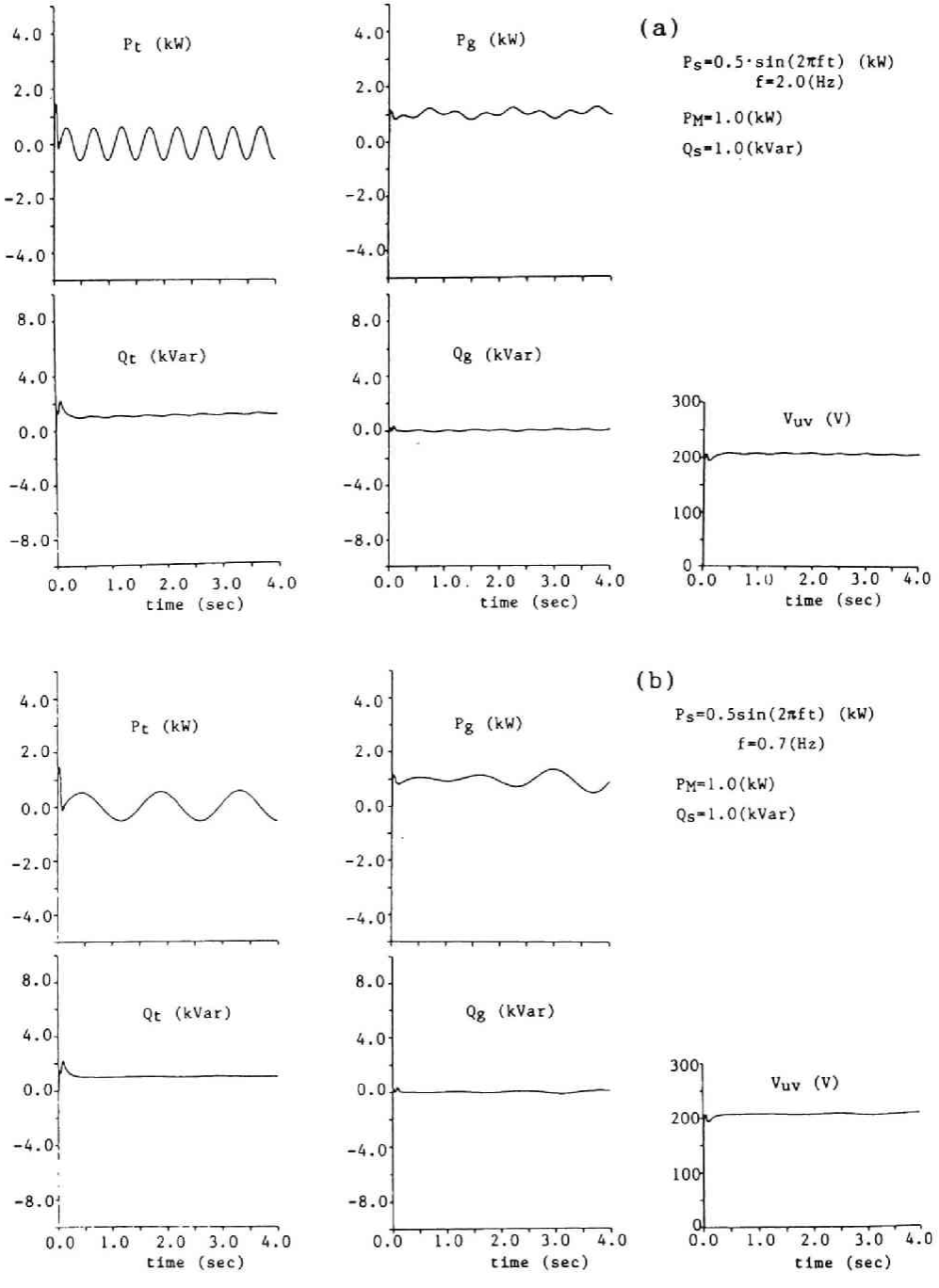

Fig.3-14 Simulation results for power swing of generator.

SMES sinusoidal active power
constant reactive power
Generator P_M = 1.0[kW], i_f = 12[A]
Filters :installed

3-5. CONCLUDING REMARKS

When SMES having a capacity comparable to power systems is operated in power system, the wave forms of voltages and currents show complex variations. Therefore it is impossible to consider SMES to be a static load.

For exact understanding the characteristics of, and the problems on SMES, computer simulation study is necessary.
In this Chapter, the following results are obtained.

[1] We propose a convenient method that a set of state equations for power system and SMES is separated by using equivalent circuit of SMES's transformers. Then we only prepare several set of equations of every commutation modes for SMES and one set of the state equations for power system. Therefore even when configuration or situation of power system change, only equations for power system which can easily obtained independently of the commutation of the converters, should be reformed.

[2] Since a operation of SMES is always in a transient state, it is necessary to determine initial values for simulation for saving computation time. A method for determining the initial values is introduced. By use of the initial values determined by the method, the simulations can start successfully.

[3] Using the above method, the computer simulation for the experiments was carried out. It can express the effects of SMES's operations on the characteristics of generator, that is, fluctuation of field current and generator swings drawn by SMES. A performance of filters can be simulated by the code. The simulation results agree well with those of the experiments described in Chapter 4 and 5.

In the simulation, unbalance of three phase system, change of reference voltage to determine firing angles and so on are neglected, which appear in experiment or real systems. It may be necessary to investigate how they affect SMES operation.

By use of the simulation code, the problems on the power system including SMES is studied in Chapter 4 and Chapter 5.

CHAPTER.4

POWER CHARGING AND DISCHARGING CHARACTERISTICS OF SMES CONNECTED TO INFINITE BUS THROUGH TRANSMISSION LINE[13)-(15)]

4-1. INTRODUCTION

Power characteristics of SMES in power system whose capacity is considered to be so large that SMES is assumed to be connected to an infinite bus are studied and discussed experimentally in Chapter 2. In real power systems, however, capacity of SMES as an energy storage plant is considered to be not so small compared with those of power systems. It is not considered to be an usual case that SMES is located near large power source. When SMES is installed at a certain point of transmission lines like a pumped hydro plants, it is necessary to take impedances of power systems viewed from terminal of SMES into account.

As a typical example for above mentioned condition, characteristics of SMES connected to an infinite bus through transmission lines are investigated in this chapter. The problems to study are;

[1]Power characteristics of SMES connected to an infinite bus through transmission lines.
[2]Power characteristics of SMES with reactive power compensator
[3]Characteristics of harmonic currents of SMES and its influences on operation of SMES.
[4]How to compensate lagging reactive power of SMES.
[5]How to suppress harmonic currents of SMES.

For the problems [4] and [5], some considerations are reported;

a) Leading or lagging reactive power of SMES is controlled by use of forced commutating power converter.[22]

b) A reactive power of SMES is reduced by changing converter arrangement.

c) Harmonic currents of SMES are suppressed by use of power filters (active or passive type)

Here, passive filters which also compensate reactive power are investigated. They are used now in HVDC(high voltage direct current transmission lines). Passive filters are used for a basic consideration on suppressing higher harmonics and compensating lagging reactive power.

Power system characteristics of SMES with filters to suppress current harmonics and to compensate lagging reactive power are considered by experiments and simulations.

An active power filter by use of superconducting magnet is also introduced. The fundamental tests were carried out.

4-2. EXPERIMENTAL SYSTEM

In order to approach the above mentioned problems, experiments were carried out by use of the artificial transmission line system and SMES system described in Chapter 2.

A configuration of experimental system is shown in Fig.4-1, where the superconducting magnet(10.8[H], 141[A]) is connected to the regional power system (considered as an infinite bus) through thyristorized converters, transformers and artificial transmission lines.

The rated capacity of transmission line system is 6[kVA] and base voltage is 220[V]. SMES system is connected to transformer (220/3300). Impedance of 3300[V] transmission line system can be changed. Transmission line of impedance 10[%] means that it is 200[km] long.

Passive filters which are also reactive power compensators are connected to the terminal of transformer (SMES system). Designs of the filters are discussed in Section 4-4-2.

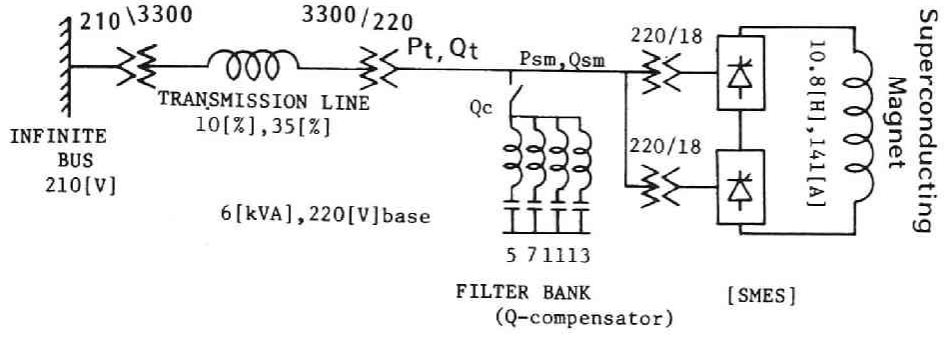

Fig.4-1 Configuration of experimental system

The active and the reactive power of SMES are controlled according to the following functions.

$$\left.\begin{aligned} Pr &= Ps + K_{ip}\int (Ps-Pt) \\ Qr &= Qs + K_{iq}\int (Ps-Pt) + Qc \end{aligned}\right\} \quad (4\text{-}1)$$

where Ps and Qs are specified active and reactive powers, respectively. A reactive power Qc is one which passive filters supply. An active power Pt and a reactive power Qt which are feedback value for controller are measured at AC terminal of SMES by power meters. Firing angles for double thyristorized converters are determined by controller from reference powers Pr and Qr and magnet current Id as mentioned in chapter 2.

4-3. POWER CHARACTERISTICS OF SMES WITH REACTIVE POWER COMPENSATOR

4-3-1. POWER CHARACTERISTICS OF SMES CONSIDERING TRANSMISSION LINE IMPEDANCE

In this section, power characteristics of SMES connected to an infinite bus through transmission lines are discussed. The terminal voltage of SMES varies with operations of SMES(including reactive power compensator) due to transmission lines impedance. Therefore, in such a system, power characteristics of SMES are affected by transmission line impedance (that is, transmission line length) and reactive power compensator. Here, we studied the above problems.

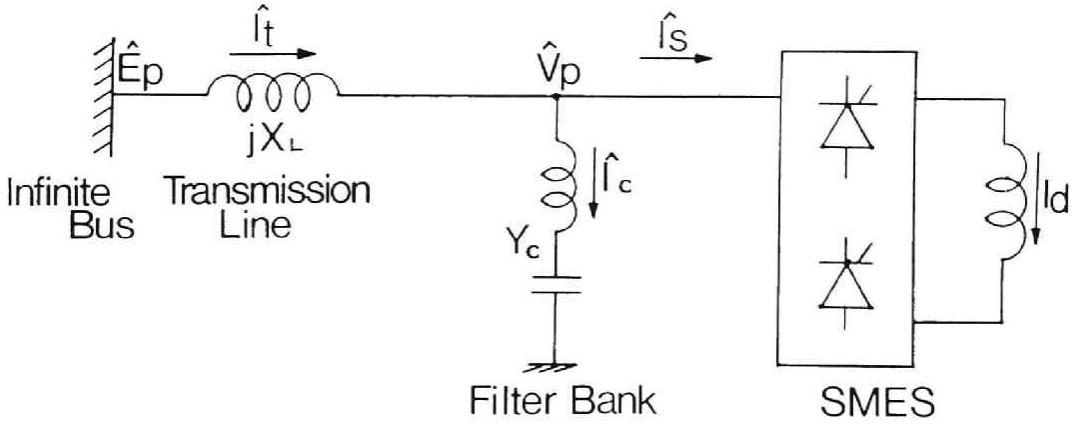

Fig.4-2 Skeleton of experimental system

Figure 4-2 shows a schematic diagram of considered system(refer to the experimental system shown in Fig.4-1). For simplification, discussions are on the basis of the following assumptions;

1) inductance of superconducting magnet is infinite.

2) commutation period is neglected.

3) higher harmonics is neglected. (that is, only the fundamental component is taken into account.)

That is,

4) harmonics generated by SMES is assumed to be suppressed completely by filters.

5) SMES is considered to be a static load.

When the superconducting magnet current is Id, the r.m.s. values of transformer currents I_{s1} and I_{s2} ($\hat{I}_s=\hat{I}_{s1}+\hat{I}_{s2}$) are obtained as

$$I_{s1} = I_{s2} = \frac{\sqrt{6}}{\pi}\frac{m_1}{m2} Id \qquad (4\text{-}2)$$

$\frac{m_1}{m_2}$: turn ratio of transformer

In case of firing angles are α_1 and α_2 and a terminal voltage vector $\hat{V}_p$ is selected as a base vector, SMES's AC current $\hat{I}_s$ and a current of the reactive power compensator $\hat{I}_c$ are given as

$$\hat{I}_s = (I_{s1}\cos\alpha_1+I_{s2}\cos\alpha_2)+j(I_{s1}\sin\alpha_1+I_{s2}\sin\alpha_2) \qquad (4\text{-}3)$$

$$\hat{I}_c = jY_cV_p \qquad (4\text{-}4)$$

where Y_c denotes an admittance of a reactive power compensator and $\hat{E}_p$ is an infinite bus phase voltage.

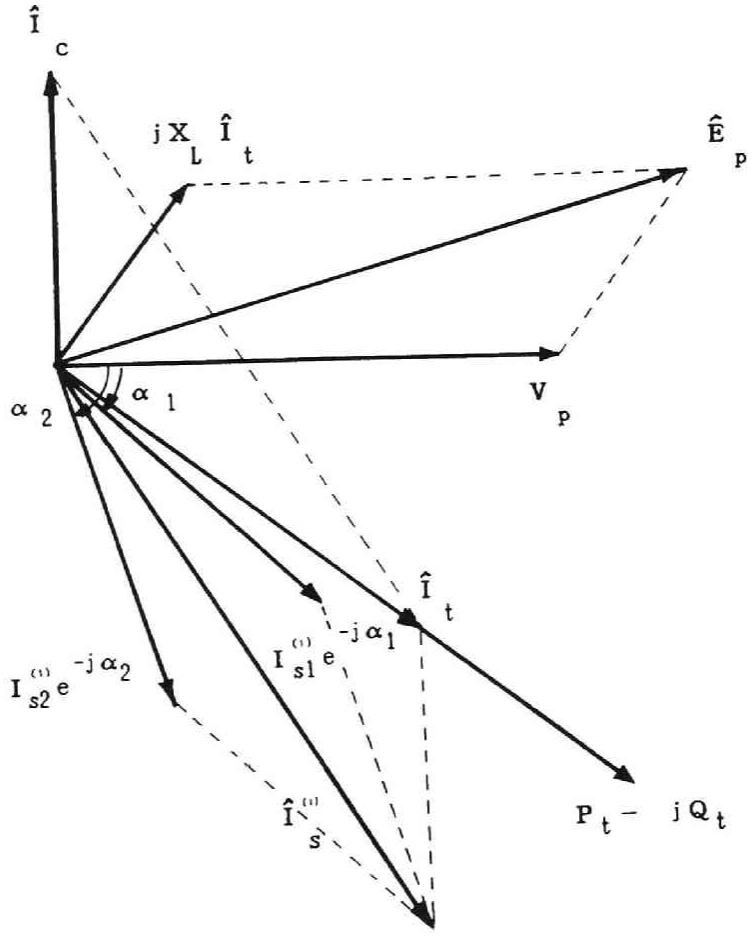

Fig.4-3 Phaser diagram of test system

The phaser diagram is shown in Fig.4-3, where X_L is a reactance of a transmission line. The terminal phase voltage Vp can be obtained as

$$\hat{E}_p - V_p = jX_L\hat{I}_t = jX_L(\hat{I}_s+\hat{I}_c) \qquad (4\text{-}5)$$

The active power and the reactive power of SMES including the reactive power compensator(filters) are given as

$$P_t - jQ_t = 3V_p\hat{I}_t \qquad (4\text{-}6)$$

The terminal voltage V_p changes according to the transmission line current $\hat{I}_t$.

The possible region for the active and reactive power simultaneous controls can be obtained in the same manner as mentioned in Chapter 2.

The characteristics of the terminal voltage V_p can be also obtained. (P-V characteristics of SMES: see Fig.4-4 or 4-5) When SMES is operated at a certain active power, it is desirable to keep a terminal voltage of SMES to be constant. P-V characteristics show a possible region for such a control. In the following sections, we discuss how transmission impedance and reactive power compensator effect on the P-Q and P-V characteristics of SMES.

4-3-2. TRANSMISSION LINE IMPEDANCE

The P-Q and the P-V characteristics of SMES by considering transmission line impedance are discussed by use of experimental system. Figure 4-4 (a) and (b) show Pt-Qt and Pt-V_p characteristics of SMES with magnet current Id(=60, 100 and 140[A]) where line reactance is (a)10[%] and (b) 35[%], respectively. No reactive power compensator is installed. The larger the line reactance X_L is, the larger the terminal voltage drop is and the smaller the Pt-Qt simultaneous controllable region is. In case of the line reactance 35[%], the terminal voltage decreases to be almost 60[%] of rated voltage (220[V]) at Id=140[A] and Pd=0.0[kW]. SMES cannot operate normally with such a low voltage. A reactive power compensator is necessary.

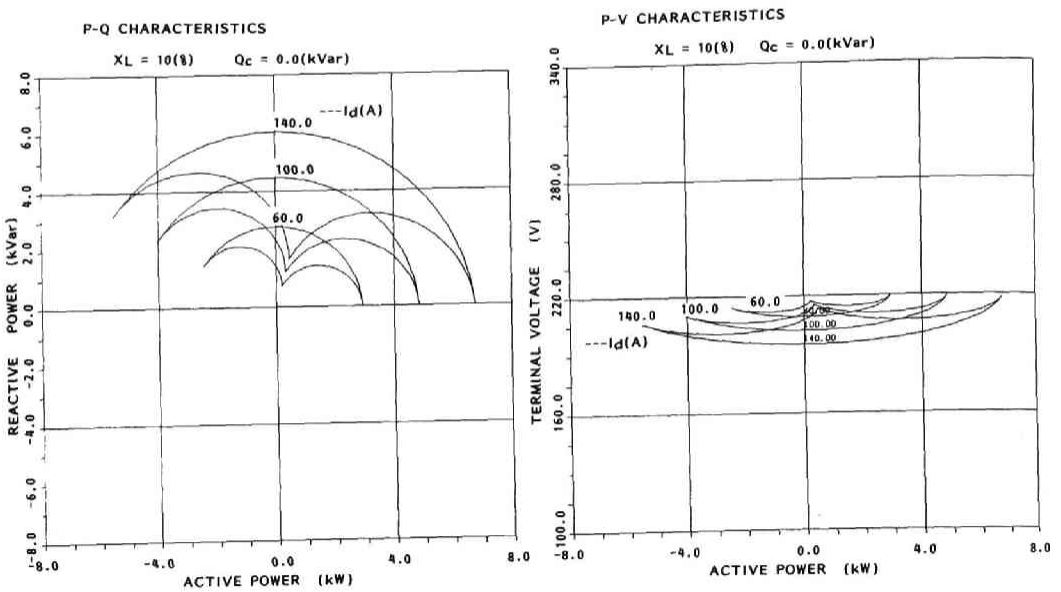

(a)transmission line reactance X_L=10[%]

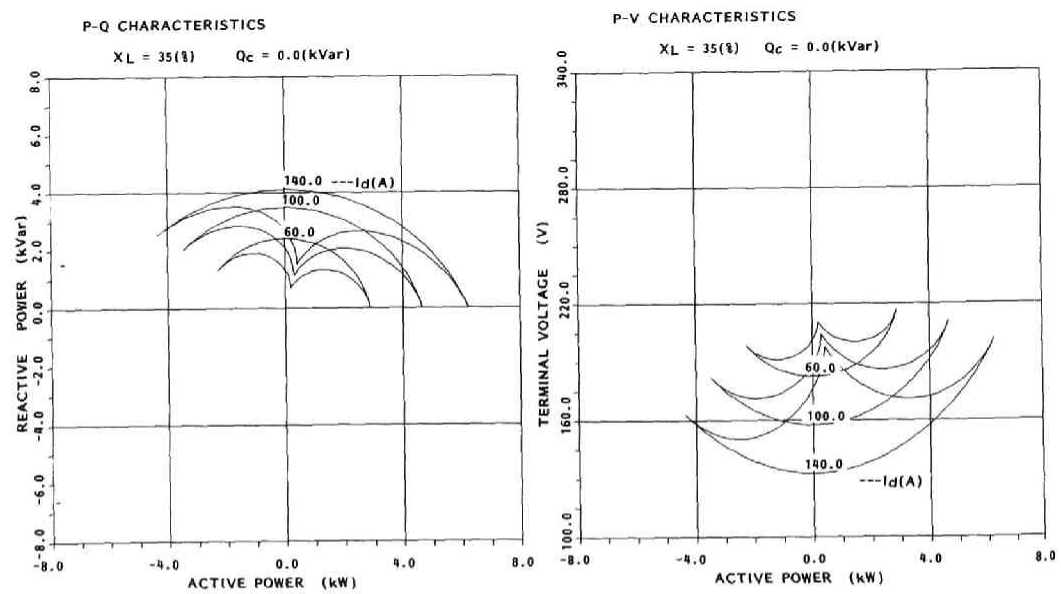

(b)transmission line reactance X_L=35[%]

Fig.4-4 Active and reactive power characteristics and active power and terminal voltage characteristics

4-3-3.REACTIVE POWER COMPENSATION[16]

Here, effects of a reactive power compensator on Pt-Qt and Pt-V_p characteristics are considered. Figure 4-5 shows the Pt-Qt and Pt-V_p characteristics of SMES where a capacity of a reactive power compensator is (a)1.0[kVar](0.17p.u.) (b)3.5[kVar] (0.58p.u.) with line reactance 35[%]. From Fig.4-5 (b), it is found that the terminal voltage can be kept 220[V] for a proper set of Pt and Qt.

The area S of the Pt-Qt simultaneous controllable region at magnet current 100[A] is shown in Fig.4-6 as a function of the line reactance X_L with Q_c(capacity of reactive power compensator). The area S is normalized by the area where the line reactance is zero.

When a line reactance is 0.3 p.u., the area S of Pt-Qt simultaneous controllable region is almost half of that of X_L=0.0p.u.(S_O). However, when a reactive power compensator (capacity :Q_C=0.5p.u.) is set to the terminal of SMES, the ratio S/S_O becomes up to 1.0.

A capacity of filters (one of reactive power compensators) is determined under the above discussions in Section 4-4-2.

4-4. PASSIVE FILTER

4-4-1. CURRENT HARMONICS[17]

In power controls of SMES with thyristorized converters, firing angles vary with time. Even if active power is controlled to be constant, wave forms of AC currents vary with time. Furthermore in active and reactive power simultaneous controls, wave forms of AC currents have more complex variations. Ratios of harmonics in AC current change with time and operating conditions of SMES. In order to design

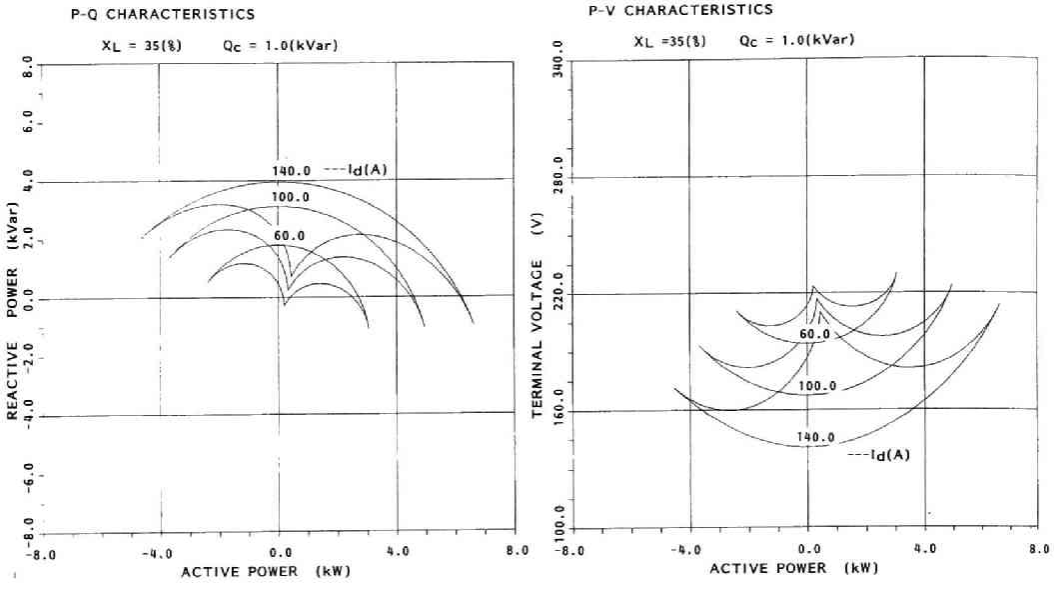

(a)transmission line reactance X_L=35[%],
reactive power compensated Q_C=16.7[%](1.0[kVar])

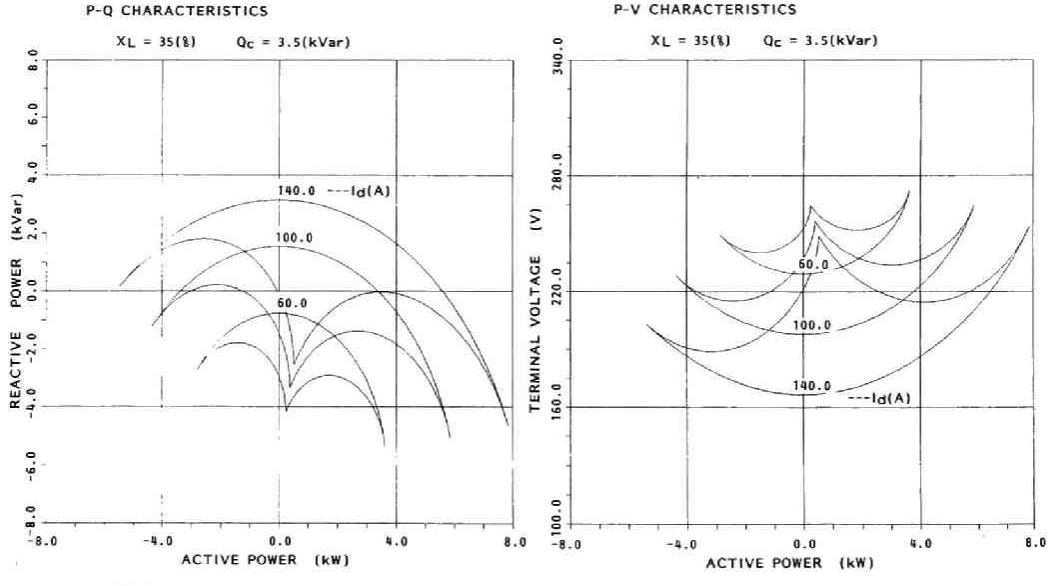

(b)transmission line reactance X_L=35[%],
reactive power compensated Q_C=58.3[%](3.5[kVar])

Fig.4-5 Active and reactive power characteristics and active power and terminal voltage characteristics with reactive power compensator.

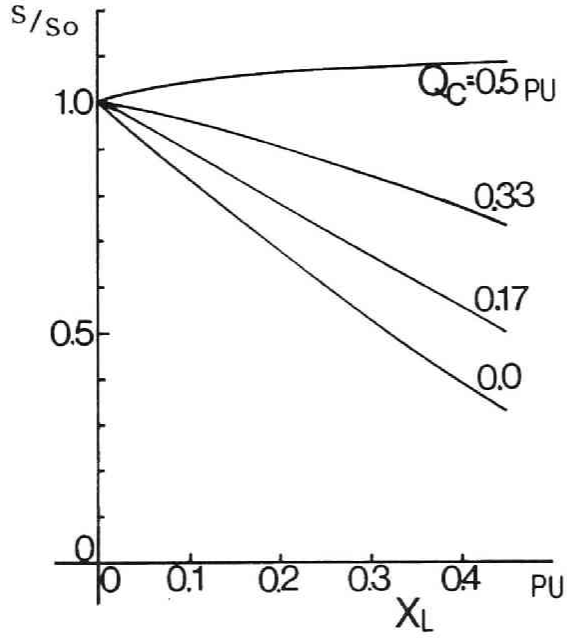

Fig.4-6 Area S of Pt-Qt simultaneous control region corresponding to line reactance X_L with parameter Q_C(capacity of reactive power compensator)

filters for suppressing current harmonics, characteristics of current harmonics evolved at operation of SMES are examined and discussed.

Theoretical harmonics

Assumed that inductance of a superconducting magnet is infinite and commutating reactance can be neglected, SMES is considered to be a current source. Wave forms of AC currents through high voltage terminals of transformers are of square shapes. (see Fig.4-7) In Fig.4-7, a sinusoidal wave shows a u-phase voltage of transformers. The upper wave I_{s1} shows a current flowing into the upper transformer and the lower one I_{s2} shows the current for the lower transformer. The dotted waves is in case of $\alpha_1=\alpha_2=0$. When each thyristorized converter is controlled with firing angles α_1 and α_2, respectively, the

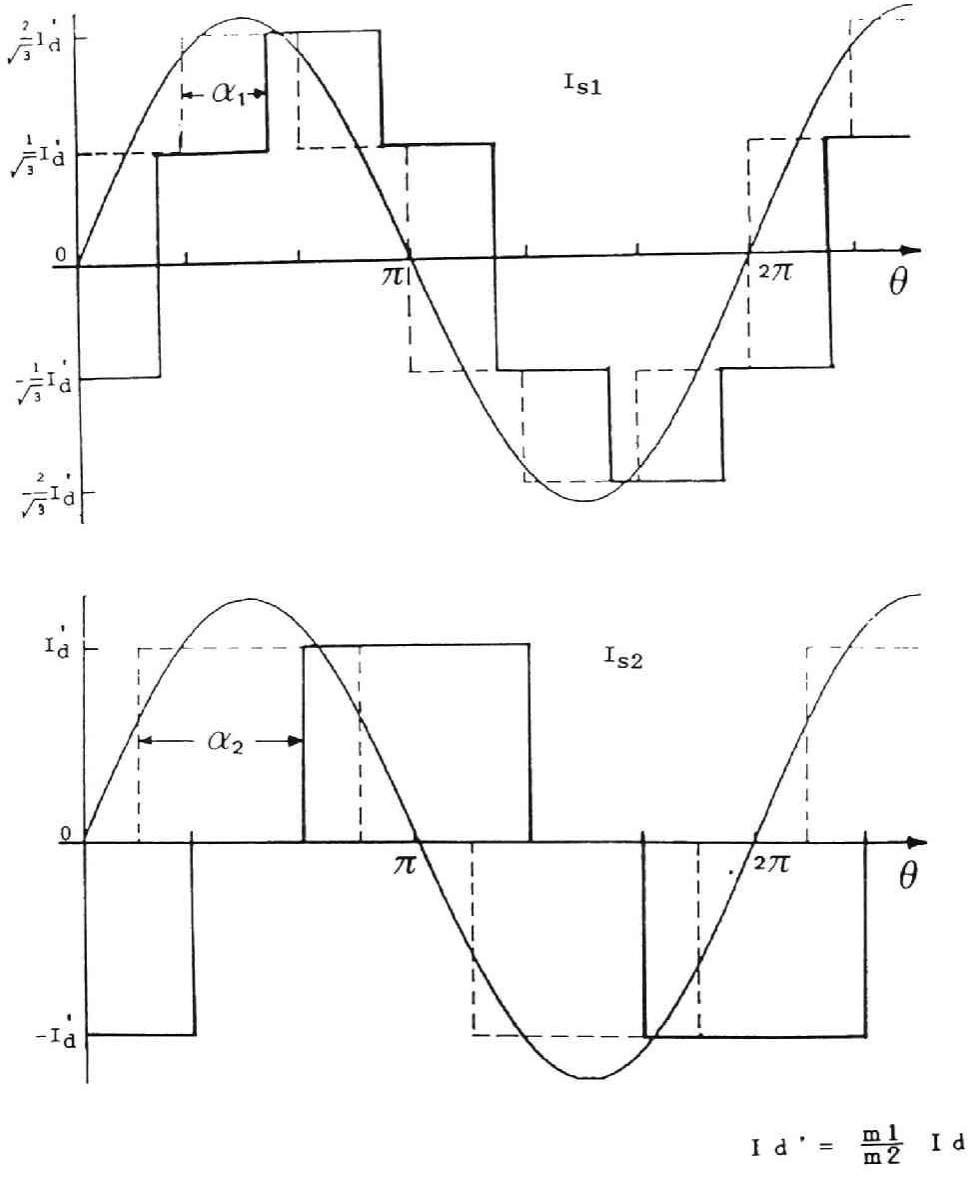

Fig.4-7 Current through transformer windings at high voltage terminal (magnet current Id).

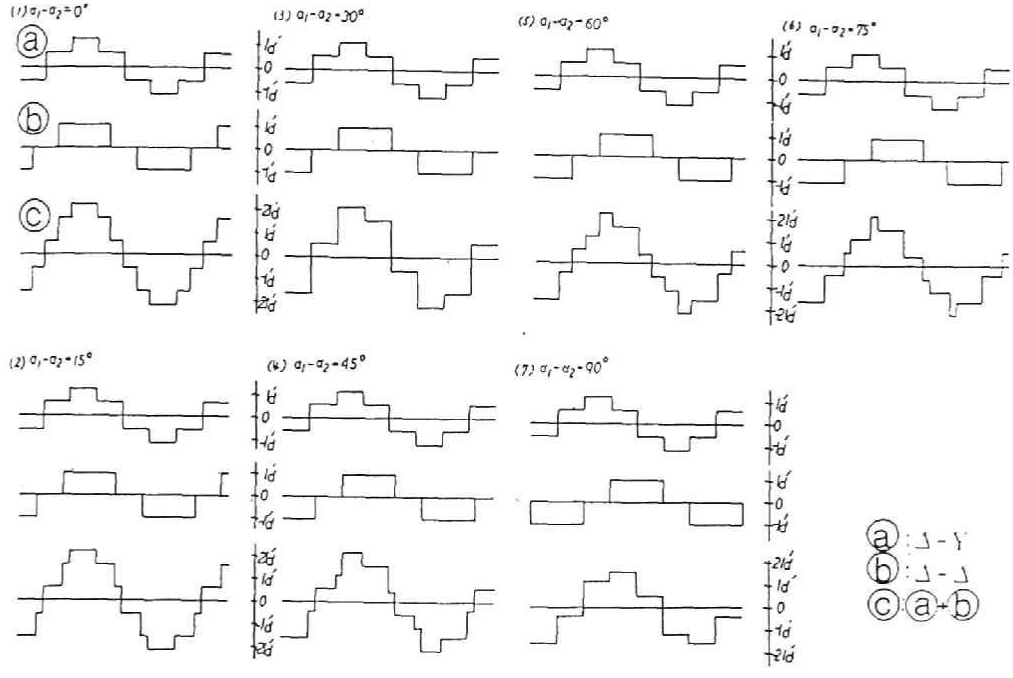

Fig.4-8 Wave shape of AC current of SMES with $|\alpha 1-\alpha 2|$

currents I_{s1} and I_{s2} are delayed by angles α_1 and α_2, individually, in phase. Since firing angles change according to operating conditions of SMES, SMES's AC current $\hat{I}_s(=\hat{I}_{s1}+\hat{I}_{s2})$ is given as a function of difference of α_1 and α_2. (see Fig.4-8)

The currents I_{s1} and I_{s2} through each transformer can be obtained by means of Fourier series where $\alpha_1=\alpha_2=0$.

$$I_{si}(\theta)\sim\frac{a_{io}}{2}+\sum_{n=1}^{\infty}[a_{in}\cos n\theta+b_{in}\sin n\theta] \qquad (4\text{-}7)$$

$$a_{in}=\frac{1}{\pi}\int_{-\pi}^{\pi} I_{si}(\theta)\cos n\theta$$

$$b_{in}=\frac{1}{\pi}\int_{-\pi}^{\pi} I_{si}(\theta)\sin n\theta$$

$$i=1,2 \qquad \theta=2\pi ft$$

The coefficients a_{in} and b_{in} are written as

$$\left.\begin{aligned} a_{1n} &= \begin{cases} \dfrac{2\sqrt{3}}{n\pi} I_d' & (n=1,6k\pm 1;\ k=1,2,\cdots) \\ 0 & (n:\text{rest}) \end{cases} \\ a_{2n} &= \begin{cases} \dfrac{2\sqrt{3}}{n\pi} I_d' & (n=1,12k\pm 1;\ k=1,2,\cdots) \\ -\dfrac{2\sqrt{3}}{n\pi} I_d' & (n=(12k-6)\pm 1;\ k=1,2,\cdots) \\ 0 & (n:\text{rest}) \end{cases} \\ b_{1n} &= b_{2n} = 0 \qquad (n:\text{all}) \end{aligned}\right\} \quad (4\text{-}8)$$

In the case of the firing angles are α_1 and α_2, the fundamental components of I_{s1} and I_{s2} delay by such angles. Therefore the SMES AC current Is is expressed as

$$\begin{aligned} I_s(\theta) &= \sum_{n=1}^{\infty} [a_{1n}\cos n(\theta-\alpha_1) + a_{2n}\sin n(\theta-\alpha_2)] \\ &= \sum_{n=1}^{\infty} [a_n\cos n\theta + b_n\sin n\theta] \qquad (4\text{-}9) \\ a_n &= a_{1n}\cos n\alpha_1 + a_{2n}\cos n\alpha_2 \\ b_n &= a_{1n}\sin n\alpha_1 + a_{2n}\sin n\alpha_2 \end{aligned}$$

Then the magnitude of the n-th component of $I_s(\theta)$ is obtained as

$$C_n = \{(a_{1n}^2 + a_{2n}^2) + 2a_{1n}a_{2n}\cos n(\alpha_1-\alpha_2)\}^{1/2} \qquad (4\text{-}10)$$

Substituting Eq.(4-8) to Eq.(4-10), we obtain

$$C_n = \begin{cases} K\{2+2\cos n(\alpha_1-\alpha_2)\}^{1/2} & (n=1,\ 12k\pm 1;k=1,2,\cdots) \\ K\{2-2\cos n(\alpha_1-\alpha_2)\}^{1/2} & (n=(12k-6)\pm 1;k=1,2,\cdots) \\ 0 & (n:\text{rest}) \end{cases}$$

$$K = \frac{2\sqrt{3}}{n\pi} I_d' \qquad (4\text{-}11)$$

Then the current $I_s(\theta)$ contains harmonics of the $(6k\pm1)$-th order $(k=1,2,\ldots)$. In the operation of $\alpha_1=\alpha_2$, $I_s(\theta)$ contains harmonics of the $(12k\pm1)$-th order. A content ratio of each order harmonics to the fundamental component is obtained as a function of $(\alpha_1-\alpha_2)$ shown in Fig.4-9. The ratio of harmonics of n-th order given as $[Is^{(n)}/Is^{(1)}]$ ($Is^{(n)}$: amplitude of the n-th harmonic current and $Is^{(1)}$: amplitude of the fundamental one).

In simultaneous controls of constant active and reactive powers, difference between two firing angles $|\alpha_1-\alpha_2|$ varies with time. Operating regions for $|\alpha_1-\alpha_2|$ are shown in Fig.4-10 for active powers 1 to 4[kW] and reactive power 4 [kVar].(See Fig.4-10) For example, when SMES is operated by constant active and reactive power control (Ps=2.0[kW], Qs=4.0[kVar]), the ratio $[Is^{(n)}/Is^{(1)}]$ varies with magnet current Id as shown in Fig.4-11. Harmonics of the 5-th order has its maximum value (almost 20(%)) at magnet current Id=97[A]. Harmonics of the 7-th order has its maximum value (almost 18(%)) at the end of charging(Id=120[A]). Since the content ratio $[Is^{(n)}/Is^{(1)}]$ varies in power control operation, filters must be designed according to the maximum value of harmonics of each order through operations.

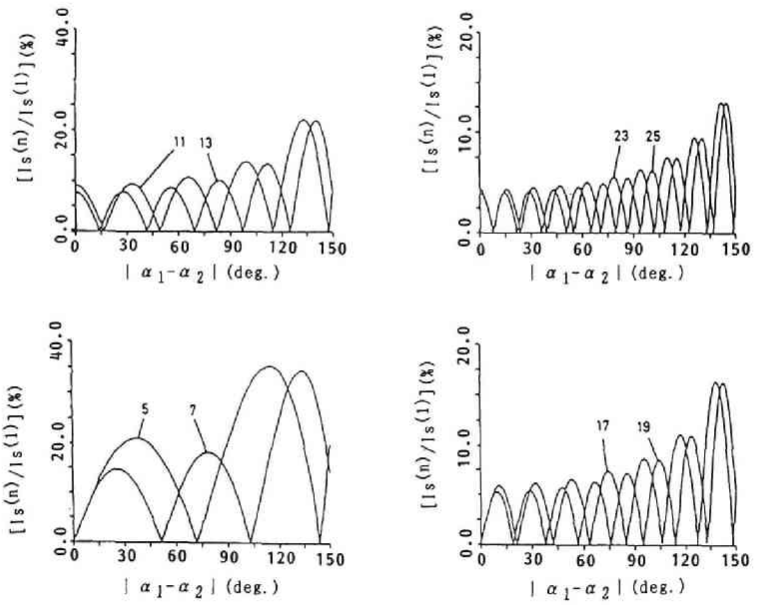

Fig.4-9 Content ratio of harmonics of i-th order to fundamental component as a function of | α1-α2 |

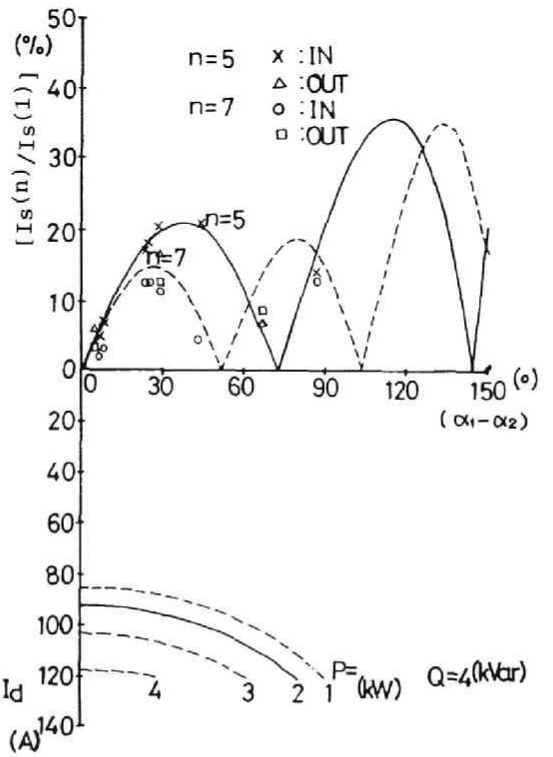

Fig.4-10 Harmonics of n-th order as a function of | α1-α2 | and operating region in constant power control.

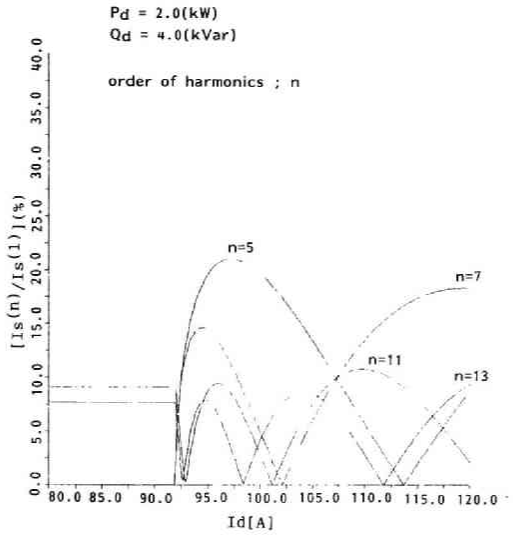

Fig.4-11 Ratio $[Is^{(n)}/Is^{(1)}]$ as a function of Id at power control (Ps,Qs)=2.0[kW],4.0[kVar]).

4-4-2.FILTER DESIGN

In this section, passive filters for the experimental system are designed, for example. We decide the followings:

1] orders of harmonics to be suppressed by filters.
2] total reactive power supplied by filters.
3] how to share the reactive power among filters for each order of harmonics.

The lower the frequency of harmonics is, the greater the peak value of the harmonics is. Then harmonics of higher orders can be neglected. Orders of harmonics for design of filters are determined to be the 5-th, the 7-th, the 11-th and the 13-th under the discussions in Section 4-4-1, that is, the number of filters is four.

A total reactive power supplied by filters is determined to be 3.5[kVar](220[V]) such that possible region for the simultaneous control of constant active and reactive power of

SMES is large at power factor 1.0. Figure 4-12 shows possible region of the simultaneous active and reactive power control with designed filters for the experimental system. The shaded area is possible region for simultaneous controls of constant active and reactive powers with magnet current 100[A]<Id<140[A]. However, an amount of reactive power 3.5 [kVar] is rather large for system capacity(6[kVA]). Then a parallel resonance between the filters and the transmission lines may appear at low frequencies. The parallel resonance is discussed in Section 4-6-4.

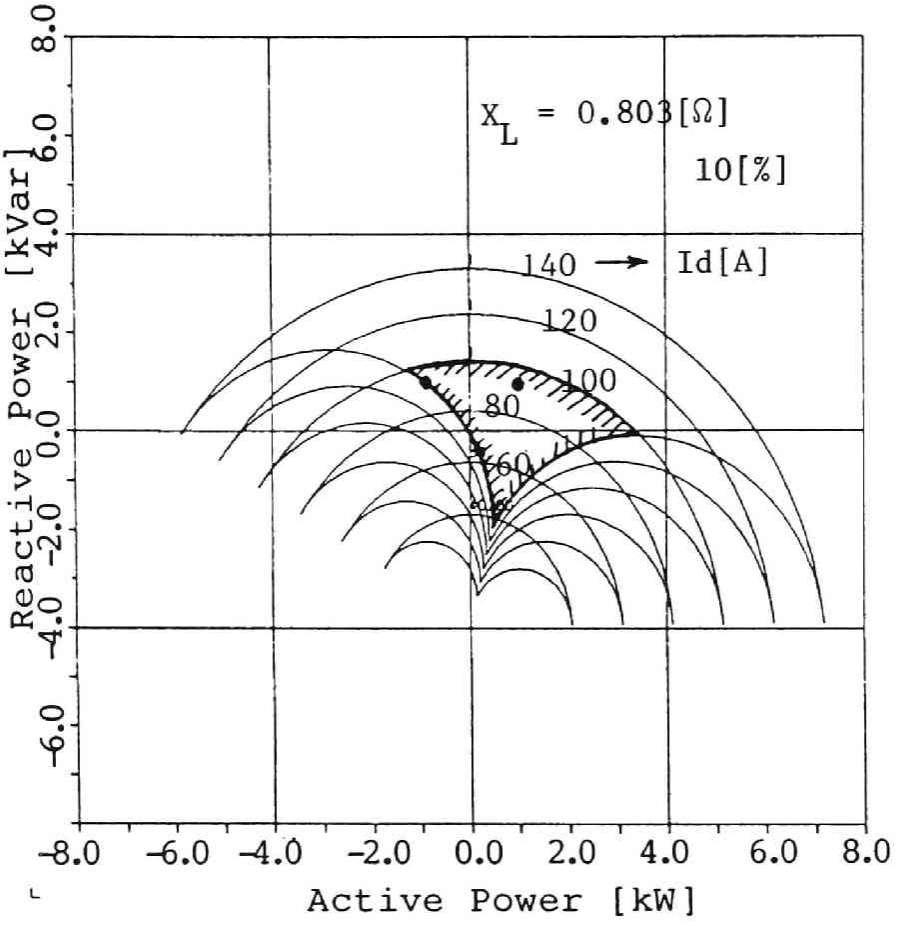

Fig.4-12 Pt-Qt characteristics with designed filters and possible region for P-Q simultaneous control (shaded region; Id 100[A]-140[A])

$I_s^{(n)}$:harmonic current source of n-th order
Z_{sn} :impedance of power system for harmonics of n-th order
C_{fn}, L_{fn}, R_{fn}:parameters of filters for harmonics of n-th order

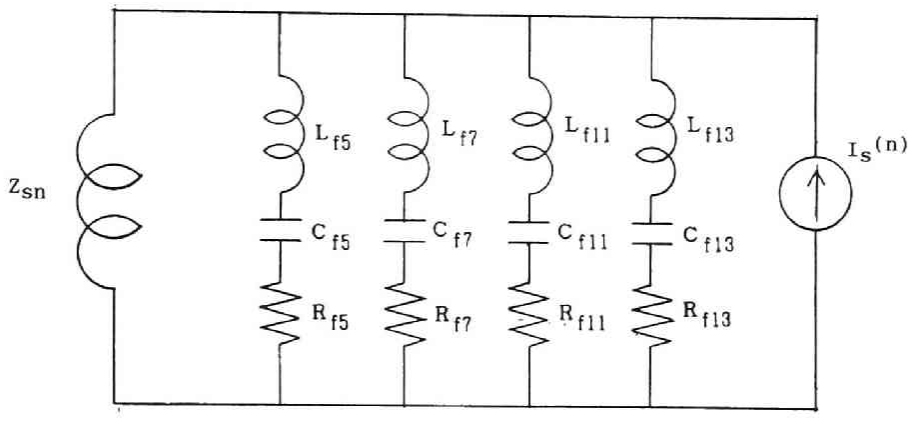

Fig.4-13 Equivalent circuit of experimental system with filters for higher frequency

Let us consider how to determine an amount of reactive power supplied by each filters. An equivalent circuit for higher frequencies (harmonics of the n-th order) is shown in Fig.4-13. Harmonic current source of the n-th order (that is, SMES) is $I_s^{(n)}$. Impedance of power systems viewed from SMES terminal for harmonics of the n-th order is Z_{sn}. When SMES generates current harmonics of a certain frequency($I_s^{(n)}$), current flowing through transmission lines is examined. Calculated results of frequency response are shown in Fig.4-14, (a) only shunt capacitor (b) the reactive power of the filter for the 5-th harmonic is largest and (c) that for the 13-th harmonic is largest. "Current ratio" means ratio of the current flows into system to the current generated by harmonic source(SMES).

A frequency for parallel resonance between filters and transmission lines is roughly determined by reactive power compensated by filters. As shown in Fig.4-14, a order of harmonics, which expresses a parallel resonance, is between the

a)

Cf(μF)	Lf(mH)	Rf(Ω)	Q	Var
190.0	0.004	0.0001	1000	3467

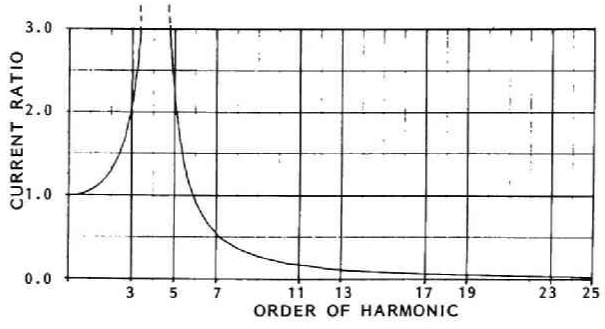

b)

	Cf(μF)	Lf(mH)	Rf(Ω)	Q	Var
5	20.0	14.072	0.8842	30	380
7	20.0	7.180	0.6316	30	373
11	50.0	1.163	0.1608	30	920
13	100.0	0.416	0.0680	30	1835

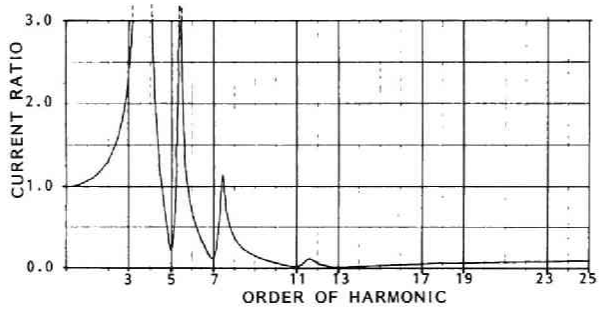

c)

	Cf(μF)	Lf(mH)	Rf(Ω)	Q	Var
5	100.0	2.814	0.1768	30	1901
7	50.0	2.872	0.2526	30	931
11	20.0	2.908	0.4019	30	368
13	20.0	2.082	0.3401	30	367

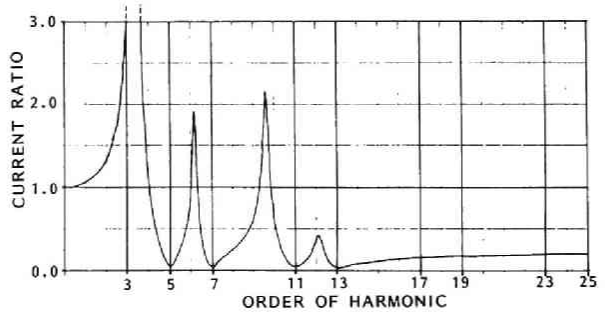

IMPEDANCE OF TRANSMISSION LINE

Z_n = 0.0 + j 0.807 (10(%))

Fig.4-14 Frequency response of system including passive filter
Current ratio: ratio of current flow into the system to current generated by harmonic source
a)with only capacitor
b)capacitor for the 5-th harmonic filter is largest
c)capacitor for the 13-th harmonic filter is largest

Table 4-1 Specifications of designed passive filter

order	C [μF]	L [mH]	R [Ω]	Q	VAR
5	100	2.814	0.1768	30	1901
7	50	2.872	0.2526	30	931
11	20	2.908	0.4019	30	368
13	20	2.082	0.3401	30	367

3.3-th and the 4-th, which depends on how to share a total compensating reactive power to each filter. If reactive power supplied by a filter for harmonics of higher order is large, it is disadvantage that an inductance of filter for harmonics of lower order become large and characteristics of frequency response is sensitive near the frequencies of harmonics suppressed by filters. In practice, a filter is not always tuned exactly to the frequency of the harmonic that is intended to suppress. Detuning of filters or deviation of power system frequency should be considered.

After calculating characteristics of several kinds of filters by use of simulation code described in Chapter 3. Filters were made according to the design as shown in Table 4-1. Characteristics of designed filter are examined in Section 4-5.

4-5. COMPUTER SIMULATION OF PASSIVE FILTER PERFORMANCE[18]

By use of computer simulation described in Chapter 3, performance of the designed filters is confirmed. Simulation studies for installation of filters are performed. How scatter of firing angles affects the harmonic current of SMES is also discussed.

4-5-1. INSTALL OF PASSIVE FILTER

It is necessary to survey effect of filter installation on SMES's operations. By use of simulation studies, it is pointed out that damping of a transient oscillation is bad when filters are connected to power systems during power control of SMES, because of error feedback routine of controller.

The simulation results show that after the installation of the filters, large transient voltages and currents of filters appeared. Therefore condensers of the filters used in the experiments are decided to be of the rated voltage 400[V]. However, SMES current is not so distorted because inductance of superconducting magnet is large.

4-5-2. PERFORMANCE OF PASSIVE FILTER

Figure 4-15 shows one of the simulation results for constant active and reactive powers control without filters. The transmission line reactance is 10[%]. The active power and the reactive power are controlled to be 1.0[kW] and 3.0[kVar], respectively. The current through the transmission line is the same as SMES AC current i_{sv} which contains harmonics of the $(6k\pm1)$-th order. The terminal voltage V_{vw} also contains harmonics of the $(6k\pm1)$-th order. (see Fig.4-16)

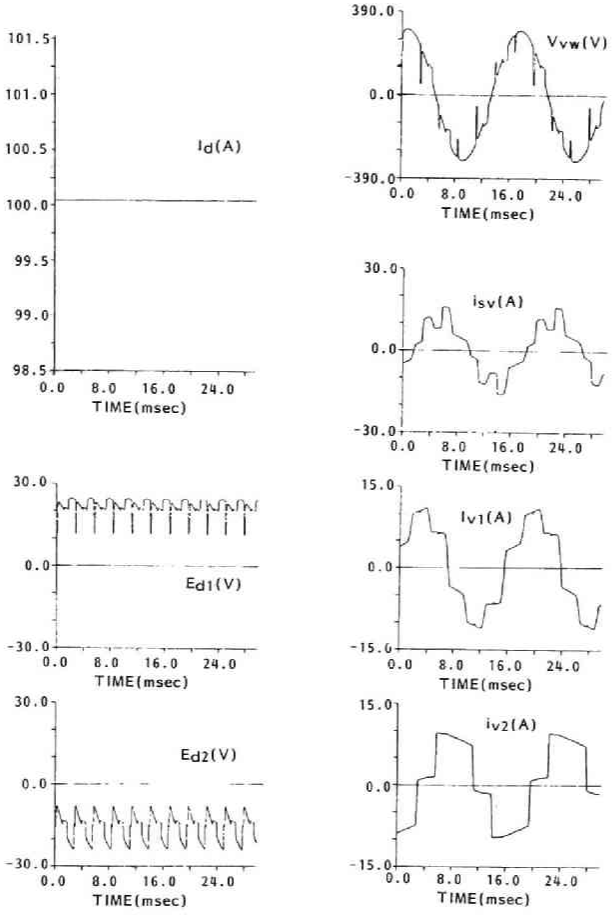

Fig.4-15 Simulation results for constant active and reactive power control without filters
transmission line reactance X_L=10[%]
Ps=1.0[kW],Qs=3.0[kVar]

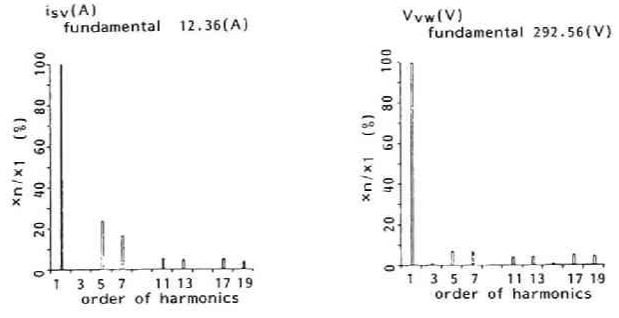

Fig.4-16 Harmonic component of terminal voltage and transmission line current in Fig.4-15

One of the simulation results for confirming effects of the designed filters is shown in Fig.4-17, where magnet current is 100[A], specified active power is 1.0[kW] and reactive power is 0.0[kVar]. The currents flowing through each filter contain the fundamental component (that corresponds to the share of the reactive power) and harmonics of each designed order. It is found that the harmonics of the transmission line current $i_{scv}(i_{tv})$ are reduced. Harmonic components of each voltages and currents are shown in Fig.4-18. Harmonics of terminal voltage are suppressed by the filters.

The other results are shown in Fig.4-19 and Fig.4-20, where the scatter of the firing angles of the thyristor is considered. (scatter of firing angles : 3 degrees delay of firing angles for thyristors connected to v-phase of upper converter.) In Fig.4-19, the voltage and the current of the transmission line contain the harmonics of the 3-rd order. Transmission line reactance is 10[%]. The order of harmonic for parallel resonance is near the 3-rd. It corresponds to the experimental result shown in Fig.4-32. In Fig.4-20, transmission line current i_{tv} contains the harmonics of the 2-nd order. Since transmission line reactance is 35[%], the order of harmonics for parallel resonance is near the 2-nd. The active and the reactive power, which should be controlled to be constant, contain fluctuation of 60[Hz].

The above mentioned case where the harmonics of lower order expand is studied by use of the simulation on several conditions of transmission line reactance and reactive power to be compensated. The result is shown in Fig.4-21. It shows that the lower the order of the harmonic is, the worse the power control is. In the simulation, the unbalance of the three phase system, the change of the reference voltage to determine the firing angles and so on are neglected, which appear in the experimental or real systems. It may be necessary to investigate how they affect SMES operation.

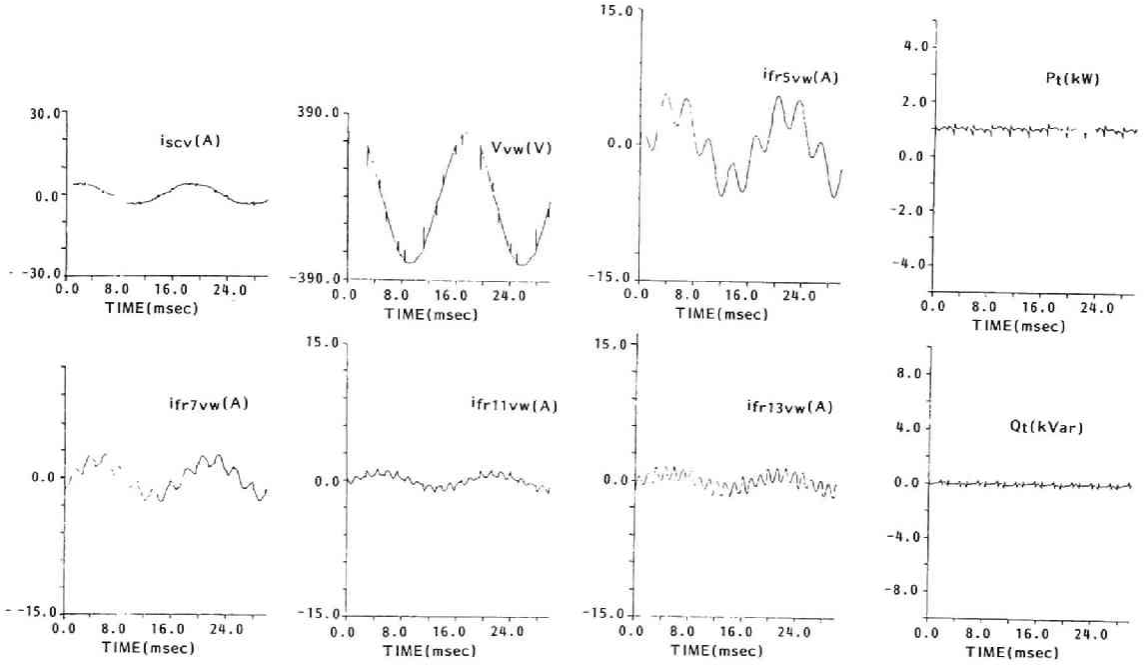

Fig.4-17 Simulation results for constant active and reactive power control with designed filters
transmission line reactance X_L=10[%]
Ps=1.0[kW],Qs=0.0[kVar]

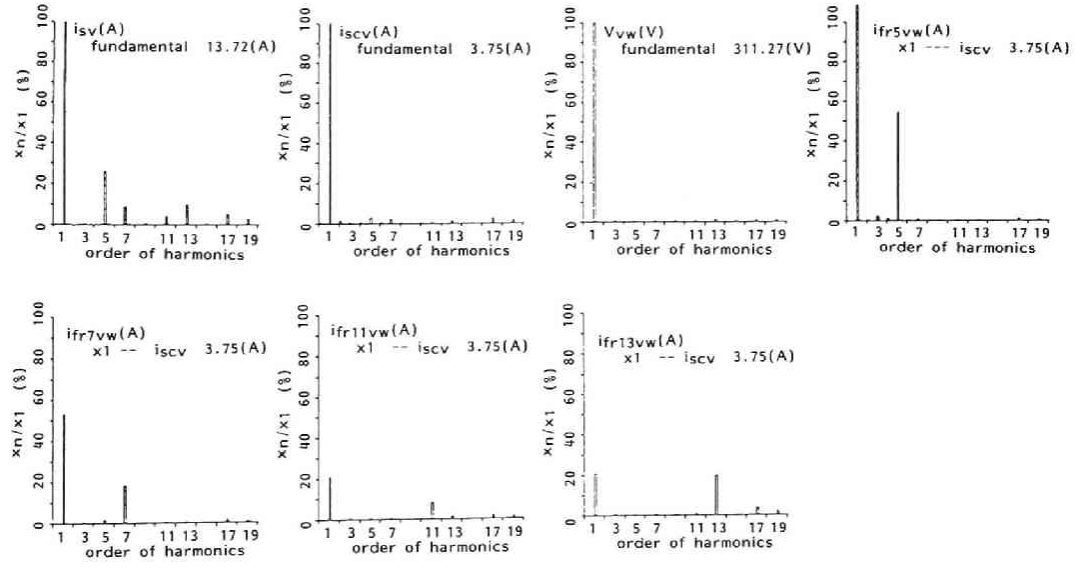

Fig.4-18 Harmonic component of voltages and currents in Fig.4-17

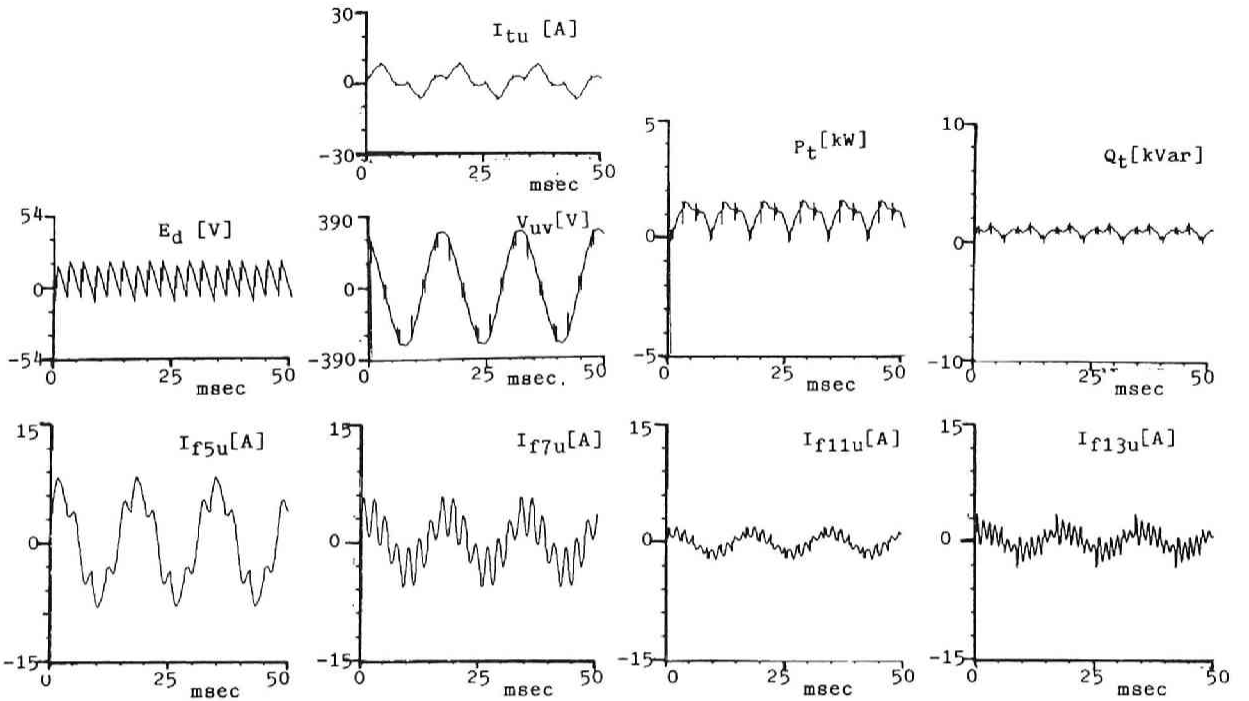

Fig.4-19 Simulation results for performance of passive filter: parallel resonance of the third order.
(with scatter of firing angles)
transmission line reactance X_L=10[%]
Ps=1.0[kW],Qs=0.0[kVar]

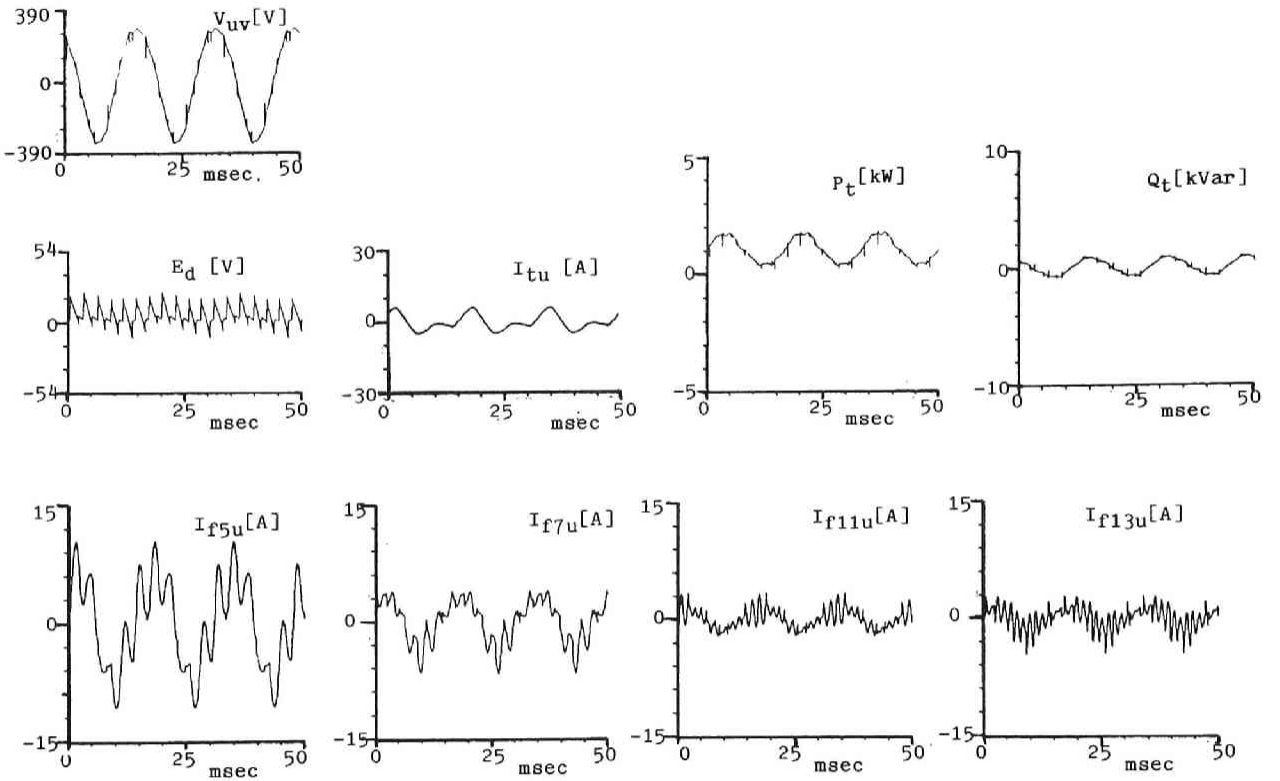

Fig.4-20 Simulation results for performance of passive filter: parallel resonance of the second order.
(with scatter of firing angles)
transmission line reactance X_L=35[%]
Ps=1.0[kW],Qs=0.0[kVar]

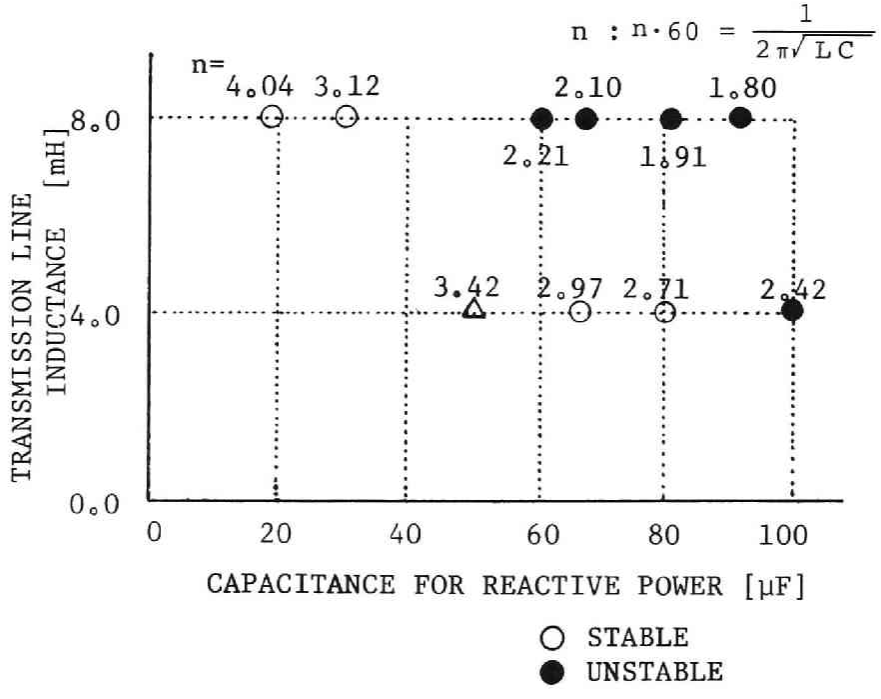

Fig.4-21 Stability of power control of SMES and parallel resonance related to inductance of transmission line and capacitance for reactive power compensated.

4-6. EXPERIMENTAL RESULTS AND DISCUSSION[19]

4-6-1. EFFECT OF TRANSMISSION LINE

At first, consider a case where SMES is connected to an infinite bus without transmission lines. An experimental result is shown in Fig.4-22, where active power Pt is± 1.0[kW] and reactive power Qt is 4.0 [kVar]. The active and the reactive powers are well controlled.

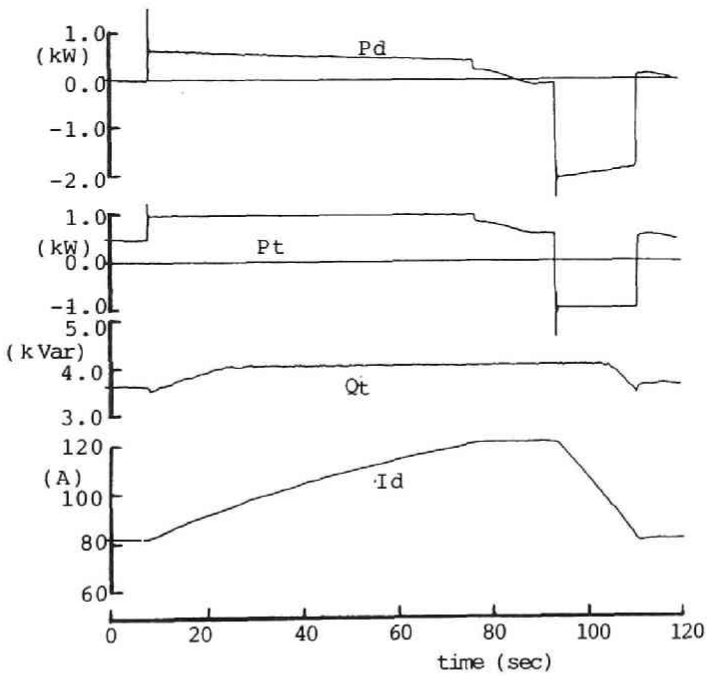

Fig.4-22 Experimental result of Pt-Qt simultaneous control (1)
SMES is directly connected to infinite bus

An experimental result is shown in Fig.4-23 where the SMES is connected to the infinite bus through the transmission line of 10[%] (6[kVA], 220[V] base). The average active power and the reactive power are controlled to be ±1.0[kW] and 4.0[kVar], respectively. However, the oscillation appears in the wave forms of the active and the reactive power, which may be due to the change and the distortion of the terminal voltage.

In the case of the transmission line of 35[%], the commutation failure of the converter occurs and the power cannot be controlled.

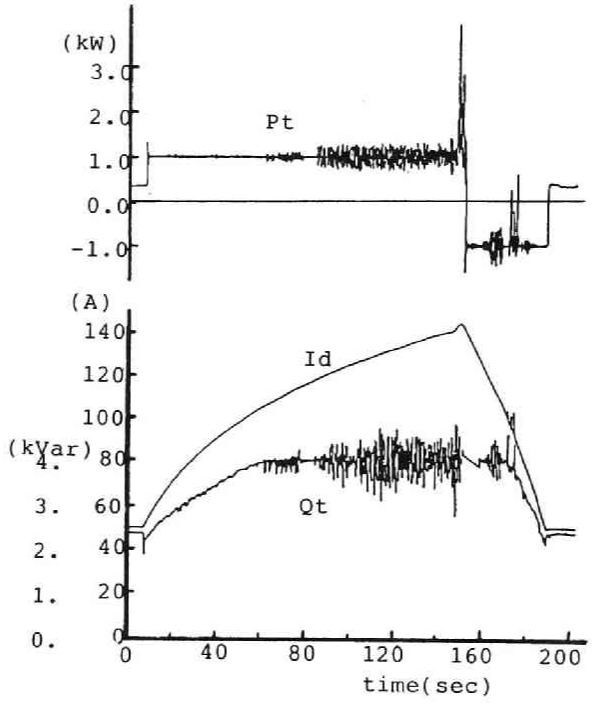

Fig.4-23 Experimental result of Pt-Qt simultaneous control (2) SMES is connected to infinite bus through 10[%] transmission line.

4-6-2. CURRENT HARMONICS OF SMES

In this section, current harmonics generated by SMES which is directly equipped to an infinite bus are measured and discussed.

The ratios of harmonics to the fundamental vary with the magnet current Id as shown in Fig.4-24.(refer to Fig.4-11) When the magnet current is small, only the active power is controlled. Then the ratios of harmonics are small. However, when the current exceeds 85 A, the active and reactive power are also controlled. Then the ratios of harmonics become larger. The ratios are calculated as a function of $|\alpha_1-\alpha_2|$ from the experiments, which are marked in Fig.4-10. Non-theoretical harmonics, which also vary with the current Id, are measured to be smaller than the theoretical ones.

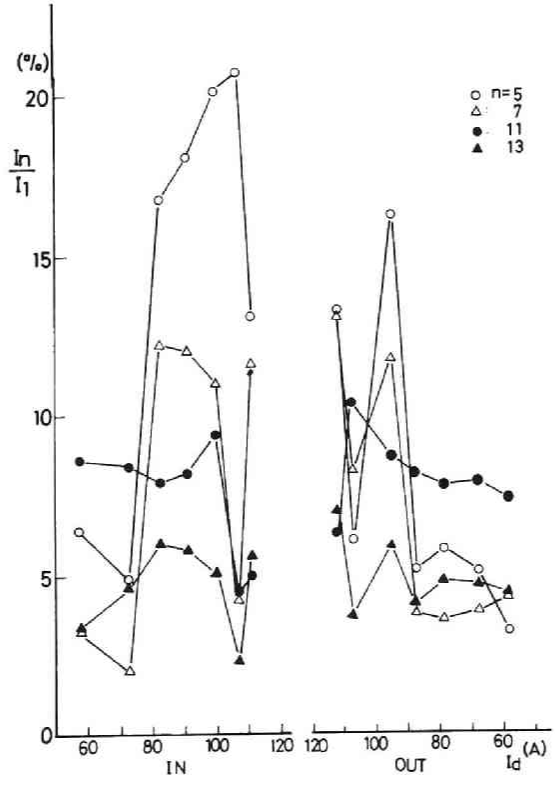

Fig.4-24 Ratio $[Is^{(n)}/Is^{(1)}]$ as a function of Id (experiment) (refer to Fig.4-11)

4-6-3. EFFECT OF PASSIVE FILTER

At connecting filters:

Let us consider the experiments with filters. A transient oscillation at connecting filters to power system is pointed out in the simulation results. In the experiments, the filters are connected without the power control of SMES. Fig.4-25 shows the experimental result. The transient oscillation is damped within several cycles at the connecting.

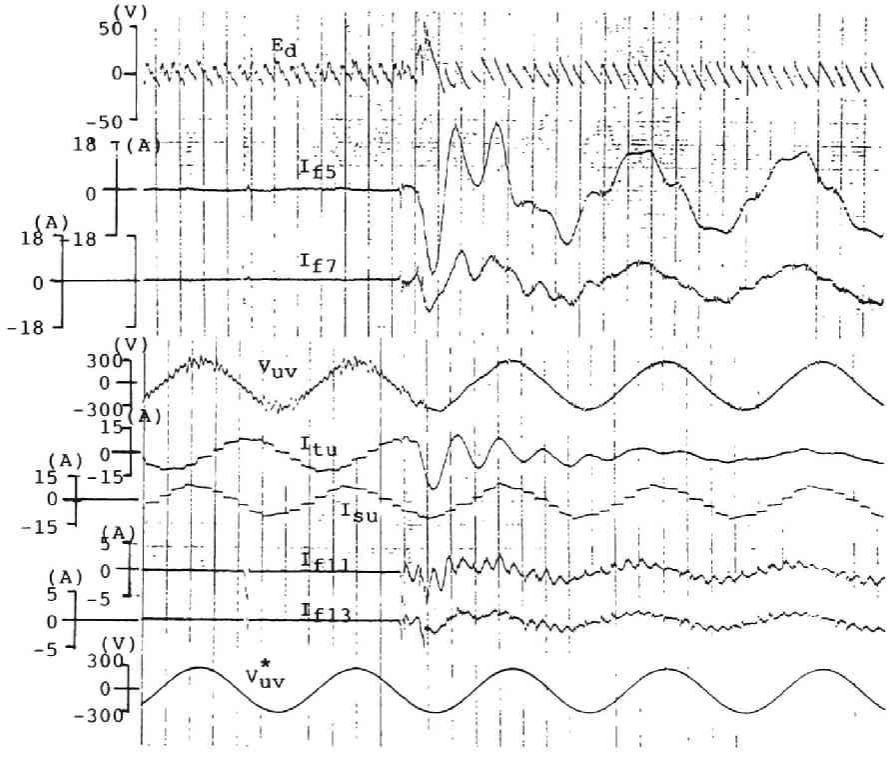

Fig.4-25 Installation of passive filter

Effectiveness of filters:

An experimental result of the power control of SMES with the filters is shown in Fig.4-26, where the specified active power is ± 1.0[kW] and the reactive power is 1.0[kVar]. The simultaneous constant active and reactive power control can be performed while the magnet current is between 104[A] and 140[A] in the charging mode and between 140[A] and 106[A] in the discharging mode. The operating point is dotted on Fig.4-12. It gives the P-Q simultaneous controllable region for the magnet current Id:between 98[A] and 140[A] in the charging mode and between 140[A] and 93[A] in the discharging mode. The experimental results agree well with the calculated ones.

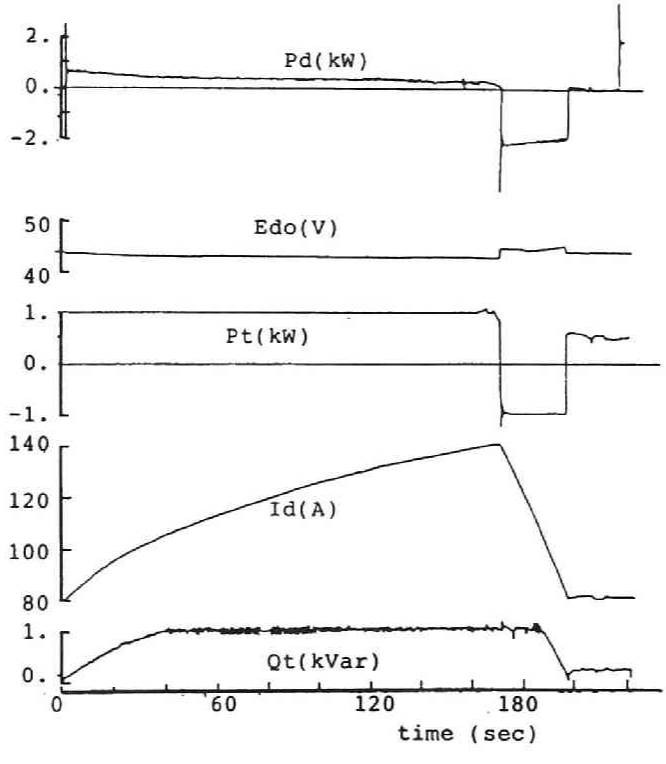

Fig.4-26 P-Q simultaneous control with passive filters and 10[%] transmission line. (Pt=± 1.0[kW],Qt=1.0[kVar])

High speed power detector[24]:

As shown in Fig.4-26, the reactive power contains small distortion. It may depend on the delay time of active and reactive power detectors, which give the signals to the power controller. Then, by use of active power and reactive power detector with small delay time, we tried to improve the characteristics of power control. The detector is based on the concept of instantaneous real power p and imaginary power q. The delay time is about 10[msec]. The experimental result by use of the detector is shown in Fig.4-27. Power controls of SMES can be successfully performed by use of the detector of quick response.

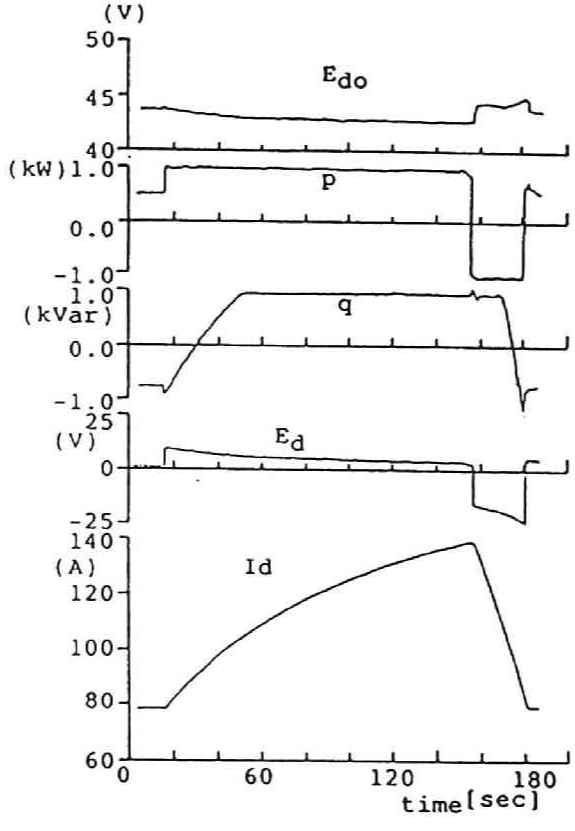

Fig.4-27 P-Q simultaneous control by use of power detector of small delay time with passive filters and 10[%] transmission line. (Pt=± 1.0[kW],Qt=1.0[kVar])

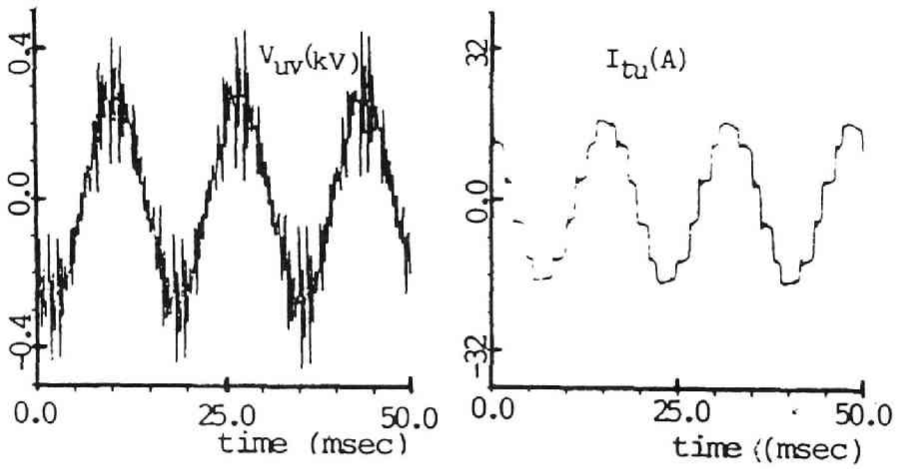

Fig.4-28 Wave form of transmission line current and terminal voltage at magnet current Id = 108[A]
without filters 10[%] transmission line.

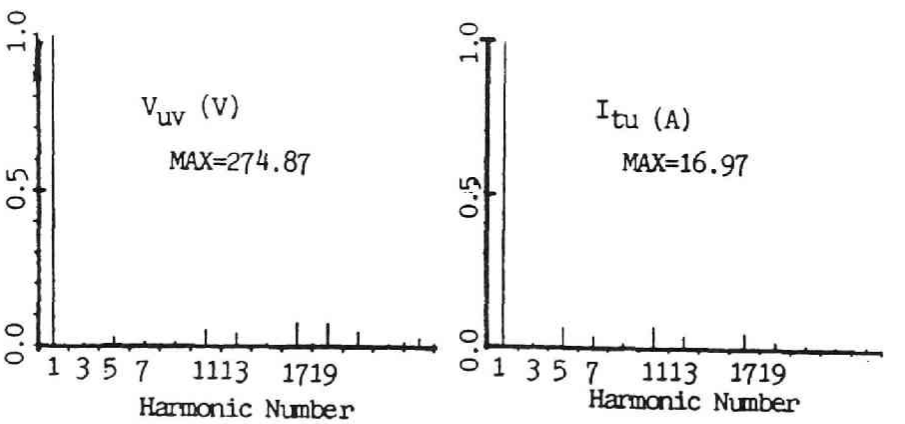

Fig.4-29 Magnitude of harmonic components of each order to the fundamental one.

Suppress harmonics by filter:

The current i_{tu} through the transmission line (10[%]) and the terminal voltage V_{uv} without the passive filters are shown in Fig.4-28, where the specified active power is 1.0[kW], the reactive power is 4.0 [kVar] and magnet current Id=108[A]. The current contains the harmonics. Because of the harmonic currents, the terminal voltage is distorted. Then good power

control of SMES cannot be performed. The magnitude of harmonics contained in the voltage and the current are shown in Fig.4-29, which nearly equal to calculated ones as expected.

Figure 4-30 shows the voltages and the currents with passive filter, where the specified active power is 1.0[kW], the

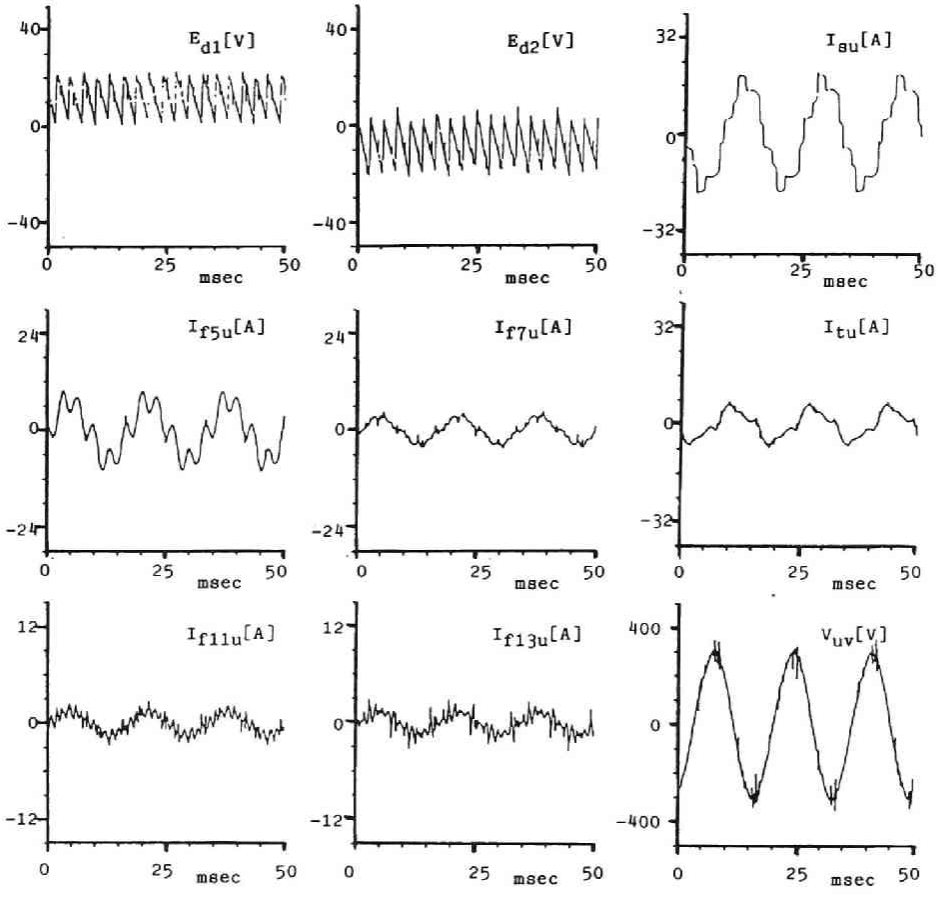

Fig.4-30 Wave forms of voltages and currents at the test with filters and 10[%] transmission line

Id=112[A]

Edi: DC voltage of the i-th converter
Vuv: AC voltage at terminal of SMES
Isu: AC current of SMES
Itu: AC current of transmission line
If..u: AC current of filters associated with subscript

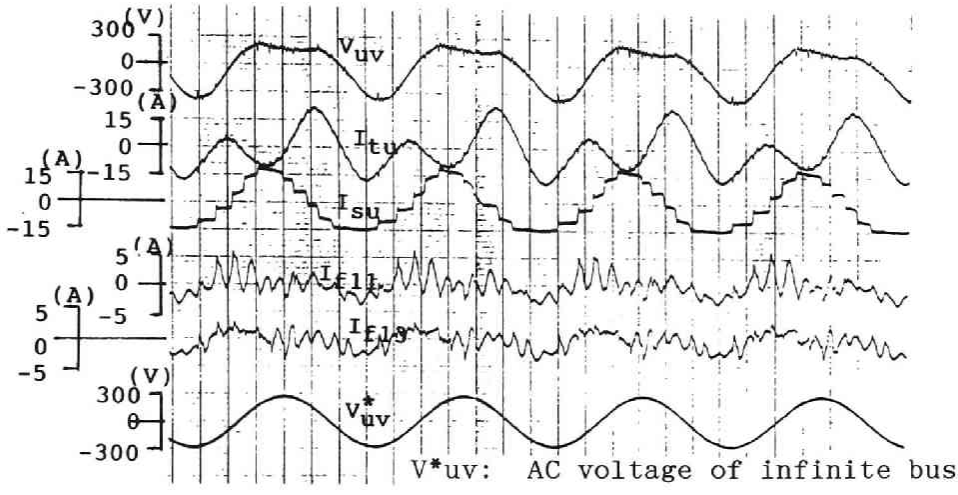

Fig.4-31 Wave forms of voltages and currents at the test with filters and 35[%] transmission line

reactive power 1.0[kVar] and the magnet current = 112[A]. The theoretical harmonics in the current are reduced by the filters as shown in the figure. The distortion of the terminal voltage is much smaller than that without filter. The filtering effect is confirmed. However, the non-theoretical harmonics are contained.

4-6-4. NON-THEORETICAL HARMONICS

In an ideal system, non-theoretical harmonics do not exist. However, in real systems, non-theoretical ones are generated because of unbalanced three phase voltage and transmission line impedances, scatter and change of firing angles of thyristors. On the other hand, the parallel resonance for the designed filters exists at about the 3.3-th harmonics for the impedance 10[%] of the transmission line and about the second for that of 35[%]. Then if the non-theoretical harmonics for parallel resonance are contained, they expand.

In the case of 35[%] transmission line impedance, the line current I_{tu} shown in Fig.4-31 is distorted due to the second harmonics as expected. The distortion affects the control, then it expands and at last, the power control cannot be performed.

4-7. ACTIVE FILTER[20),(21).[23]

As mentioned before, because of wide change of firing angles and unbalance of three phase system, it is in some sense unavoidable problem that not only the theoretical harmonics but the non-theoretical ones are generated in power control operation of SMES.

In order to solve the problem, we pick up an active filter for harmonic suppression in AC system. An active filter has the following merits: that is,

(1) it can suppress the distortion which contains the harmonics of several frequencies, even if the distortion is unbalance in three phase system.

(2) it can respond to variation of the distortion within its capacity, and even if the distortion become larger than its capacity, it will not be over-loaded.

By considering that an active filter must suppress current harmonics which are changing in frequency and in magnitude, it is proposed to consist of DC current source, GTO(Gate turn off thyristor) converter and a filter bank. To match SMES system, we use a small superconducting magnet as a DC current source.

In order to generate the harmonic currents, GTO converter is controlled under the concept of three phase PWM(Pulse Width Modulation) method. The major harmonic components of modulated currents are injected into the AC system. The rest of the harmonic components which are small in magnitude and much higher in frequency are controlled to be small and filtered out.

DESIGN OF ACTIVE FILTER

A schema of an active filter is shown in Fig.4-32. In addition to the schema, a passive filter to reduce much higher-frequency harmonic components is needed. It is an important problem to decide turn ratio of transformer, inductance and rated

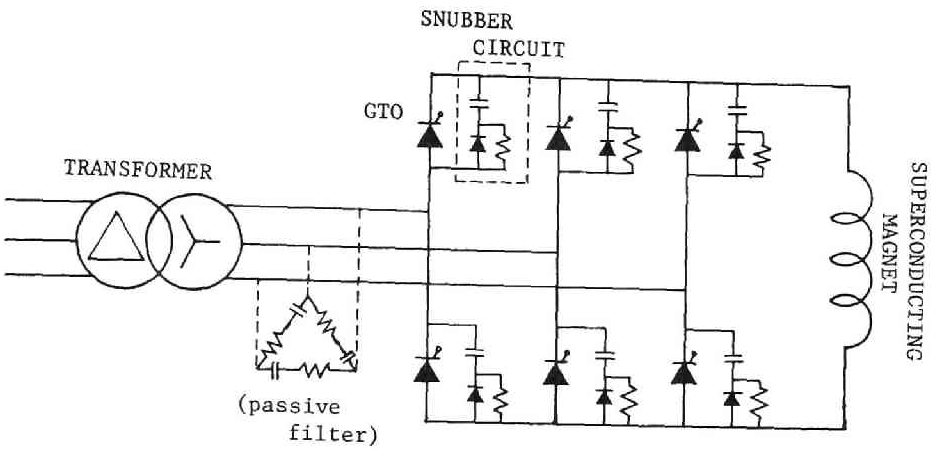

Fig.4-32 Schema of active filter

Table 4-2 Specification of active filter

Superconducting magnet

Inductance	(H)	.505
Rated current	(A)	125
Stored Energy	(kJ)	3.95
Conductor		Nb-Ti

Transformer

Rating Capacity	(kVA)	6
Turn ratio		220/18
Connection		D-Y

GTO

On-state current	(A)	125
Off-state voltage	(V)	1200
Reverse voltage	(V)	1200

Snubber circuit

Capacitor	(μ F)	0.47
Resistor	(Ω)	10

current of superconducting magnet and so on. For the first step, we designed and made a model active filter. The basic tests on the active filter were carried out to confirm a possibility of suppressing the current harmonics of SMES. The specification of GTO, snubber circuit, transformer and superconducting magnet is shown in Table 4-2. In practice, because of turn-off or turn-on time of GTO, the highest frequency of the current injected into AC system by the active filter is limited.

The active filter is designed to generate currents up to 13-th harmonic frequency (780[Hz]). The frequency of the carrier wave (triangular wave) for PWM is 2040[Hz].

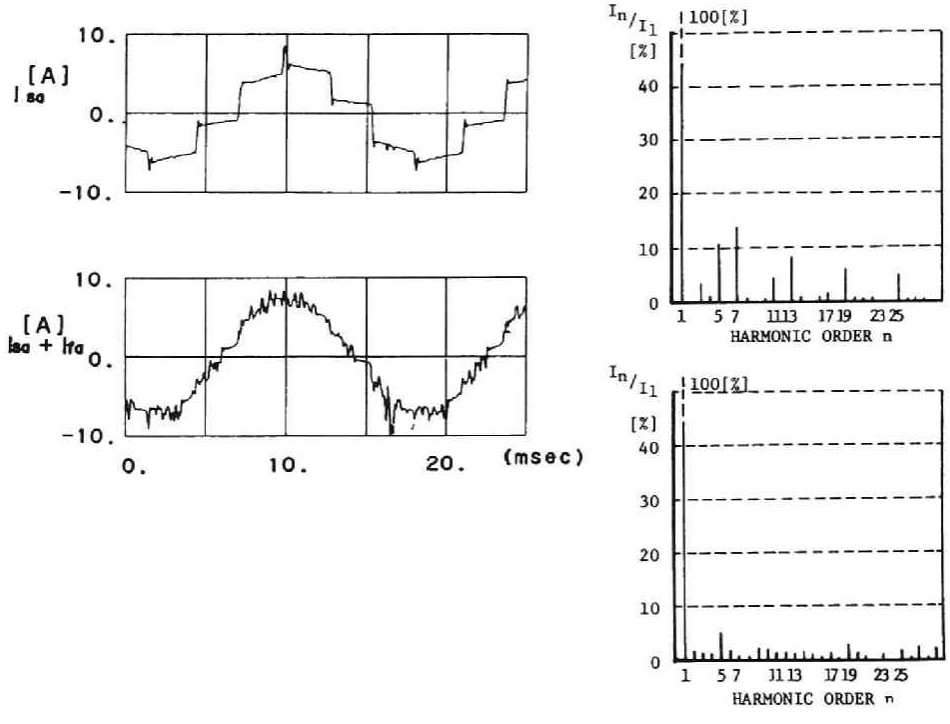

Fig.4-33 Test result for suppression of harmonics of SMES current.

TEST RESULT

At first, we operated the active filter to generate the harmonic current of single order. As a result, it was confirmed that the active filter can generate current up to 13-th harmonic frequency without any large phase shift.

Second, we operated the active filter to generate the harmonic components of SMES current. One of the test results is shown in Fig.4-33. The upper(Isa) is the SMES AC current and its harmonic components (experimental data recorded on a data- recorder). This is the input signal for the active filter. The sum of Isa and the filter current Ifa, which is considered as the current through the transmission line, is shown in the lower figure of Fig.4-33. These tests were performed under various conditions. The possibility of suppressing the current harmonics of SMES was confirmed.

4-8. CONCLUDING REMARKS

When SMES having a capacity comparable to power systems is operated in the power system, it is impossible to consider SMES to be a static load. In this chapter, the result of the experiments and the computer simulations for investigating influences of transmission line on characteristics of SMES are described.

[1] Terminal voltage is distorted by the harmonic current of SMES through the transmission line. The performance of SMES is affected by the distortion and the change of the terminal voltage.

[2] Lagging reactive power of SMES causes the voltage drop at the terminal of SMES.

In order to meet these problems, the passive filters were

designed and made. By experiment and simulation, the power system characteristics of SMES with filters to suppress current harmonics and to compensate the reactive power was studied. We obtained the results as follows

[3] Active and the reactive powers of high power- factor are controlled.

[4] Current harmonics through the transmission line are reduced to be small.

[5] Terminal voltage across SMES remains almost constant.

[6] The non-theoretical harmonics is observed. It may be due to the parallel resonance of the transmission line and the filters.

The passive filter may not be so good for the power system including SMES. An active filter composed of a superconducting magnet was studied. Good performance was confirmed by the experiment.

CHAPTER.5

CHARACTERISTICS OF SMES CONNECTED TO ONE-MACHINE AND AN INFINITE BUS SYSTEM(22)

5-1. INTRODUCTION

SMES is considered to be a power control plant of quick responsibility. Then it is expected to be a power system stabilizer as well as a energy storage plant. As for such kinds of purposes, some simulation and experimental results have been reported. SMES has different properties from those of other power system apparatus as described in the previous chapters. Therefore, before studying SMES as a power system stabilizer, characteristics of power systems including SMES should be studied. One of the most important problems in such power systems is how SMES operations affect the other power system apparatus, especially, generators.

In order to investigate the problem, we carried out some experiments on an experimental network. In the network, a small superconducting magnet is connected to a small synchronous generator through a double thyristorized converter and transformers. The generator is connected to the regional power system through artificial transmission lines. The active power into or out of SMES and the reactive power are controlled. For the experiments, simulation studies by use of the simulation code described in Chapter 3 were performed.

For the experiments and the simulation, the harmonic current flow, power flow, characteristics of the generator and so on, are discussed.

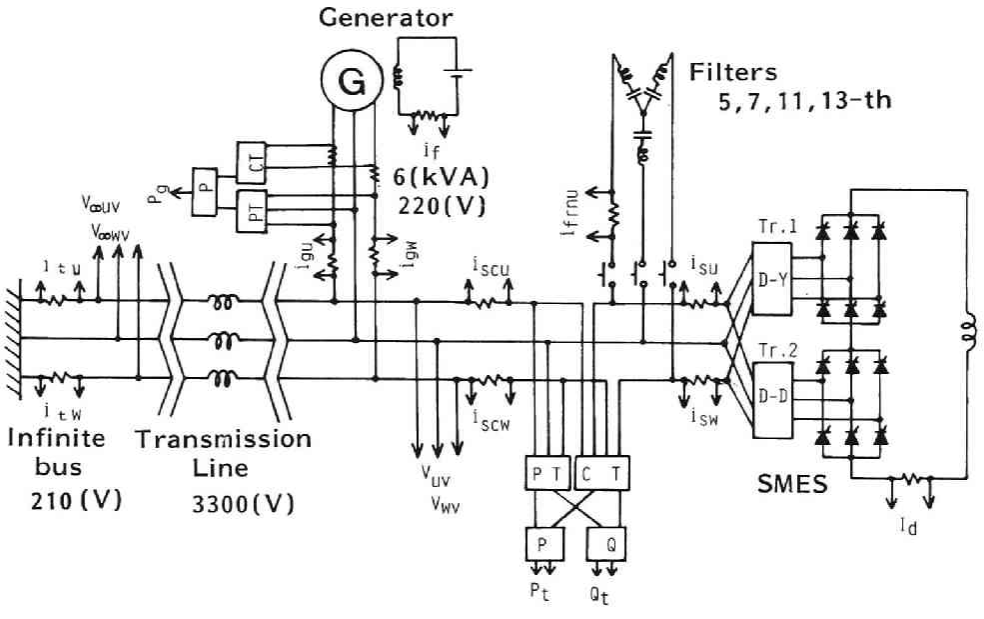

Fig.5-1 Configuration of experimental system for one-machine and infinite-bus with SMES.

5-2. EXPERIMENTAL SYSTEM

A configuration of a model transmission system used in the experiments are shown in Fig.5-1. Main elements of the system are a three phase synchronous generator, transformers, transmission lines and a model SMES system.

Since a generator connected to SMES may be a large scale thermal plant or a nuclear power plant, we used a generator of cylindrical rotor type in the experiment. The specification of the generator is shown in Table 5-1. The generator is of a 4 poles cylindrical rotor. The rated capacity is 6[kVA], the

rated current, 15.7[A] and the rated power factor, 0.9. The generator is equipped with an AVR and a governor system, but these equipments were not used in the experiments, since the purpose of the experiments is to investigate fundamental characteristics of the power system. Because of the same reason, we used a constant voltage DC power supply as an exciter of the field current. The generator is driven by a DC motor of 15[kW].

Table 5-1 Specification of generator

Synchronous generator		
Cylindrical-rotor type		
Frequency	60	Hz
Number of poles	4	poles
Rated rotating speed	1800	rpm
Rated capacity	6	kVA
Rated voltage	220	V
Rated current	15.7	A

Table 5-2 Machine constant of generator

Xd	X2	Xo	Xd'	Xd''	Xq''
185.0	58.0	24.2	43.0	39.8	114.6 (%)

Td'	Td''	Ta	Tdo'	
0.038	0.011	0.036	0.106	(sec)

The results of no-load test and short-circuit test of the test generator are shown in Fig.5-2. The no-load characteristics curve of the generator is almost linear. A field current I_f is 11.8 [A] for the rated voltage 220 [V] on no-load. The machine constants given by tests are shown in Table 5-2. Synchronous reactance is 185(%).

The model system corresponds to a 157 [kV] double-circuit transmission system and a 13[MVA] generator.

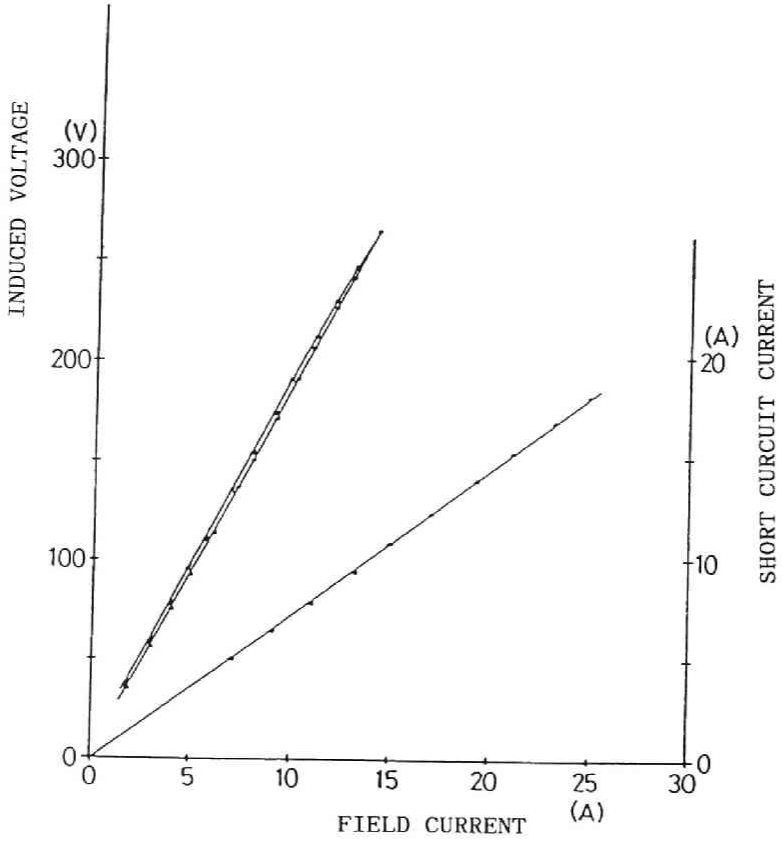

Fig.5-2 No-load characteristic curve and Short-circuit characteristic curve

The transmission lines mainly used in the experiments is of 3300[V] two lines, one of them is for the fault test. By use of the experimental system, the maximum output power of the generator for the steady state stability is obtained as shown in Fig.5-3 without SMES experimentally. Specified powers of SMES are set considering this characteristics so that the system will not step out.

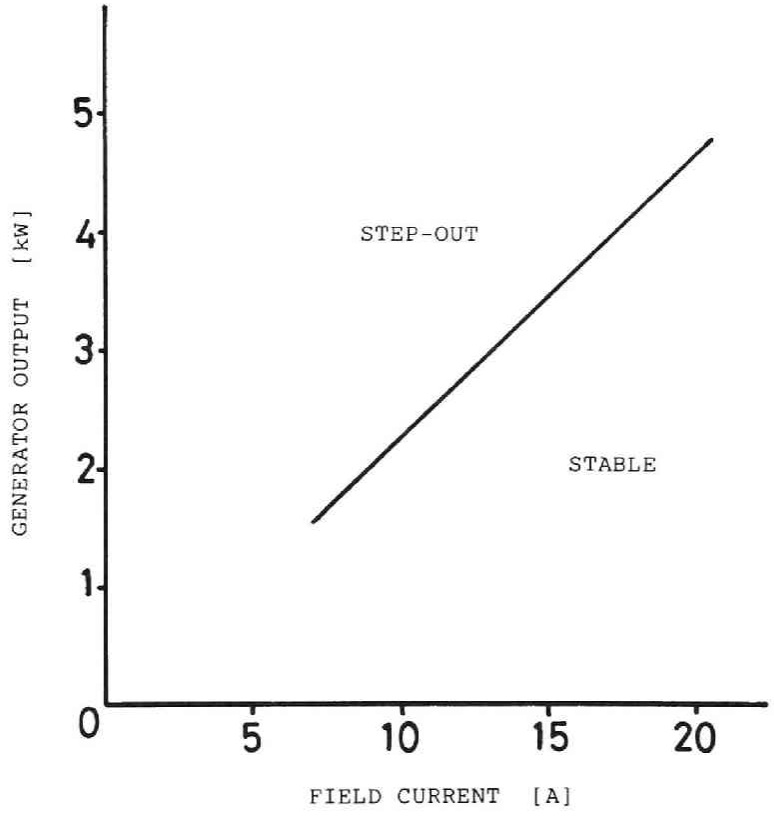

Fig.5-3 Maximum output power of generator for steady state stable with 36.6[%] transmission line.

As described in Chapter 2, the model SMES system designed and made is composed of a superconducting magnet and two thyristorized Graetz bridges connected in series as a converter. It is connected to AC three phase system through two transformers of 6[kVA]. The specification of the transformers, the thyristors and the superconducting magnet used in the experiments are presented in Table 2-1, 2-2. Capacity of the converters and transformers is the same as that of the test generator. That is, a power controller of large capacity which can behave as not only a load but also a generator controlled by the thyristorized converters is installed near a generator.

The passive filters (reactive power compensator) designed and made in Chapter 4 were used in the experiment.

5-3. EXPERIMENTS OF POWER CONTROL OF SMES CONNECTED TO ONE-MACHINE AND AN INFINITE BUS SYSTEM

By use of the above experimental system, experiments for power controls of SMES were carried out. In Section 5-3-2, investigations were performed about SMES with no filters and no reactive power compensator. In Section 5-3-3, investigations were performed about a case that passive filters are installed at SMES terminal.

5-3-1. PURPOSE

The purposes of the experiments are to investigate problems on operations of SMES in power systems including generators.

1] To study the simultaneous controls of active and reactive powers of SMES in one-machine connected to an infinite bus system. How the power controls of SMES affect on the performance of a generator? Are a generator able to operate regardless to operating conditions of SMES? On the contrary, how

conditions of a generator affects on the performance of SMES?

2] To analyze the harmonics flow of voltages and currents of the system. The current harmonics generated by SMES flow into the power system. They are distributed to an infinite bus through transmission lines and a generator. How they affect a generator performance.

3] To study the behavior of the generator and the power flow in the power system under the above conditions.

5-3-2. POWER CHARGING AND DISCHARGING WITHOUT FILTER[23)-(25)]

The experiments are carried out under the conditions as;

1]the generator generates a certain constant active power to the infinite bus (regional power source) through the transmission lines.

2]the field winding of generator is excited by a constant DC voltage source.(AVR is not used)

2]SMES is connected to the system at the generator terminal.

3]No filter is installed.

4]SMES is charging or discharging at a constant active power.

When the field current I_f of the generator is set to be 11.8[A](for rated voltage 220[V] at no-load), the terminal voltage decreases as the reactive power produced by SMES increases. Therefore SMES can not be operated successfully with a large magnet current because of the terminal voltage drop.

Then the field current of the generator is set at 20[A] so that the generator supplies a part of reactive power produced by SMES. One of the experimental results of simultaneous control of active and reactive powers of SMES is shown in Fig.5-4. The operating conditions are as follows ;

1) Generator field current If = 20[A],
2) The generator output power Pg = 3.0[kW],
3) The required active and reactive powers of SMES Ps=±1.0[kW], Qs=3.0[kVar],
4) The magnet current 60[A]<Id<120[A].
5) Transmission line reactance is 36.6[%].

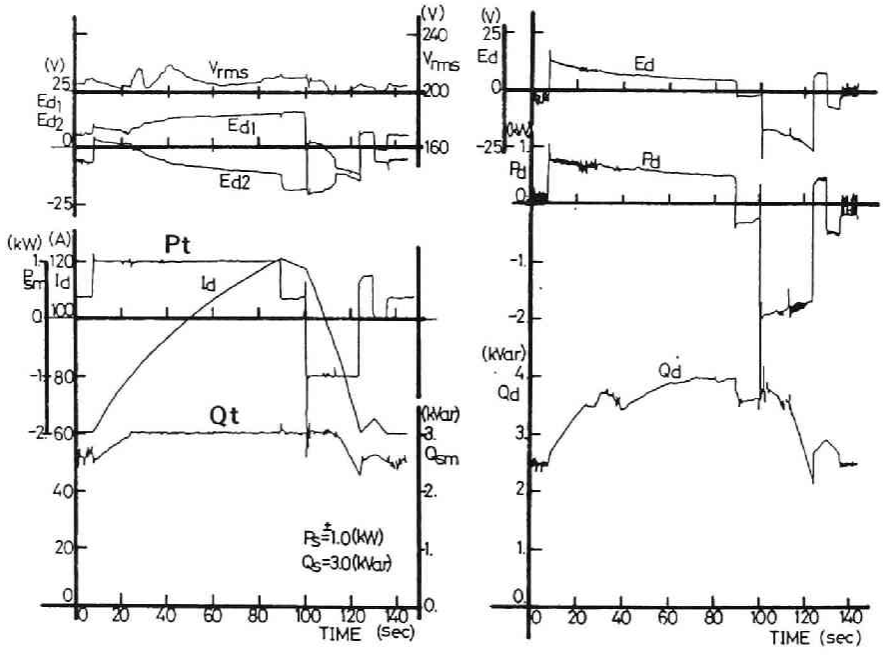

Fig.5-4 P-Q simultaneous control of SMES(experiment).
If=20[A], Pg=3.0[kW], (Ps,Qs)=(± 1.0[kW],3.0[kVar])

In Fig.5-4, a voltage Vrms denotes r.m.s. value of the generator terminal voltage. Powers Pt and Qt are the active power and the reactive power (+ : lag.) into or out of SMES. A voltage Ed is the magnet terminal voltage. Powers Pd and Qd of SMES are calculated by converter voltages and superconducting magnet current.

When the magnet current Id exceeds about 80 [A], the operating condition comes into the simultaneous controllable region. Hence Pt and Qt are controlled to be constant.

Let us compare the test result with that without a generator shown in Fig.4-23 in Chapter 4. In Fig.4-23, active and reactive powers are not controlled to be constant where the transmission line reactance is 10[%]. In comparison with this, SMES is operated successfully with the generator though the transmission line reactance is 36.6[%] in Fig. 5-4. It is considered that the generator compensates a part of the reactive power for SMES and also absorbs the higher harmonic currents generated by SMES to a certain extent.

Figure 5-5 and 5-6 show the active power and the reactive power flows, respectively. While the active power Pt flowing into or out of SMES is controlled to be $\pm$ 1.0 [kW], the generator produces a constant active power Pg = 3.0 [kW]. However the active power P_L flowing through the transmission line changes 2.0 [kW] (charge) to 4.0 [kW] (discharge). Thus a power flow through transmission lines is controlled by operations of SMES without changing generator output power.

The reactive power Qt produced by SMES varies with the magnet current Id where constant P-Q control is impossible. In P-Q controllable region, it is controlled to be almost constant 3.0[kVar]. The reactive power Qg supplied by the generator is almost constant of about 1.2[kVar]. The difference of Qt and Qg is supplied from the infinite bus through transmission lines(Q_L). The reactive power Q_L leads to the voltage drop at the SMES terminal.

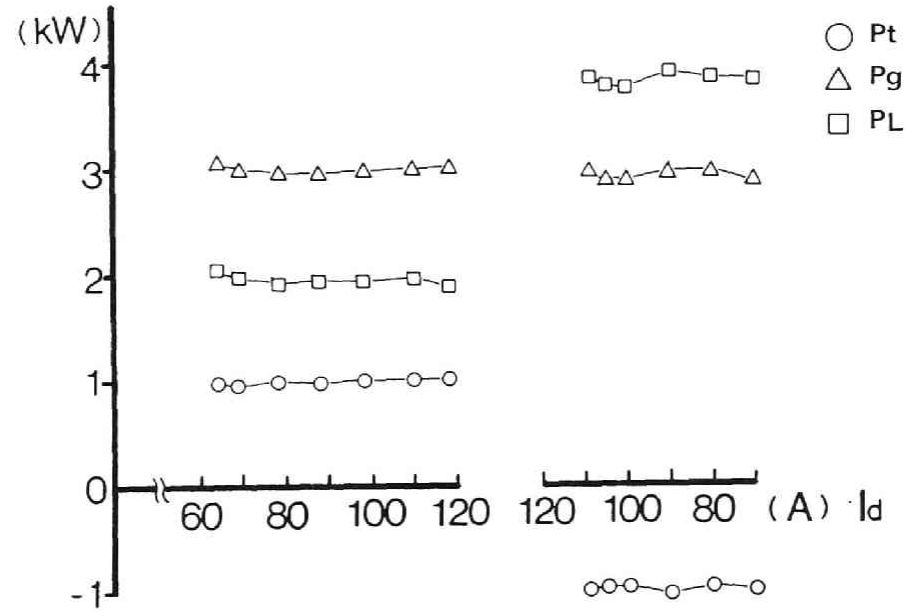

Fig.5-5 Active power flows

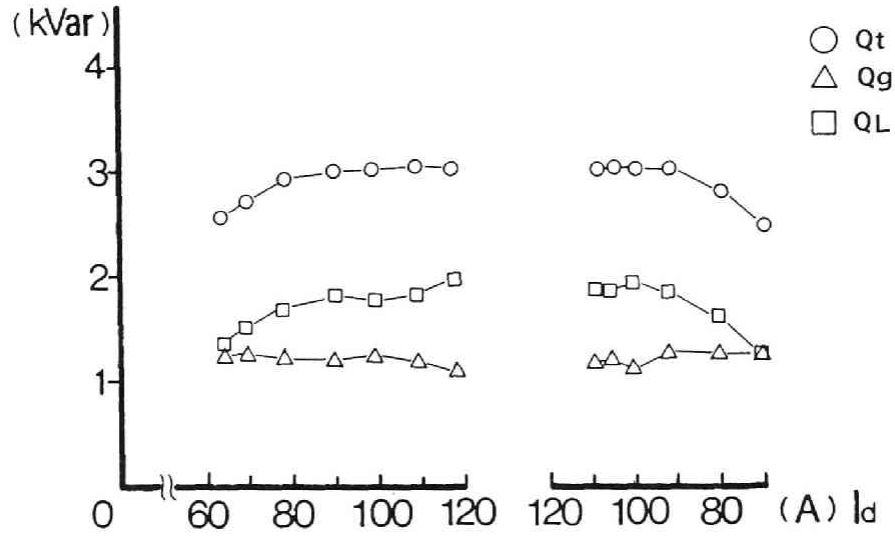

Fig.5-6 Reactive power flows

Figure 5-7 shows wave forms of the voltages and the currents with the magnet current Id; about a] 100, b] 110 and c] 120 [A] in charging mode of SMES. Symbols of each voltages and currents are shown in Fig.5-1. The larger the magnet current becomes, the larger the difference between two firing angles of converter is. Therefore the wave form of the SMES current I_{su} varies with time. Then the harmonic components of the generator current I_{gu} and the transmission line currents I_{tu} also change with time. The wave forms of the generator terminal voltage are distorted. The field current I_f has fluctuations corresponding to commutation of the converters.

Figure 5-8 shows the content ratios of harmonics of the 5-, 7-, 11- and 13-th order to the fundamental ones for the magnet current Id. (V_{wv} :generator terminal voltage, I_{sw} :SMES AC-side current, I_{gw} :the generator armature current, I_{tw} : transmission line current.) The content ratios of harmonics for I_{sw} depend upon the commutation pattern of SMES, that is, the operating conditions of SMES. Especially, those of the 5-th or the 7-th harmonic components increase up to almost 20[%].

The higher harmonic currents evolved from SMES are distributed into the generator and the transmission line. The harmonic contents of I_{gw} and I_{tw} change with time. The higher order of the harmonics flows into the generator more than into the transmission line. For the lower order, it is reverse. It is considered that it is because an impedance of generator for higher harmonics is small.

The field current I_f contains ripples of the 6-th and 12-th order as shown in Fig.5-9. It is caused by the commutation of the thyristors. DC component of If is 20 [A]. The r.m.s values of the ripple currents begins to increase up to almost 0.7 [A] when the magnet current Id exceeds 80 [A], that is, P-Q simultaneous control of SMES begins.

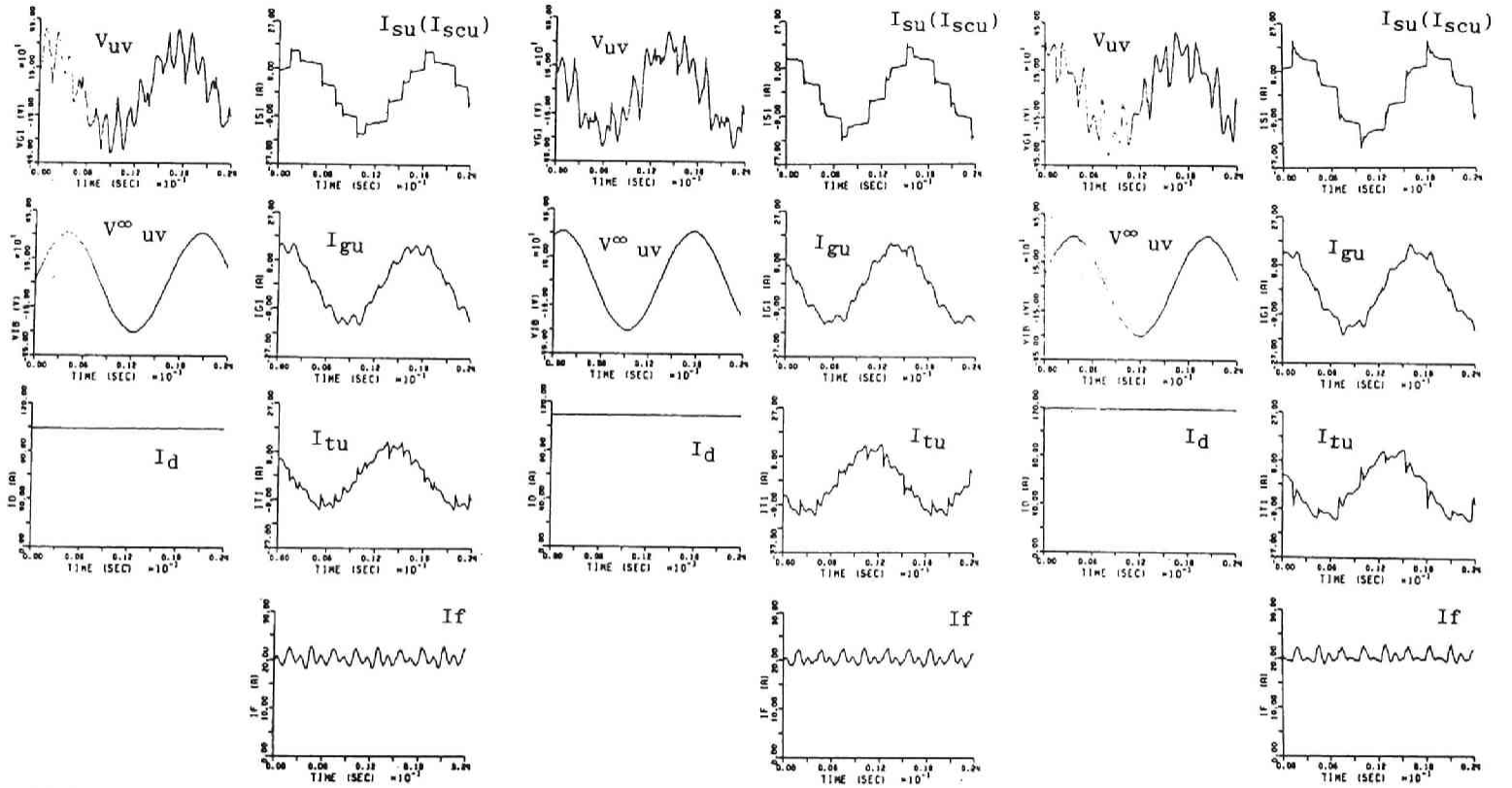

a)(charging mode Id is about 100[A]) b)(charging mode Id is about 110[A]) c)(charging mode Id is about 120[A])

Fig.5-7 Wave forms of voltages and currents.
a)(charging mode Id is about 100[A])
b)(charging mode Id is about 110[A])
c)(charging mode Id is about 120[A])

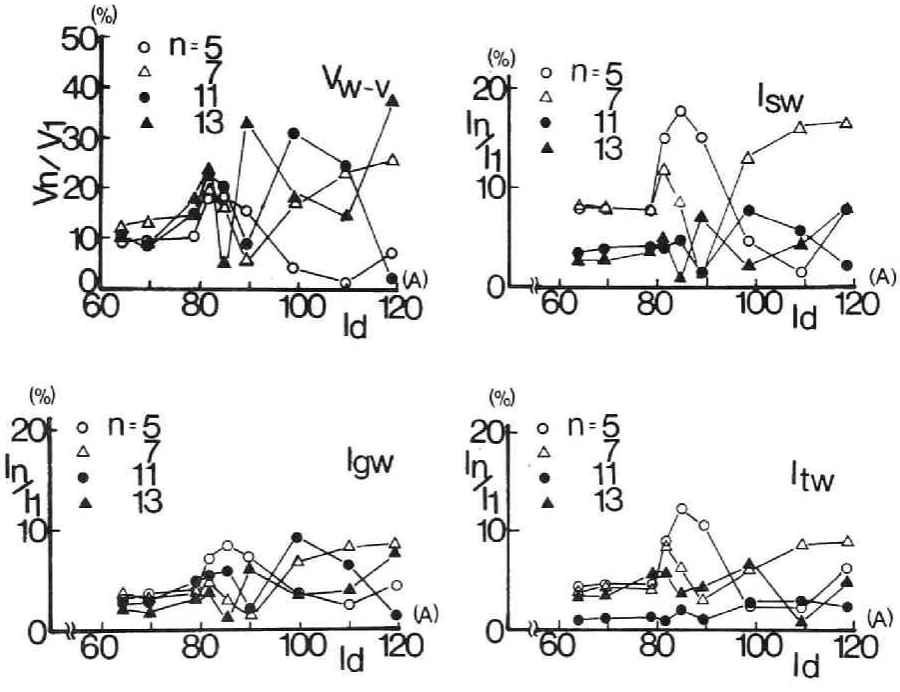

Fig.5-8 Ratios of higher harmonic components of voltages and currents(charging mode)

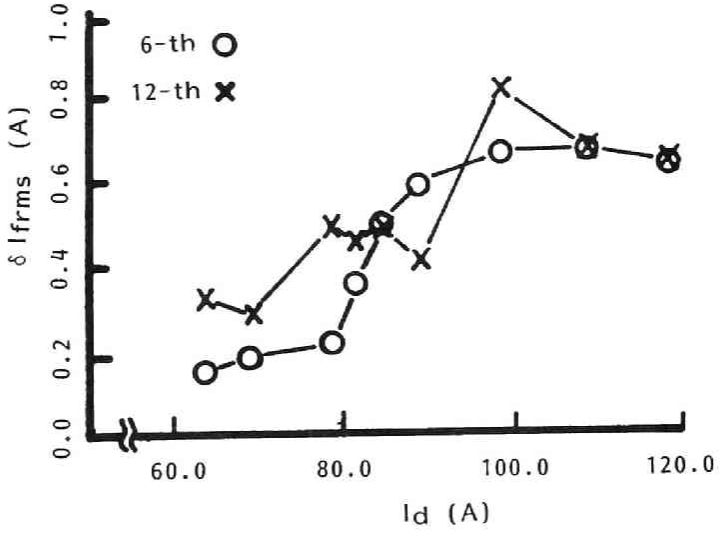

Fig.5-9 Higher harmonic ripples of field current If [r.m.s.] (charging mode)

Figure 5-10 shows the phaser diagram for the fundamental components of voltages and currents at the charging mode of SMES (Id=98.7[A]). The phase difference between phaser $V^{\infty}{}_{W}$ (infinite bus voltage) and phaser V_W (SMES terminal voltage) is about 8° . The phase difference between phaser $V^{\infty}{}_{W}$ and the phaser E_{OW} (generator induced voltage) is about 50° .

The synchronous reactance and the line reactance obtained from the phaser diagram are almost equal to those for the steady state condition without SMES.

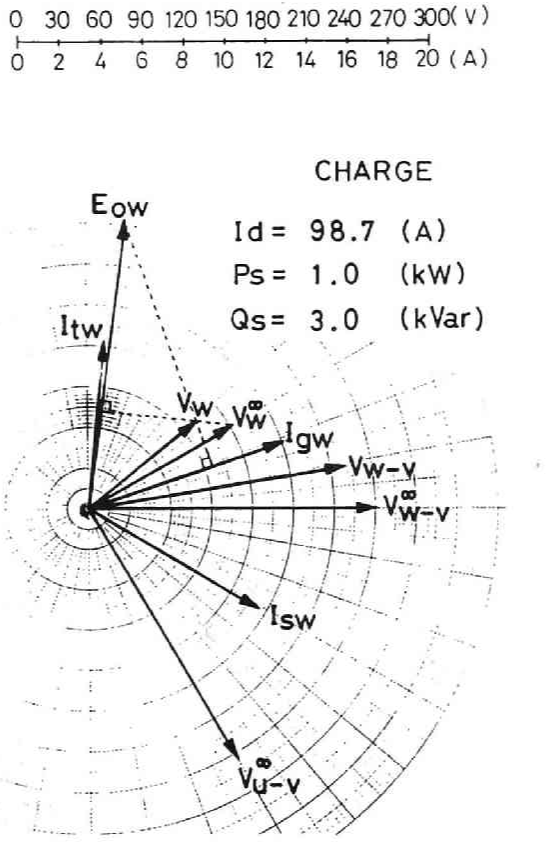

Fig.5-10 Phaser diagram for fundamental components of voltages and currents (charging mode).

5-3-3. POWER CHARGING AND DISCHARGING WITH FILTER(26),(27)

As mentioned above, SMES can not operate successfully when the generator do not supply a part of reactive power consumed by SMES. The instantaneous terminal voltage and the current are distorted by harmonic currents of SMES. Therefore passive filters are set at the terminal of SMES.

Figure 5-11 shows voltages and currents at the filter installation. The power feedback control is not used at the filter installation in the same manner as is mentioned in section 4-6-3. The ripples of the terminal voltage V_{uv} are cleared out. Ripples of the armature current I_{gu} are also removed. Each filter current If_5, If_7, If_{11} and If_{13} contains the fundamental component (;for reactive power compensation) and the higher harmonics of each order.

Experiments for the power control of SMES with filters were curried out. Figure 5-12 shows one of the experimental results. The active power of SMES Pt is controlled to be of a sinusoidal wave. The frequency is set at 0.1[Hz]. In some period of the operation, the sinusoidal active and constant reactive powers simultaneous control was performed. The r.m.s. value of the terminal voltage Vt is kept almost constant (210[V]). The generator output power Pg is kept at 1.0[kW]. However, at the mode change of the control, the small swing (frequency is about 0.7[Hz]) appeared. It is the characteristic frequency of the swing of the generator. When the power of SMES is controlled to be a sinusoidal wave of 0.7[Hz], the generator becomes to swing at the frequency of about 0.7[Hz].(refer to Section 3-4-3)

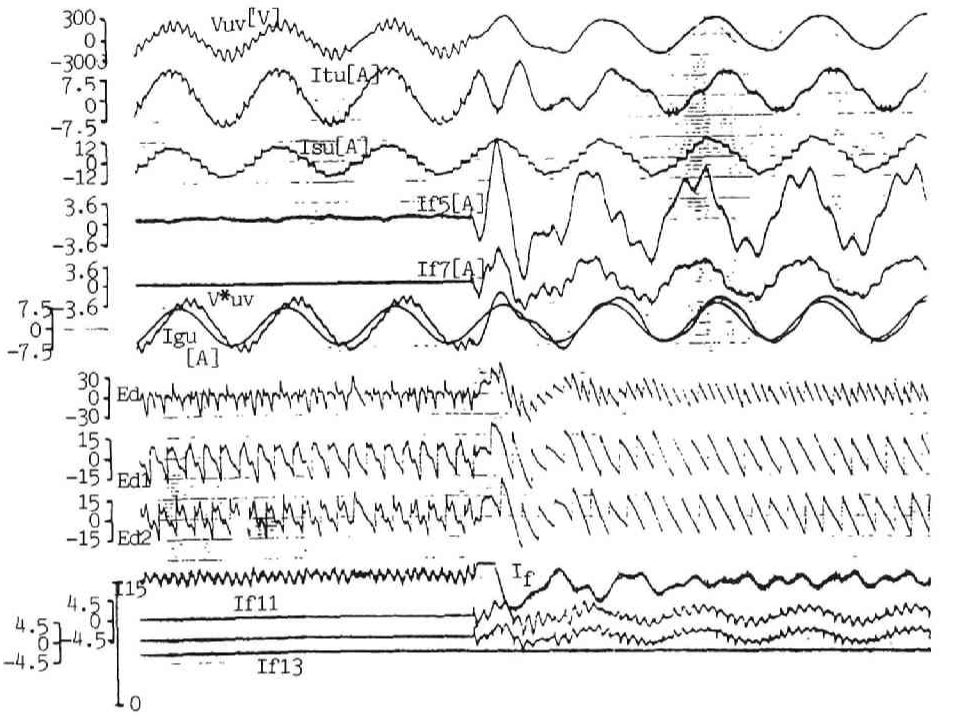

Fig.5-11 Wave forms of voltages and currents at the filter installation. (magnet current Id=50[A])

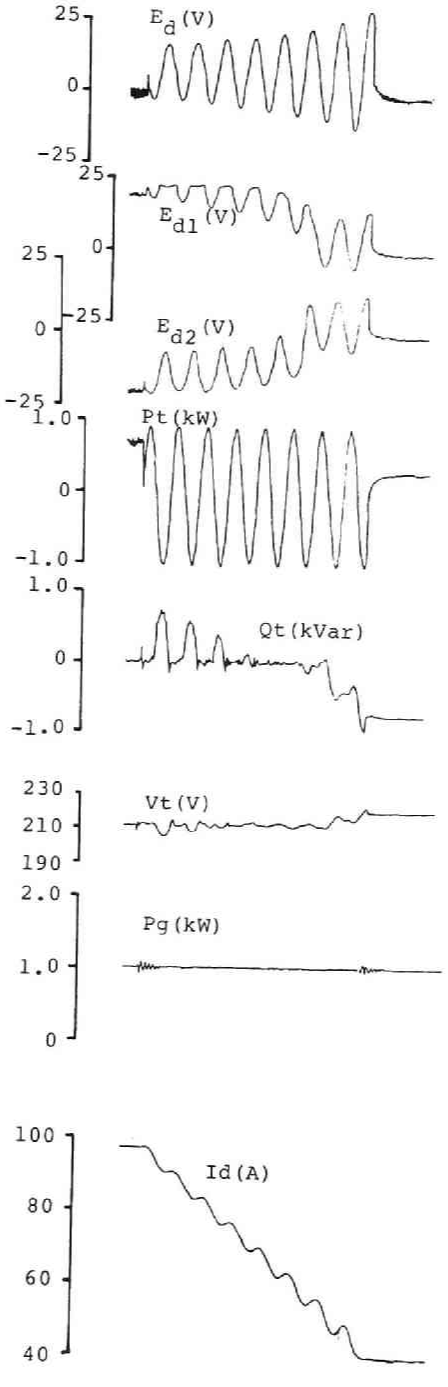

Fig.5-12 Experimental result for power control of SMES.
SMES's power Ps=1.0 sin(2π ft) f=0.1[Hz]

The constant active and reactive power control of SMES are also carried out. The wave forms of the voltages and currents at a certain time during the operation are shown in Fig.5-13. a) is for the charging mode, b) is for the discharging mode and c) is for the charging mode without the filters. The conditions are;

*The generator output power is 2.0[kW].

*The transmission line length is 36.6[%].

*SMES is operated with the powers

$$(Ps,Qs)=(\pm 1.0[kW],1.0[kVar])$$

The amplitude of current harmonics of each order are listed in Table 5-2. The AC current of SMES I_{su} contains the fundamental and the theoretical harmonics (5,7,11,13-th). The harmonics are filtered out to be the current I_{scu}. The fundamental component of the current I_{scu} becomes small for the reactive power compensation by the filters. The theoretical harmonics are damped to a certain value by the filters. However the 2-nd or the 3-rd order of harmonics increase because of the parallel resonance of the filters and the power system.

HARMO.NO.	Itu	Isu	Igu	Iscu	If5	If7
R.M.S.	4.07	11.70	6.00	3.91	5.15	2.44
1	5.56	16.23	8.45	5.25	6.45	3.24
2	0.18	0.10	0.06	0.24	0.14	0.06
3	0.72	0.56	0.50	1.20	0.83	0.37
5	0.63	2.21	0.19	0.72	3.20	0.36
7	0.09	0.84	0.05	0.12	0.06	0.75
11	0.05	0.95	0.03	0.03	0.03	0.16
13	0.03	1.30	0.01	0.02	0.07	0.01

[A]

Table 5-2 Amplitude of each order of harmonics

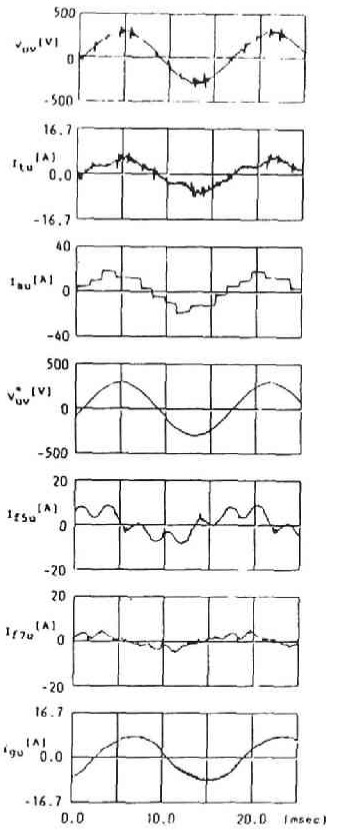

a)charging mode

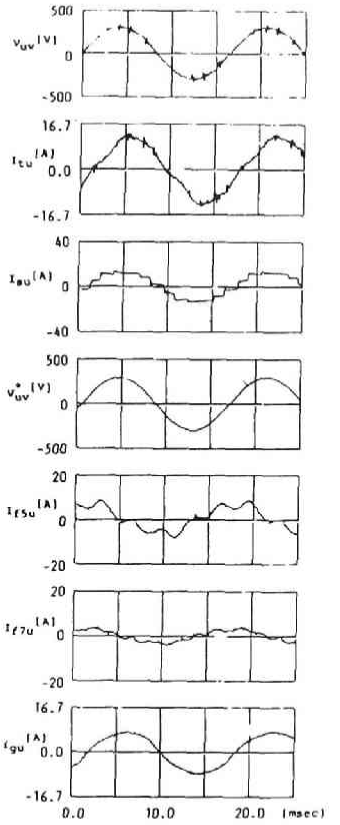

b)discharging mode

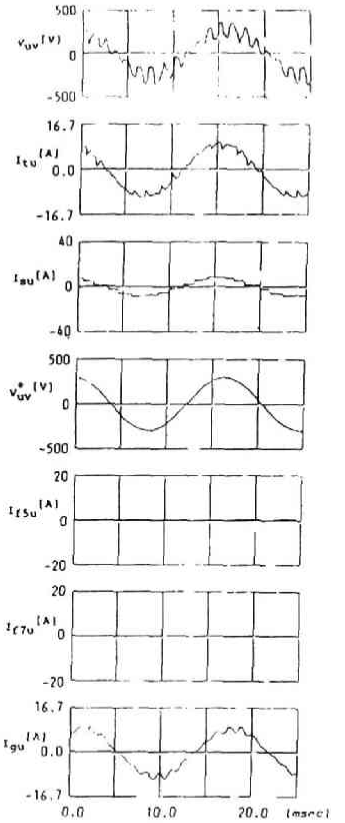

c)charging mode without filters

Fig.5-13 Wave forms of voltages and currents in constant active and reactive power control.
a)charging mode
b)discharging mode
c)charging mode without filters

The non-theoretical harmonics are considered to be caused partly by the scattering of the firing angles. By use of the simulation described in Chapter 3, the relation between the non-theoretical harmonics and the deviation of the firing angles is investigated.

One of the simulation results is shown Fig.5-14 where the conditions are as follows ; passive filter is installed, generator output power is 1.0[kW], field current is set at 12[A], and SMES is charging at active power 1.0[kW], reactive power 0.0[kVar] and magnet current is about 100[A]. Transmission line reactance is 36.6[%] (6[kVA],220[V] base). The SMES AC current i_{sw}, the generator current i_{gw} and field current i_f are shown for example. The scattering of firing angles (3 degrees) are considered, that is the firing angles for the thyristors connected to the u-phase are delayed by 3 degrees. The wave form of the field current i_f shows that it is affected by the commutation of SMES's converters. Fig.5-15 shows the experimental result corresponding to the above simulation.

The armature and the field currents of generator are influenced by the operation of SMES. It requires much consideration from various angles. The problems on the design of the generator or the methods for excluding the influences of SMES should be studied.

5-4. CONCLUDING REMARKS

In this chapter, in order to investigate the characteristics of SMES in power systems, the charging and the discharging experiments of SMES in the artificial transmission system with one generator were performed. And the computer simulation for the experimental system were also carried out. As a result of these investigation, we obtain the following:

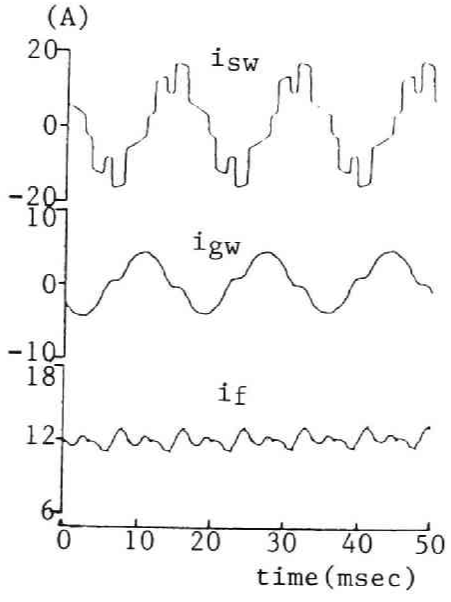

Fig.5-14 Simulation result considering the scatter of firing angles.

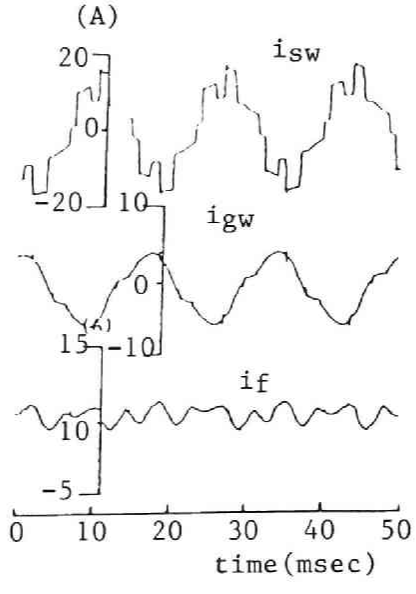

Fig.5-15 Experimental result corresponding to the simulation result as shown in Fig.5-14

[1]-Without filters, because the reactive power of SMES is supplied almost from the infinite bus, the terminal voltage drop is so large that SMES could not be operated successfully.

[2]-When the field winding of the generator is over-excited, the reactive power of SMES is partly supplied from the generator. Therefore we can operate the power control of SMES.

[3]-When the control pattern of the SMES's active power contains the component of the natural frequency of the swing of the generator, the output power of the generator can be controlled. Conversely, when the control pattern do not contains the component of the natural frequency, the power flow through the transmission line can be controlled by SMES without influence on the generator.

[4]-The harmonic current of SMES is distributed to the generator and the infinite bus through the transmission lines. The armature and the field currents of generator are under the influences of the operation of SMES. It requires much consideration from various angles. The problems on the design of the generator or the methods for excluding the influences should be studied.

REFERENCES

[1]Boenig, H.J., et.al, "Application of Superconducting coil to Reactive Power control in Electric power systems", IEEE MAG. Vol-MAG-17 No.1, p.517, 1981.

[2]Boenig, H.J., Paice, D.A., "FAULT CURRENT LIMITTER USING A SUPERCONDUCTING COIL", Applied Superconductivity Conference, Knoxville, TN, Nov. 30- December 3, 1982.

[3]Rogers, J.D., et.al, "Superconducting Fault current Limitter and Inductor Design", IEEE MAG Vol-MAG-19 No.3, p.1054, 1983.

[4]Boom, R.W., et.al, "Wisconsin Superconductive Energy Storage Project", Vol.I to IV. 1974 to 1981, Univ. of Wisconsin.

[5]Hassenzahl, W.V., et.al, "1-GWh Load-Leveling Superconducting Magnetic Energy Storage system Reference design", Proc. 1st International Symposium of Superconductive Energy Storage, p.68, 1979.

[6]Iwamoto, M., "Concept Design of SMES", proc. US-Japan Work Shop on SMES, p.155, 1981.

[7]Eyssa, Y.M., "Magnetic Design of Energy Storage Magnet", ibid, p.135.

[8]"Feasibility study on superconducting energy storage", NEDO-P-8408 June 1985

[9]Mitani, Y., Tsuji, K. and Murakami, Y., "A Method for Evaluating the Stabilizing Effect of Superconducting Magnet Energy Storage in Power system", Trans. I.E.E.J., Vol.104-B, No.9, pp.553-560, Spt., 1984.

[10]Ohsawa, S., Miyauchi, H. and Hayashi, "Stabilizing Control for Power Systems by Means of Superconducting Magnetic Energy Storage", Trans. I.E.E.J., Vol.105-B, No.1, pp.23-30, Jan., 1985.

[11]Kaminosono, H., et.al, "Characteristics of Superconducting Magnetic Energy Storage Connected to Model Power System", Conference Record of IPEC tokyo, p.820, 1983.

[12]Ohsawa, Y., et.al, "Stabilizing Control for Power system by means of SMES", Proc.of U.S.-Japan workshop on SMES, p.79, 1981.

[13]Rogers, J., et.al, "30 MJ-SMES Unit for Stabilizing on Electric Transmission System", IEEE MAG-15, 1979.

[14]Kaminosono, H., et.al, "Power System Stabilization by Superconducting Magnetic Energy Storage", Proc. of U.S.-Japan Workshop on SMES, p.120, 1981.

[15]Rogers, J.D., "Superconducting magnetic Energy Storage for BPA transmission Line Stabilization", IEEE MAG. Vol-MAG-19 No.3, pp.1078-1085, 1983.

[16]Boenig, H.J., Ranken, W.S., "DESIGN AND TESTS OF A CONTROL SYSTEM FOR THYRISTORIZED POWER SUPPLIES FOR SUPERCONDUCTING COILS", 7th Symposium on Engineering Problems of Fusion Research knoxville, TN = Oct. 25-28, 1977.

[17]Boenig, H.J., Turner, R.D., Neft, C.L. and Sueker, K.H., "DESIGN AND TESTING OF A 13.75 MW CONVERTER FOR A SUPERCONDUCTING MAGNETIC ENERGY STORAGE SYSTEM", Proc. of 9th Symposium on Engineering Problems of Fusion Research, Chicago, Il, Oct. 26-29, 1981.

[18]Kaminosono, H., Tanaka, T., Ishikawa, T. and Akita, S., "CHARACTERISTICS OF SUPERCONDUCTING MAGNETIC ENERGY STORAGE(SMES) ENERGIZED BY A HIGH-VOLTAGE SCR CONVERTER"

[19]Nitta, T., et.al, "Controls and Characteristics of SMES Connected to Power system", Proc. of U.S.Japan Work shop on SMES, p.64, 1981.

[20]Nitta, T., et.al, "Experiment for Power Charging and Discharging of SMES", Static Apparatus Seminar of I.E.E.J. SA-80-19, Nov. 1980.

[21]Ise, T., Tsuji, K. and Murakami, Y., "Power and Reactive power Simultaneous Control by 0.5 MJ Superconducting Magnet Energy Storage", Trans. I.E.E.J., Vol.104-B, No.9, pp.545-552, Spt., 1984.

[22]Murakami, Y., "GTO converter as an Interface between SM and AC Power Lines", ASC LF 16, 1982.

[23]Kawahira, H., Nakamura, T., Nakazawa, S. and Nomura, M., "Active Power Filter", Conference Record of IPEC-TOKYO 83, pp.981-992 March 1983.

[24]Akagi, H., Kanazawa, Y., Fujita, K. and Naniwae, A., "Generalized Theory of the Instantaneous Reactive power and its Application", Trans. I.E.E.J., Vol.103-B, No.7, pp.483-490, July., 1983.

[25]Kuh,E.S., Layton,D.M. and Rohrer,R.A., "Network analysis and synthesis via state variables", in network and switching theory, G.Biorci, Ed., Newyork Academic, N.Y., pp.140-148, 1968.

(1)Nitta, T., Shirai, Y. and Okada, T., "Controls and Characteristics of Superconductive Magnetic Energy Storage connected to Power System", Conference Record of IPEC-TOKYO 83, pp.832-843 March 1983.

(2)Nitta, T., Shirai, Y. and Okada, T., Convention Records of Kansai branch of I.E.E.J. G4-25, 1980.

(3)Ohsawa, S., Shirai, Y., Nitta, T. and Hayashi, S., Convention Records of Kansai branch of I.E.E.J. G4-24, 1980.

(4)Nitta, T., Shirai, Y., Kishima, A. and Okada, T., I.E.E.J. Proc. on S.A., SA-82-23, pp.59-67, 1982.

(5)Shirai, Y., Nitta, T. and Okada, T., 56-th Convention record of Japan Society for Power Electronics Vol.9 pp.76-85, 1983.

(6)Shirai, Y., Tanaka, S., Nitta, T. and Okada, T., Convention Records of Kansai branch of I.E.E.J. G4-6, 1981.

(7)Shirai, Y., Nitta, T. and Okada, T., Convention Records of Annual Meeting of I.E.E.J. 860 1982.

(8)Shirai, Y., Nitta, T. and Okada, T., "Computer Simulation for Power System Including Superconducting Magnetic Energy Storage", Submitted to PESC '88.

(9)Shirai, Y., Kondoh, H., Nitta, T. and Okada, T., I.E.E.J. Proc. on P.E., PE-87-123, pp.53-62, 1987.

(10)Nitta, T., Shirai, Y., Fijita, K. and Okada, T., Convention Records of Annual Meeting of I.E.E.J. 851 1983.

(11)Tanaka, Y., Shirai, Y., Nitta, T. and Okada, T., Convention Records of Annual Meeting of I.E.E.J. 849 1984.

(12)Kondoh, H., Shirai, Y., Nitta, T. and Okada, T., Convention Records of Kansai branch of I.E.E.J. G3-35, 1986.

(13)Nitta, T., Shirai, Y. and Okada, T., "Power System Characteristics of Superconducting Magnetic Energy Storage", 21st Intersociety Energy Conversion Engineering Conference, August, p.895- 900(1986)

(14)Shirai, Y., Tanaka, Y., Nitta, T. and Okada, T., I.E.E.J. Proc. on P.E., PE-85-62, pp.41-50, 1985.

(15)Nitta, T., Shirai, Y., Tanaka, Y. and Okada, T., I.E.E.J. Proc. on S.A., SA-85-21, pp.11-20, 1985.

(16)Tanaka, Y., Shirai, Y., Nitta, T. and Okada, T., Convention Records of Kansai branch of I.E.E.J. G3-67, 1984.

(17)Shirai, Y., Kishima, A., Ohsawa, C., Nitta, T. and Okada, T., Convention Records of Kansai branch of I.E.E.J. G4-23, 1982.

(18)Tanaka, Y., Shirai, Y., Nitta, T. and Okada, T., Convention Records of Kansai branch of I.E.E.J. G3-43, 1985.

(19)Shirai, Y., Tanaka, Y., Nitta, T. and Okada, T., Convention Records of Annual Meeting of I.E.E.J. 924 1985.

(20)Shirai, Y., Nitta, T., Okada, T., Seriu, H. and Imura, E., "Active Filter using Superconducting Magnet", 68-th Convention record of Japan Society for Power Electronics.

(21)Seriu, H., Shirai, Y., Nitta, T. and Okada, T., Convention Records of Annual Meeting of I.E.E.J. 934 1986.

(22)Nitta, T., Shirai, Y. and Okada, T., "Power Charging and Discharging Characteristic of SMES connected to Artificial Transmission Line", IEEE trans. on MAG. vol.MAG-21 no.2 pp.1111-1114 March 1985.

(23)Shirai, Y., Kishima, A., Nitta, T. and Okada, T., I.E.E.J. Proc. on P.E., PE-84-67, pp.123-134, 1984.

(24)Kishima, A., Shirai, Y., Nitta, T. and Okada, T., Convention Records of Kansai branch of I.E.E.J. G4-4, 1983.

(25)Shirai, Y., Ueda, K., Nitta, T. and Okada, T., Convention Records of Annual Meeting of I.E.E.J. 852 1984.

(26)Shirai, Y., Nitta, T. and Okada, T., Convention Records of Annual Meeting of I.E.E.J. 930 1986.

(27)Shirai, Y., Kondoh, H., Nitta, T. and Okada, T., Convention Records of Annual Meeting of I.E.E.J. 915 1987.